

T  
H41-92  
SHA

# PROCEDURES FOR ANALYSIS OF DIGITAL TELEMETERED SEISMIC ARRAY DATA

A THESIS  
*submitted in fulfilment of the  
requirements for the award of the degree  
of*  
DOCTOR OF PHILOSOPHY  
*in*  
EARTHQUAKE ENGINEERING



**Ph.D. THESIS**  
BY  
MUKAT LAL SHARMA



DEPARTMENT OF EARTHQUAKE ENGINEERING  
UNIVERSITY OF ROORKEE  
ROORKEE-247 667 (INDIA)

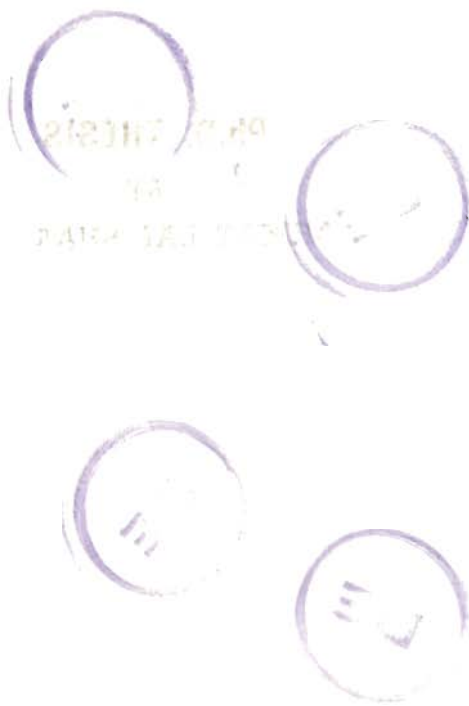
MAY, 1992

PROCEDURES FOR ANALYSIS OF  
DETERMINATION OF BIRCH AND

of the data

RESULTS

TABLE



of the data

RESULTS

*Dedicated to my Mother*

## CANDIDATE'S DECLARATION

I hereby certify that the work which is being presented in the thesis entitled "PROCEDURES FOR ANALYSIS OF DIGITAL TELEMETERED SEISMIC ARRAY DATA" in fulfillment of the requirement for the award of the Degree of DOCTOR OF PHILOSOPHY and submitted in the Department of Earthquake Engineering, of the University is an authentic record of my own work carried out during a period from September, 1987 to May, 1992 under the supervision of Dr. H. R. Wason.

The matter presented in this thesis has not been submitted by me for the award of any other Degree of this or any other University.



(Mukat Lal Sharma)

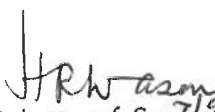
This is to certify that the above statement made by the candidate is correct to the best of my knowledge.



(Dr. H. R. WASON)  
Reader in Geophysics  
Department of Earth Sciences  
University of Roorkee  
Roorkee - 247667, INDIA

Date : 11/5/92

The Ph. D. Viva - Voce examination of Sri M. L. Sharma,  
Research Scholar, has been held on 7th Sept., 1992.



Signature of Supervisor  
7/9/92



Signature of H.O.D.  
7/9/92



Signature of External Examiner  
7/9/92

## A B S T R A C T

Monitoring of earthquakes provides basic data for seismological investigations and research. The advancement of digital technology has made it possible to record the seismic signals from many seismometer stations simultaneously in digital mode at a centralized site for rapid as well as on-line analysis of the recorded digital data. Such data has now become available from the Sample Short Aperture Telemetered Digital Seismic Array in Garhwal Himalaya (TDSA). The data acquisition system in TDSA uses Short Term Average (STA) and Long Term Average (LTA) event detection technique for the recording of the triggered events on 9 track half inch magnetic tapes feeding common time reference from OMEGA world standard time.

The main objective of this study is to develop the methods and techniques of digital seismic data processing from array of seismic stations. The complete ground motion time histories were monitored as received from individual stations, initially, to find the optimal values of trigger parameters i.e., STA and LTA periods, threshold level for trigger ratio (STA/LTA) of individual seismometer outstations, trigger window, pre and post event recording periods and maximum event recording period. These parameters were selected on the lower side so as not to miss any seismic event resulting in recording of many false alarms (Sharma et al., 1987). The background noise level of individual seismometer outstations, array geometry, line of sight conditions of the stations with respect to the central recording station and environmental disturbances were kept in view in selecting the trigger parameters. TDSA being located in a rough terrain and quite remote area, the system has not run on continuous basis due to lack of uninterrupted power supply. In the present study the data for total run time of 781 hours during the period 13-02-89 to 07-05-89 comprising of 530 triggered events has been analyzed and an attempt has been made to optimize the post processing of the recorded events.

The initial exercise carried out consisted of development of the software package for Transfer of Magnetic tape Data (TMD) on DEC-2050 computer system (Sharma, 1990) from the data tapes written as blocks of 4096 bytes in industrial compatible format. Based on bit manipulations

TMD software reads two 16 bit words (PDP 11/23) at a time as single 36 bit word (DEC 2050) and then according to the prescribed format the data is demultiplexed and saved in different files changing the binary mode into the integer mode. TMD takes care of the parity bit by supplying the value of previous sample to the corrupt sample in the time series. TMD provides digital seismogram files for each station and a separate file for date and time of the first sample, sampling rate and the total number of samples of each seismogram. The data files are then transferred on PC XT/AT for post processing of the recorded data.

Another software package for automatic determination of on-set time of the first arrivals of seismic signals at different stations has been developed under the present study (Sharma et al., 1990). The automatic Phase Picker (APP) incorporates the function of an event detector and also obtains precise values of first arrivals for determining hypocentral parameters. APP developed in this study is based on a characteristic function which is a modified time series of ground motion time history. The characteristic function enhances the changes in the amplitudes and/or frequencies of the original time series. STA representing the current signal value and LTA representing the back ground noise level are computed over the characteristic function in a manner to enhance the signal to noise ratio. Once the first arrival is picked, the algorithm enters into confirmatory tests for seismic event and if the time series is passed through the tests then the onset time of the first arrival, up/down first motion characteristic, maximum amplitude and coda length are recorded. The tests performed are frequency dispersion test, coda shape test and the test for arrival times at different seismometer outstations which is applied after the times from each channel are picked. A modified version of APP software package has been developed in which the threshold value for the trigger ratio is decided by the background noise level. The results of both the techniques are comparable.

For the processing of the recorded data, single pole high pass and low pass digital filters are applied to remove DC bias and the high frequency content from the recorded time series. The software package APP is then run to first select the seismic events from the triggered events. APP further computes the onset times of the first arrival of the seismic phases, up/down first motion characteristic, maximum amplitude and the coda length. For the verification of the results obtained by the APP, the filtered digital seismograms are plotted on the screen of the PC for visual inspection and the onset time and characteristics of seismic signals are marked. This procedure, called visual

analysis, can achieve the accuracy in picking the first arrival to 2.77 milli sec. However, any error made in marking the right sample on the screen shall affect the accuracy of the first arrival.

APP has marked 17 events as seismic events out of 530 triggered events recorded at three or more stations. Only one seismic event is rejected as false alarm due to failing of third confirmatory test in which some noise peak has come just before the first seismic arrival and could not be filtered by the filtering process. All the triggered events are processed by visual analysis and the same 18 events as marked by APP are confirmed to be the only seismic events. The higher number of false alarms are mainly due to environmental disturbances (transmission errors) giving rise to sudden increase in the amplitudes up to  $\pm 32768$  micro volts and the choice of trigger parameter values so as not to miss low magnitude events. Qualitywise with respect to the times of first arrival of seismic phases as noted down by visual analysis, APP gives the same arrival time for 36 seismograms whereas a difference of 0.0 to 0.5 sec in case of 19 seismograms and 0.5 to 1.0 sec in case of 7 seismograms is noticed. In 2 seismograms the first arrival is marked by the visual analysis only and in 5 seismograms the first arrival is picked only by APP. A comparison of the results of APP with other reported phase picker algorithms (Stewart, 1971, Allen, 1978) shows that APP is better in quality and quantity in respect of first arrival time pickings.

The first arrival times obtained by the procedures laid down for the analysis of the events are used to determine the hypocentral parameters for the 18 seismic events from HYPO 71 computer program (Lee and Lahr, 1975). Source parameters like stress drop, seismic moment and source dimension etc. have been computed for some events using Brune's model (Brune, 1970) of seismic source. Based on the data from these events, an empirical seismic moment - magnitude relationship has been proposed for this region. The shallow microearthquake events with low stress drops indicate the low resisting power of the upper crust to withhold the strain energy arising due the plate motions in the region.



## ACKNOWLEDGEMENTS

I express my gratitude to Dr. H. R. Wason, Reader Department of Earth Sciences for his guidance, discussions and help in carrying out the studies and preparation of the thesis.

Govt. of India, Department of Science and Technology, provided necessary funds for the deployment of 'Short Aperture Telemetered Digital Sample Seismic Array in Garhwal Himalaya' (Ganga-Yamuna Valley) as part of the 'All India Coordinated Project on Himalaya Seismicity and Seismotectonics' and the analysis of the recorded data. M/S. Earth Data Ltd., Nutsey Lane, Southampton, U. K. provided training in operation and maintenance of the data acquisition system in Roorkee and at their works. Prof. L. S. Srivastava, the Principal Investigator of the Research Scheme encouraged me to participate and carry out the studies from the initial stages and provided continued support and direction at various stages of the study.

Prof. P. N. Agrawal, Head of the Department and Prof. B. V. K. Lavania and Prof. A. S. Arya, previous Heads of the Department provided all facilities to carry out the work.

Prof. K. N. Khattri, Prof. R. Chander, Prof. P. S. Moharir, Prof. V. N. Singh and Mr. A. D. Pandey gave valuable suggestions at different stages of the work.

I am thankful to all the staff employed in the project for their help in maintenance and operation of the array. Mr S. C. Gupta, Mr. Manoj Sharma and Mr. S. C. Sharma provided all help and assistance in preparation of the thesis.

I will be failing in my duties if I do not mention the constant encouragement by my father and my wife, Neelam, which inspired me through out the work.

Lastly, but not the least I would also like to express my sincere thanks to all of them who have helped me directly or indirectly during this period.

I am thankful to 'Computer Link' for printing the thesis.



# CONTENTS

# CONTENTS

	Page	No.
CERTIFICATE		i
ABSTRACT		11
ACKNOWLEDGEMENT		v
CONTENTS		vi
GLOSSARY OF SYMBOLS		x
LIST OF ABBREVIATIONS		xii
LIST OF FIGURE CAPTIONS		xiii
LIST OF TABLES		xlx
<b>Chapter 1 INTRODUCTION</b>		
1.1 PREAMBLE		1
1.2 RELEVANCE OF THE STUDY		7
1.3 PLAN OF THE WORK		9
<b>Chapter 2 THE TELEMETERED DIGITAL SEISMIC ARRAY IN THE GARHWAL HIMALAYA</b>		
2.1 INTRODUCTION		11
2.2 EARTHQUAKE STATION NETWORKS		13
2.2.1 Why Telemetered Array of Seismic Stations?		13
2.2.2 Why Digital Telemetered Array of Seismic Stations?		14
2.2.3 Digital Telemetered Arrays - A Review		15
2.3 SHORT APERTURE SAMPLE TELEMETERED DIGITAL SEISMIC ARRAY IN THE GARHWAL HIMALAYA		18
2.3.1 The Himalaya		18
2.3.2 The Array		23
2.3.3 Description of the System		27
2.3.4 Software for Data Acquisition		31

2.3.4.1, Station averaging	34
2.3.4.2 Event detection technique	35
2.3.4.3 Saving event data on magnetic tapes	37
2.3.4.4 Event data log	37
2.3.4.5 Analog output of the event	38
2.3.4.6 PDP 11/23 data storage format	39
2.3.4.7 Outstation data format	40
<b>CHAPTER 3 DATA ACQUISITION AND PARAMETER SELECTION</b>	
3.1 INTRODUCTION	43
3.2 PRESENT KNOWLEDGE ABOUT THE AREA	44
3.2.1 Seismicity of the Area	44
3.2.2 Focal Depths	46
3.2.3 Velocity Structure	47
3.2.4 Focal Mechanisms	48
3.3 SELECTION OF TRIGGER PARAMETERS FOR TDSA	49
3.3.1 Long Term Averaging Period	49
3.3.2 Short Term Averaging Period	50
3.3.3 Trigger Parameters	52
3.3.4 Recording Periods	55
<b>Chapter 4 SOFTWARE DEVELOPED FOR DATA PROCESSING</b>	
4.1 INTRODUCTION	60
4.2 SOFTWARE DEVELOPED FOR FORMAT CHANGE AND ARCHIVING	60
4.3 VISUAL ANALYSIS OF THE RECORDED DATA	68
4.3.1 Procedure	68
4.3.2 Filtering Process	73

**CHAPTER 5 PHASE PICKER**

5.1 INTRODUCTION	85
5.2 PHASE PICKING ALGORITHM - A REVIEW	87
5.2.1 Time Domain Algorithms	87
5.2.1.1 Logical Structure	88
5.2.1.2 Different time domain algorithms	93
5.2.2 Frequency Domain Algorithms	101
5.3 PHASE PICKER DEVELOPED	102
5.3.1 Automatic Phase Picker Algorithm (APP)	104
5.3.2 Dynamic Threshold	114
5.3.3 APP Computer Program	116

**CHAPTER 6 RESULTS AND DISCUSSIONS**

6.1 INTRODUCTION	118
6.2 DATA SET	119
6.3 RETRIEVAL OF THE DATA	120
6.4 VISUAL ANALYSIS OF THE DATA	121
6.5 AUTOMATIC ANALYSIS BY PHASE PICKER	123
6.6 VISUAL Vs AUTOMATIC ANALYSIS	134
6.7 FURTHER ANALYSIS OF THE DATA	137
6.7.1 Location and Magnitude of the Events	137
6.7.2 Fault Plane Solutions	146
6.7.3 Source Parameters	148
6.7.4 Interpretation of the Source Parameters	178

## CHAPTER 7 CONCLUSIONS AND SUGGESTIONS

7.1 CONCLUSIONS	180
7.2 SUGGESTIONS FOR THE FURTHER WORK	184

## APPENDIX

I LISTING OF COMPUTER PROGRAMS	186
II DETAILS OF THE MAGNETIC TAPE FORMAT USED IN PDP 11/23 SYSTEM	213

REFERENCES	218
------------	-----

## G L O S S A R Y   O F   S Y M B O L S

The following list defines the principal symbols used in the thesis. On many occasions, additional ones have to be used in a minor context. It is hoped that appropriate text explanations will avoid confusions.

<u>SYMBOL</u>	<u>MEANING</u>
A	Constant
$a_1$	Coefficient for filters
AVE(i)	Short Term/Long Term Average
$b_0, b_1$	Coefficient for filters
CF(i), CF	Characteristic function
D	Epicentral distance (km)
D(i)	First difference of time series
$D_{max}$	Maximum distance between any two out stations
$f, F, f_1$	Frequency
H(f)	Gain of the filter
h(i)	Impulse function
J	$(-1)^{1/2}$
L1, L2, L3, LA, LB, LC, LD	Information of particular bits in a 16 - bit word
M	16 - bit word
$M_L$	Magnitude
$M_0$	Seismic moment
N, N1, N2, N3, N4	Information of particular bits in a 16 - bit word

NC	Component identification bits
ND	Data not valid bit
NE	Parity bit
NR	Range bits
r	Source radius
$R_{\theta\phi}$	Radiation pattern
$R(i)$	Modified time series
$\circ$	
$R(i)$	First Difference of $R(i)$
S1, S2	Threshold levels
$S(i)$	Variance
t	Time index
T, $\Delta t$	Sampling interval
u	Slip
$V_{50}$	Median of distribution
$V_{75}$	75th percentile of distribution
V	Velocity
$V_p$	P-wave velocity
$x(i)$	Input time series
$y(i)$	Output time series
$\alpha_1, \alpha_2$	Coefficients for filters
$\beta_1, \beta_2, \beta_3, \beta_4$	Coefficients for filters
$\rho$	Density
$\Delta\sigma$	Stress drop
$\mu$	Modulus of rigidity
$\tau$	Travel time divided by quality factor Q





## LIST OF ABBREVIATIONS USED IN THE THESIS

<u>ABBREVIATION</u>	<u>MEANING</u>
APP	Automatic Phase Picker ( Software)
BCD	Binary Coded Decimals
BT	Basement Thrust
CHK	Chakrata
CRS	Central Recording Station
DAS	Data Acquisition System
DHR	Dhargaon
EOF	End Of File mark
GRD	Format change program (software)
LIU	Line Interface Unit
LTA	Long Term Average
LTAP	Long Term Average Period
MBT	Main Boundary Thrust
MCT	Main Central Thrust
NNR	Narendranagar
NT	Number of stations to trigger
PCM	Pulse Coded Modulation
POR	Pauri
POSTEVP	Post Event Recording Period
PREVP	Pre event Recording Period
PRTCT	Software to replace noise spikes
RRK	Roorkee
SMS	Seismic Monitoring System
SMRT	Software to decrease sampling rate
STA	Short Term Average
STAP	Short Term Average Period
SUR	Surkanda
TDSA	Telemetered Digital Seismic Array
TR	Trigger Ratio
TW	Trigger Window
TMD	Transfer of Magnetic tape Data (Software)
UTK	Uttarkashi
VDU	Visual Display Unit

## LIST OF FIGURE CAPTIONS

FIG NO.	CAPTION	PAGE NO.
2.1	Tectonic map (Fuchs and Sinha, 1978) showing the locations of Central Recording Station and Outstations	25
2.2	Block diagram of the configuration of the seismic telemetry system.	29
2.3	Parameters for event trigger and recording	36
2.4	Bit structure of the 16-bit word recorded by Data Acquisition System	41
4.1	Flow chart for software package TMD	63
4.2	Plot of ground motion time histories of the seismic event recorded by DAS on 25-11-88 at three stations	70
4.3	Plot of a false alarm recorded by DAS at five stations	71
4.4	Example of post processing of the seismogram recorded at Surkanda station on 12-04-89. (a) Plot of original time series as recorded by DAS having two noise spikes, (b) Plot of the same time series on an expanded y-scale, and (c) Plot of the same time series after replacement of the noise spikes by average trend	72

- 4.5 Procedure of digital processing of the seismogram recorded by DAS at a station to mark characteristic parameters of the seismic event. (a) Plot of the full seismogram, (b) Plot of the original seismogram taking expanded y-axis and, (c) Plot of a segment containing P-arrival on expanded x- and y-scale 75
- 4.6 Example of a microearthquake ( $M_L = 3.0$ ) recorded by DAS. The accuracy for P-phase onset as in (a) marked with  increases in (b) with  mark. The epicentral distances are given in parenthesis 76
- 4.7 Gain of the low pass filter for different  $\alpha$  82
- 4.8 Example of post processing of the seismogram recorded at POR ( Pauri) station on 2-04-89 (a) Full plotting of original time series as recorded by DAS, (b) Portion of seismogram containing P-arrival and, (c) Filtered time series containing P-arrival 84
- 5.1 Generalised logical structure for a phase picker 89
- 5.2 Different types of Characteristic Functions (Plotted on different vertical scale) 92
- 5.3 Gain of the high pass filter with  $\beta_1 = 0.995$  107
- 5.4 Gain of the low pass filter with  $\alpha = 0.33$  used for STA 110

5.5	Gain of the low pass filter with $\alpha = 0.992$ used for LTA	111
5.6	Flow chart of software package for Automatic Phase Picker	117
6.1	Comparison of records for Narendranagar observatory obtained by Banioff Seismograph and TDSA for the same event	124
6.2	Frequency dispersion values of time series obtained using APP. The time series corresponding values marked as (o) and ( $\Delta$ ) are passed by this test as seismic event whereas those corresponding to values marked as ( $\bullet$ ) are rejected as false alarms	127
6.3	Coda shape values obtained by APP. The values marked as (o) and ( $\Delta$ ) are passed as seismic events while the value marked as ( $\bullet$ ) are rejected as false alarms	130
6.4	Block diagram showing procedure laid down for data processing using visual analysis and phase pickers	135
6.5	Example of P-phase picking by visual analysis (V) and APP (A) at five stations of seismic event dated 12-4-89. The blocks show display of 1 sec data containing the P-onset	139
6.6	Comparison of the performance of different phase picker algorithms in confirming events triggered at 3 or more stations as seismic events	140

6.7	Hypocentral locations of seismic events using Visual analysis (●) and APP (O)	144
6.8	Composite fault plane solution of seismic events recorded by DAS	147
6.9	Displacement Spectra of P-wave for seismic event dated 25-11-88 used for computation of seismic source parameters	152
6.10	Displacement Spectra of P-wave for seismic event dated 08-03-89 used for computation of seismic source parameters	153
6.11	Displacement Spectra of P-wave for seismic event dated 16-03-89 used for computation of seismic source parameters	154
6.12	Displacement Spectra of P-wave for seismic event dated 29-03-89 used for computation of seismic source parameters	155
6.13	Displacement Spectra of P-wave for seismic event dated 30-03-89 used for computation of seismic source parameters	156
6.14	Displacement Spectra of P-wave for seismic event dated 02-04-89 used for computation of seismic source parameters	157
6.15	Displacement Spectra of P-wave for seismic event dated 04-04-89 used for computation of seismic source parameters	158
6.16	Displacement Spectra of P-wave for seismic event dated 09-04-89 used for computation of seismic source parameters	159

6.17	Displacement Spectra of P-wave for seismic event dated 11-04-89 used for computation of seismic source parameters	160
6.18	Displacement Spectra of P-wave for seismic event dated 11-04-89 used for computation of seismic source parameters	161
6.19	Displacement Spectra of P-wave for seismic event dated 12-04-89 used for computation of seismic source parameters	162
6.20	Displacement Spectra of P-wave for seismic event dated 16-04-89 used for computation of seismic source parameters	163
6.21	Displacement Spectra of P-wave for seismic event dated 19-04-89 used for computation of seismic source parameters	164
6.22	Displacement Spectra of P-wave for seismic event dated 22-04-89 used for computation of seismic source parameters	165
6.23	Displacement Spectra of P-wave for seismic event dated 23-04-89 used for computation of seismic source parameters	166
6.24	Displacement Spectra of P-wave for seismic event dated 03-05-89 used for computation of seismic source parameters	167
6.25	Displacement Spectra of P-wave for seismic event dated 03-05-89 used for computation of seismic source parameters	168

6.26	Displacement Spectra of P-wav for seismic event dated 04-05-89 used for computation of seismic source parameters	169
6.27	Master curves used to mark $f_0$ and $\Omega_0$	170
6.28	Linear regression curve of seismic moment ( $m_0$ ) with magnitude ( $M_L$ ) on semi-log scale	174
6.29	Linear regression curve of stress drop ( $\Delta\sigma$ ) with magnitude ( $M_L$ ) on semi-log scale	174
6.30	Linear regression curve of source dimension ( $r$ ) with magnitude ( $M_L$ ) on semi-log scale	175
6.31	Linear regression curve of slip ( $u$ ) with magnitude ( $M_L$ ) on semi-log scale	175
6.32	Linear regression curve of energy ( $E$ ) with magnitude ( $M_L$ ) on semi-log scale	176



## LIST OF TABLES

TABLE NO.	CAPTION	PAGE NO.
2.1	DESCRIPTION OF THE OUTSTATIONS	26
3.1	RANGE AND SELECTED VALUES OF TRIGGER PARAMETERS	58
4.1	COEFFICIENTS FOR DIFFERENT TYPES OF FIRST ORDER DIGITAL FILTERS ( $0 < \alpha < 1$ )	79
6.1	RESULTS OF VISUAL ANALYSIS OF TRIGGERED EVENTS RECORDED BY TDSA. ONLY THE SEISMIC EVENTS ARE TABULATED	125
6.2	RESULTS OF AUTOMATIC ANALYSIS OF TRIGGERED EVENTS RECORDED BY TDSA. '*' SHOWS THE CODA LENGTH IS TAKEN TO BE THE END OF THE RECORD.	131
6.3	COMPARISON OF THE P-ONSET TIMES (VISUAL - AUTOMATIC) AS OBTAINED FROM VISUAL AND AUTOMATIC ANALYSES	138
6.4	COMPARISON OF THE RESULTS OF APP WITH TWO OTHER ALGORITHMS AT VARIOUS STAGES TO CONFIRM THE TIME SERIES AS SEISMIC EVENT.	141
6.5	HYPOCENTRAL PARAMETERS OF THE EVENTS AS COMPUTED FROM RESULTS OBTAINED BY VISUAL ANALYSIS (V) AND AUTOMATIC ANALYSIS (A).	142
6.6	SOURCE PARAMETERS OF THE SEISMIC EVENTS	173
6.7	'a' AND 'b' VALUES COMPUTED FOR SEISMIC MOMENT-MAGNITUDE RELATIONSHIP ' $(\log m_0 = a + b$ $M_L)$ FOR DIFFERENT AREAS BY VARIOUS AUTHORS.	177

# CHAPTER # 1

## INTRODUCTION

---

## INTRODUCTION

---

### 1.1 PREAMBLE

The pursuit for knowledge has led human kind to propound new hypotheses and theories in the hope that they would prove significant in understanding the various fundamental processes of the nature. The developments of modern science began as a result of thinking and observations and the discoveries made in this way have contributed to the progress of the present civilization. The developments in basic sciences ultimately helped reveal the facts regarding the interior as well as the exterior of the earth. It is noteworthy that progress made in understanding the earth's interior using seismology has a history no longer than about one and a half century.

Seismology has played a crucial role in understanding the structure of the earth as well as the earthquake sources which release large amount of energy inside the earth. Earthquakes occur

over a continuous energy spectrum, ranging from large magnitude earthquakes, which are rare, to microearthquakes which have relatively small magnitudes ( $\leq 3$ ) but high frequency of occurrence. Introduction of the earthquake magnitude scale by C.F. Richter in 1935, and its relation with earthquake frequency by B. Gutenberg and C.F. Richter in 1941 provided a thrust in observational seismology and also lead to greater realization of importance of microearthquake studies (79,42). Implementation of seismic station network for monitoring of microearthquakes in many countries was made possible in 1960's by technological advances in instrumentation, data transmission, and data processing.

The objectives of monitoring earthquake activity in an area including earthquakes of small magnitudes by installation and operation of seismic station networks, is to obtain information which assists in determination of crustal structure, identification of geological structures as tectonic elements capable of generating major earthquakes, patterns of spatial and temporal changes in earthquake occurrence and establishing association of earthquake activity with tectonic and geological processes operative in the earth's crust and upper mantle. This information is also useful in the demarcation of earthquake source zones in areas around critical engineering project sites. Such networks are designed to record as many earthquakes as nature and instruments permit. For seismic networks in areas of relatively low seismicity, data processing do not pose any major problem. But

for networks in areas of high seismicity, or for large aperture networks the voluminous seismic data, if not available in digital mode, requires considerable efforts and time for analysis. A seismic station network generating data in digital mode produces larger amount of data compared to traditional seismological observatory providing analog records of ground motion. Though the general aspects of the data processing procedures do not differ greatly between these two types of operations, the data in digital mode obtained from a seismic station network can be processed at a much faster rate with higher resolution using modern data processing techniques and offers opportunities for a wide class of studies.

The conventional microearthquake recording instruments produce analog recordings on films or papers (photographic/heat sensitive/ ink writing). The most direct method of seismic event detection in this case is simply to examine the paper or film seismogram taken at various stations. However, analysis of large number of seismograms is a time consuming task. In case of networks of microearthquake recorders deployed for short duration, it is common to use a few drum recorders for event detection and/or portable tape recorders to collect seismic data for event processing. If a trigger algorithm is adopted for event recording, then continuous seismograms obtained from the drum recorders can be used to verify that the trigger system is functioning properly. In some applications temporary networks have also used multichannel tape recorders at a centralized site with

common time base (60). Generally, the data is recorded in analog form in such networks and processing is done manually by measuring the times of seismic arrivals, their amplitudes and the coda lengths. The manual method has the advantage that it is straightforward. In analog recording the dynamic range and the resolution of the data recorded depend on the transducer (i.e., seismometer in most of the cases) and the recorder and is found to be generally low. Another disadvantage is that only a small part of information contained in the analog signals can be extracted.

The advancement in technology have made it possible to record the seismic data in digital form. The seismic station networks with the help of digital computers are able to record the data at one centralized site by telemetering the data from many seismometer out stations (1,18,19,26,39,61,63,64,65). Such type of networks take care of most of the limitations of the conventional recording. Since earthquake signals constitute only a small part of the continuous recording, triggered event recording techniques have been used in telemetered digital seismic networks to monitor events above a desired magnitude. Until digital electronic components became widely available, event detection techniques were based on analog technology and were not satisfactory (60). As seismic signals are now being recorded in digital mode, various algorithms have been developed in the past decade which allow an automated event detection even on real time systems.

The automated event detection techniques make use of the amplitudes and the frequency contents of the incoming signal for

seismic analysis and discrimination (5,6,12,16,18,63,94,95). Much effort in computer aided seismic analysis and discrimination has been devoted to the development of the mathematical algorithms. A major task in this regard is the selection of the seismic event based on the mathematical algorithms and their recording on the magnetic media.

To detect seismic events in the incoming time series, one must exploit their signal characteristics. The background noise typically have a low amplitude and because of the instrumental noise and cultural activities, transient signals over a broad range of amplitudes and periods are often present. Briefly, the incoming signals from a local network can have a wide range of amplitudes, but local earthquakes are characterized, generally, by their impulsive onsets, high frequency content, exponential envelope and decreasing signal frequency with time.

Triggered event recording involves two automated tasks. The first is to detect an earthquake event and to initiate recording. The second task is to determine when to stop recording and return to the detection mode. In addition, a delay time memory is required so that at least a few seconds of the signal before and after the earthquake is recorded. Recording directly on computer compatible magnetic media is preferred so that further data processing can be carried out on the computers.

On-line processing of the incoming signals from a local network is required if real-time earthquake location is desired



for earthquake prediction purposes. Most of the networks make use of off-line processing of the data after recording the time series of the seismic event. Event processing is being done for measuring some basic parameters from the recorded seismic traces that describe the earthquake ground motion. These parameters are generally known as phase data and include (i) the onset times and the direction of the first P-arrival, (ii) the onset time of the later arrivals, such as S-arrival(if possible), (iii) the maximum trace amplitude and its associated period and, (iv) the signal duration of the earthquake. Precise measurement of the phase data is essential because they are used to compute the origin time, hypocenter and magnitude of the earthquake and deduce its focal mechanism. In the automated method, digitized seismic data are first acquired and phase data is determined by some algorithm. The hypocentral parameters, fault plane solution, magnitude etc. are then computed.

The present study was initiated on deployment of a Short Aperture Sample Telemetered Digital Seismic Array in Garhwal Himalaya as part of the 'All India Coordinated Project on Himalaya Seismicity and Seismotectonics' funded by Department of Science and Technology, Govt of India. Since the software for decoding of the recorded data was not available, the first task was to read the data tapes recorded on PDP 11/23 computer based data acquisition system on to the available DEC 2050 system for the post processing of the data. The software package TMD has been developed for this purpose under this study. Since this was the

first array deployed in this area using event detection technique, the next big task was to acquire useful data by the system by selecting the trigger parameters for the array. This was done by studying the geology and tectonics of the region, the seismicity and the expected hypocenters in the region. The data acquired from 13-02-89 to 7-05-89 is used for the present study. The necessary software package for the post processing of the recorded data on the PCs are developed and the processing is carried out in two steps : (i) the visual interactive analysis of the recorded data on the screen of the PC and, (ii) the automatic procedure developed for the selection of the seismic events and the computation of the phase parameters.

## 1.2 RELEVANCE OF THE STUDY

Evaluation of earthquake hazards and consequent risks at a site requires information on earthquake occurrence. The data on earthquake occurrence consists of earthquake parameters in terms of origin time, location, depth and size of the event. The pattern and geological distribution on earthquake occurrence in relation to a specific site or an area provide the basic data for the analysis to evaluate the earthquake hazards.

The smaller the magnitude of earthquake one can record, the greater the amount of data one can collect. Microearthquakes may provide in a comparatively short time, seismological information about a region that would otherwise require years and decades if only data from large magnitude earthquakes were used.

Location of earthquake source in terms of their geographical coordinates and depth is obtained by installation and careful operation of seismic networks.

A short aperture sample telemetered digital seismic array with dedicated data acquisition system was installed in the Garhwal Himalaya to acquire data on earthquake occurrence to provide requisite information to understand the ongoing physical processes in the region. Being the first array of its type in India, developments of algorithms and methods and techniques of data processing were taken up for the acquisition of the requisite data on the earthquake occurrence and its post processing in optimal way on the PCs to produce useful results.

Different techniques for the event detection and phase picking algorithms have been examined critically (5,12,95). A Phase picker has been developed for the automation of the processing for the quasi on-line/real time systems. To demonstrate the developed algorithms the data acquired by the system from 13-02-89 to 7-05-89 is used to determine the phase data of the seismic events. Further, using the results, the hypocentral parameters, magnitude of the events, the composite fault plane solution and the source parameters are computed. Linear regression analysis has been carried out and relationships between magnitude and different source parameters are determined. The parameters computed are interpreted in terms of geological and tectonic environment of the region.

### 1.3 PLAN OF THE WORK

Microearthquake studies are an important component of seismological research. Microearthquake station networks, by probing into seismically active areas, are powerful tools in studying the nature and state of physical processes related with earthquake occurrences. The problem of acquisition of digital data by telemetered sample seismic array in Garhwal Himalaya and its processing aspects are studied in the present work.

In Chapter 2, the underlying principles of telemetered digital seismic arrays and important digital data acquisition systems are reviewed. Further, the main features of the short aperture digital telemetered sample seismic array deployed in Garhwal Himalaya and the software used for data acquisition are described in addition to a brief overview of the Himalaya. The present knowledge about the seismicity of the region under study and the selection of various trigger parameters for TDSA to monitor seismic activity are discussed in Chapter 3.

Chapter 4 contains the details of the software packages developed for data archiving and the procedures for visual analysis of the recorded data. In Chapter 5, the automatic phase picker algorithms in time and frequency domains are reviewed, and the details of the algorithm used for the phase picker developed under this study are given.

Chapter 6 contains the results of the visual analysis and automatic analysis of the recorded triggered events, and the computation of the hypocentral parameters, magnitude, composite fault plane solution and the source parameters. A brief discussion following the results obtained is also given. The conclusions of the study and suggestions for further work are given in Chapter 7.

Appendix I contains the listing of the computer program TMD and APP. Appendix II contains the magnetic tape format used in the PDP 11/23 based DAS.

## CHAPTER # 2

### THE TELEMETERED DIGITAL SEISMIC ARRAY IN THE GARHWAL HIMALAYA

---

**THE TELEMETERED DIGITAL SEISMIC ARRAY IN THE GARHWAL HIMALAYA**

---

**2.1 INTRODUCTION**

Earthquakes are responsible for damage to property and often loss of life. The evaluation of earthquake hazards and consequent risks and the safety of structures during earthquakes requires comprehensive information about earthquake occurrence. The data on earthquake occurrence should consists of earthquake parameters in terms of time, location, depth , size and type of the event. The pattern and geographical distribution of earthquakes in relation to a specific site in an area provide the basic data for the analysis to evaluate the earthquake hazard.

Location of earthquake source in terms of their geographical coordinates and depth is obtained by installation and careful operation of seismograph networks. The objective of monitoring earthquake activity in an area including earthquakes of small size (microearthquakes having magnitude  $\leq 3$ ) is to obtain



information which assists in the identification of geological structures as tectonic elements capable of generating major earthquakes, determination of crustal structure, spatial and temporal features in earthquake occurrence and establishing association of earthquake activity with tectonic and geological processes operative in the Earth's crust and upper mantle. Such an information also assists in evaluation of earthquake risk in areas around critical engineering project sites.

Surveillance of earthquake activity is a prime requisite for seismological investigations and research. To accomplish this, appropriate instrumentation which could record and provide data in a standard format must be used. Information on earthquakes in a region can be acquired through the installation and careful operation of seismograph networks. Conventional instrumentation for micrbeearthquake surveys recording earthquake waves at individual transducer stations is not only cumbersome in operation and its routine maintenance but also introduces appreciable errors in absolute times of recorded phases. Therefore, it is highly desirable to have seismograph networks in which the seismic signal from several seismometer stations are transmitted to a central recording station via cables/telephone lines/radios for simultaneous recording with a common time reference.

## 2.2 EARTHQUAKE STATION NETWORKS

Earthquake station networks can be categorized as world wide networks, regional/national networks, and local networks. We know that the smaller the magnitude of earthquakes one can record, the greater the amount of data one can collect. Micro earthquake networks are designed to record vast amount of earthquake occurrence data as shown by frequency magnitude relationship (42). The conventional seismographs installed in world wide and regional/national networks are not designed to record microearthquake activity at short distances. Monitoring of local seismic activity enables better delineation of active faults, depth of activity and type of dislocation occurring along them. Regional/national networks supplement information on events in the far field.

### 2.2.1 Why Telemetered Array of Seismic Stations ?

Location of an earthquake event depends on several factors including the accuracy in the arrival times of P- and S-phases. Conventional microearthquake recording station networks with independent time references at individual stations, in general, provide inaccurate estimates of arrival times of P- and S-phases, thus limiting the reliability and accuracy of the location of events. Due to appreciable errors in time correlations at individual stations and subjective interpretation of arrival times, the accuracy of hypocentral coordinates is severely

restricted. The telemetered array linking the seismometer outstations to a central recording site takes care of most of the limitations of the conventional recording. The biggest advantage of the telemetered network is the central recording of the data with a common time base. Once the data is recorded from many stations at a central recording site, real time processing of the data becomes possible. Another advantage of such type of arrays is the triggered event recording which can conveniently reduce the volume of data to be stored for further processing. The four main advantages of the telemetered seismic networks can be summarized as:

1. Central recording linking remote seismometer stations.
2. Data acquisition with common time base.
3. Real time data processing feasible.
4. Facility of triggered event recording.

### 2.2.2 Why Digital Telemetered Array of Seismic Stations ?

The advantages of the digital data over the analog data in seismology are well known. Due to the advancement in digital technology it is possible now to record the seismic data in digital form. The biggest advantage is that of larger dynamic range available. Low level activity close to the network is often not picked up due to low dynamic range of the system. On the other hand, in case of large earthquakes analog records show clipping of amplitudes of the recorded data. The digital data recording has

higher dynamic range and provides better resolution. The data recorded by digital arrays is not affected by system noise and component drift. Signal quality in this case is not influenced by spurious environmental disturbances. As the software packages are available, or may be developed for data processing, on-line data processing of signal is possible in case of digital telemetered arrays. The processing can be directly done in frequency domain which is the choice of most of the scientists for post processing, due to its advantages on time-domain processing.

### 2.2.3 Digital Telemetered Arrays - A Review

Small earthquakes occur more frequently as compared to major events and the small events supplement the scarce instrumentally observed data on earthquake occurrence. Thus, in terms of historical development all over the world to obtain information on seismicity, microearthquake station networks were evolved from regional/national networks, initially through deployment of mobile/temporary networks to study aftershocks in the region affected by major earthquakes and subsequently as a practice for reconnaissance surveys and monitoring of earthquake activity for short duration. Presently, microearthquake networks are also deployed as permanent array of telemetered seismic stations with common time base. The methodology and techniques to study microearthquakes by such networks developed more or less independently by various groups in several countries notably in U.S.A., Japan and South Africa.

For accurate location of tremors connected with mining activity, Gane et al., 1949 described a 6-station radio telemetry seismic network that they designed and applied in South Africa (36). At the central recording site a multichannel photographic recorder with an automatic trigger was deployed to start recording when an earthquake was sensed. A 6-second magnetic tape loop delay line to preserve the initial P-onset was used.

In Japan, detailed study of microearthquake in Kii Peninsula, Central Japan, using temporary array of short period instruments and radio-telemetry seismograph systems was carried out by Miyamura and his colleagues in the 1950's and early 1960's (65). Timing accuracy was stressed in order to obtain precise location for microearthquakes. Miyamura et al., 1966 also used triggered magnetic tape recorders with a small 4 station array in Gifu Prefecture, Central Japan (65). An endless tape loop with a 20 second delay time allowed recording of the initial P-onsets. An automatic gain control was used to allow better recording of the S-phases.

In U.S.A. in 1950's, J.P. Eaton developed a telemetered seismograph system for the Hawaii seismic network (60). In 1961-63, Don Tocher upgraded the seismographic station at the University of California by telemetering seismic signals from individual station via telephone lines to a central recording site at Berkeley. Michael et. al., 1982, described the real time

seismic event detection and recording system for MIT seismic network (64). A regional telemetry network of digital seismographs, the Berkeley Digital Seismograph Network, is being installed in central California to upgrade the permanent seismographic stations of the University of California (18). Presently, about 40 permanent telemetered networks are operating in the United States. Recently, some of the systems like GEOS - General Earthquake Observation System (19) ; SNARE - an earthquake detection and recording system (39) ; Short period microearthquake recording system (1) ; PANDA - Portable Seismic array for local to regional scale seismic experiments (26) are also being reported. A list of such type of arrays deployed through out the world is given by Lee and Stewart, 1981.

Commercially available personal computers have now made digital seismic recording relatively inexpensive. Although the scientific advantages of digital recording of earthquakes outweigh the disadvantages(75), practical obstacles such as high costs and availability of appropriate software and storage devices, have inhibited adoption of digital ground motion acquisition (18).

In India, the first cable linked telemetered network was installed at Gauribidanur by Department of Atomic Energy to monitor nuclear explosions (90). Another cable linked telemetered array has also been installed for short duration in Kolar gold fields to study mining induced seismic activity (55). An indigenously built eleven stations wireless telemetered seismic

network was commissioned at Bhatsanagar in early 1988 to study the reservoir induced seismicity (56). A digital telemetered array is being installed in north east India around Jorhat (91). The first radio-linked digital telemetered array has been installed in the Garhwal Himalaya to monitor local earthquakes by Department of Earthquake Engineering , University of Roorkee.

## 2.3 SHORT APERTURE SAMPLE TELEMETERED DIGITAL SEISMIC ARRAY IN THE GARHWAL HIMALAYA

### 2.3.1 The Himalaya

The Himalaya occupies the northern part of the Indian subcontinent forming about 400 km wide arcuate bend which is convex to the SSW and runs unbroken for 2400 km between the mountain peaks of Nanga Parbat in the west and Namcha Barwa in the East, each of these peaks being located where the trend of the mountains changes abruptly. The detailed description of the geology and the tectonics of the Himalaya region may be found in the works of Wadia, 1953 ; Gansser, 1964 ; Le Fort, 1975 ; Fuchs, 1975 ; Valdiya, 1981 ; Windley, 1983 and Scarle et al., 1987.

The Himalaya is bounded by Indo-Gangetic plains towards south and the Trans Himalaya ranges towards north. The actual northern limit of the Himalaya may be taken as more or less continuous depression running parallel to the Himalaya trend and containing the valleys in which lie the upper reaches of the Indus

and the Tsangpo ( named Bhramputra further downstream in Assam). This depression is also called the Indus-Tsangpo zone. Within the Himalaya, the mountain ranges are arranged in various linear belts ; the Trans Himalaya belt, main central crystalline belt which is also called the Great or Higher Himalaya and comprises of high mountain peaks, 30 of which, including Mount Everest, have elevations in excess of 7300 m, the Lesser Himalaya which comprises mostly of the mountains with elevations upto 4500 m and the southern most outer Tertiary Foot Hill belt with elevations upto 1300 m. The boundaries between the various belts are marked by thrusts. The Great and the lesser Himalaya have also been dissected by transverse deep valleys carrying drainage.

The Indus-Tsangpo Suture zone is the northern boundary of the Tethys Himalaya beyond which lies the Trans Himalaya. It consists of the Paleozoic and younger beds intruded by the Cretaceous to Paleocene Calc-alkaline batholiths. This zone has long been recognized as a major crustal suture separating the Indian plate to the south from Lhasa and Xang Tang blocks in Tibet to the north.

The Higher Himalaya contains a basement of Precambrian rocks overlain by a sequence of the Tethyan sediments ranging in age from Cambrian to Eocene. The thrust slices showing high grade metamorphism are called the central crystallines. Unlike the Lesser Himalaya, fossils are present in this region in the sedimentary formations, Ophiolite nappes were thrust southwards on



to the Higher Himalaya from the Indus-Tsangpo Suture in early Eocene.

The Lesser Himalaya consists of the sediments of the Precambrian-Paleozoic and locally Mesozoic age metamorphosed and subdivided by thrusts with progressively older rocks towards the north. No fossils are present in this belt. The Lesser Himalaya has been thrust southwards over the Siwaliks of the Sub-Himalaya along the Main Boundary Thrust (MBT). The northern boundary of the Lesser Himalaya is defined by the Main Central Thrust (MCT) which separates it from the Higher Himalaya.

The Sub-Himalaya consists of the mid Miocene-Pliocene Siwalik mollase sediments which have been folded and faulted. The intensity of the deformation increases northward towards the MBT which demarcates the boundary of the Sub-Himalaya zone in the north. This zone is separated from the Ganga foredeep to the south of Himalaya frontal zone. The Ganga foredeep is composed of the alluvium, the Siwalik and the pre-Siwalik sediments overlying the rocks of the Indian shield.

The Himalaya is seismically very active. The spatial and temporal distribution of earthquakes in a region is called the seismicity of that region. The epicenters of the moderate magnitude earthquakes lie mostly between the MBT and the MCT. The seismicity of the Himalaya is not well constrained although major trend has been recognized (70). The occurrence of earthquakes is

confined to crustal depths of about 20 km (70). Different models have been postulated for the orogeny of the Himalaya. There are basic two types of explanations given by different authors - first is the plate tectonic model and second is the deep seated faults having relations to the Mantle.

Since 1973, increasing amounts of data on the Himalaya and Tibet have become available and, consequently, many plate tectonic models have been proposed for evolution of the Himalaya (e.g., Le Fort, 1975 ; Molnar et al., 1977; Bird, 1978 ; Seeber et al., 1981 ; Chen and Molnar, 1981 ; Barazangi and Ni, 1982, ; Molnar and Chen, 1983 ; Ni and Barazangi, 1984 and Molnar, 1984). Among these models, much of the debate of the tectonics of the Himalaya is concerned with the nature of MBT and MCT. According to Le Fort, 1975, the Himalaya was formed by imbrication of slices of India's northern margin assuming MBT and MCT to be similar, but successive tectonic thrusts (58). The southern thrust zone i.e., MBT becomes new boundary of the continental convergent zone, while the older thrust zone i.e., MCT becomes a less active dormant feature. On the other hand, Seeber and Armbruster, 1981 proposed a steady state model for the evolution of the Himalaya (83). This model requires that the MBT and MCT are contemporaneous features. Central to his model is a detachment surface underlying the entire Himalaya. The detachment represents the upper surface of the under thrusting Indian plate. Seeber et al., 1981 postulated the presence of a Basement Thrust (BT) where the northerly and relatively steeply dipping MCT merges with the shallow dipping

detachment surface at depth (84). The BT zone represents the front of the overriding crystalline basement and it is along this front where the sedimentary rocks above the Indian shield are scraped off.

Pande, 1991 suggest close relation between the phased orogenic movements and the metamorphic episode that took place synchronously with the phased evolutionary history of the Himalaya orogen (73). The metamorphites are mainly restricted to the ' Main Central Crystalline Axial Belt ' of the Himalaya and display high grade to low grade metamorphites. The ' Inner sub zone ' (73) of the Lesser Himalaya Belt shows only low grade metamorphism of chlorite grade. In contrast, the rocks of the Trans Himalaya Belt, 'Outer sub zone' of the Lesser Himalaya Belt are characterized by unmetamorphosed ones. These tectonic belts are separated from one another by the deep seated faults ( Mantle Faults). Each of these tectonic belts is further characterized by contrasted geology ; litho stratigraphy, texture, structure, tectonics and metamorphism as a result of their phased evolution.

The tectonic model suggested to explain the contemporary seismicity in the Himalaya belt are based on the analysis of data on earthquake occurrence specially, depth of foci and source mechanisms. The development of MCT, MBT etc. is a result of continued convergence of the Indian plate after collision along the Indus-Tsanpo Suture zone in the plate tectonics hypothesis or result of phased upheaval of the Himalaya orogen resulting in

activation of the faults forming the tectonostratigraphic belts consisting of Main Central Himalaya belt, Trans Himalaya belt, Lesser Himalaya belt and the outer Tertiary Foot Hill belt. Precise location of seismic events and the source parameter computations are considered necessary to have desired data to work out the tectonic models in various parts of the Himalaya. With this objective a digital telemetered seismic array is deployed in the Garhwal Himalaya.

### 2.3.2 The Array

A Short Aperture Sample Telemetered Digital Seismic Array has been deployed in Ganga Yamuna Valley (in short TDSA; Telemetered digital seismic Array), with five single component (vertical) seismometer stations at Chakrata (CHK), Dhargaon (DHR), Pauri (POR), Roorkee (RRK) and Surkanda Devi (SUR), and two 3-component at Uttarkashi (UTK) and Narandra Nagar (NNR) and central recording station (CRS) installed at Kaddukhal (Fig 2.1). The central receiving station has been set up at a ridge (Surkanda Devi) and is connected to CRS which is located on the down slope of the hill, by a 32 core telephone cable of about 800 meters in length. The signal in the form of digital time history of ground motion from individual remote seismometer stations are transmitted via radio link to the CRS.

The outstations were selected on the basis of the line-of-sight and background noise conditions to cover the Lesser

Himalaya belt in Tehri Garhwal region. The central receiving station was first chosen at the hill top of Surkanda Devi which form a prominent hill range with altitude of 3030 m in this part of the Himalaya. Then the seismometer stations were marked on the toposheets for carrying out the line-of-sight. The seismometer sites were inspected for the lowest background noise level by doing the background noise survey at the tentative sites. Final selection of the sites were made based on line-of-sight and the background noise survey (102). The line-of-sight conditions were assessed for the array taking into account the topography, heights of the antennas and Earth's curvature following the procedures as given by Stebbings, 1982. The selection of the seismometer outstations and the CRS for this array has been described elsewhere by Sharma and Wason, 1989. The altitudes of the selected seismometer stations are 3030, 2500, 1700, 1800, 2200, 1400, and 270 m at SUR, CHK, UTK, DHR, POR, NNR and RRK, respectively. The latitudes longitudes and the rock types of the seismometer outstations are given in Table 2.1. According to Lee and Stewart, 1981 if the crustal structure is homogeneous, stations in a seismic network should be evenly distributed (60). In a region of area A, a network consisting of approximately  $A/D^2$  stations, where D is the station spacing, is required for good control on the determination of earthquake parameters. Certain constraints like background noise of individual stations, geology and tectonics of the area to be investigated and line-of-sight conditions with respect to the CRS will also affect the station distribution.

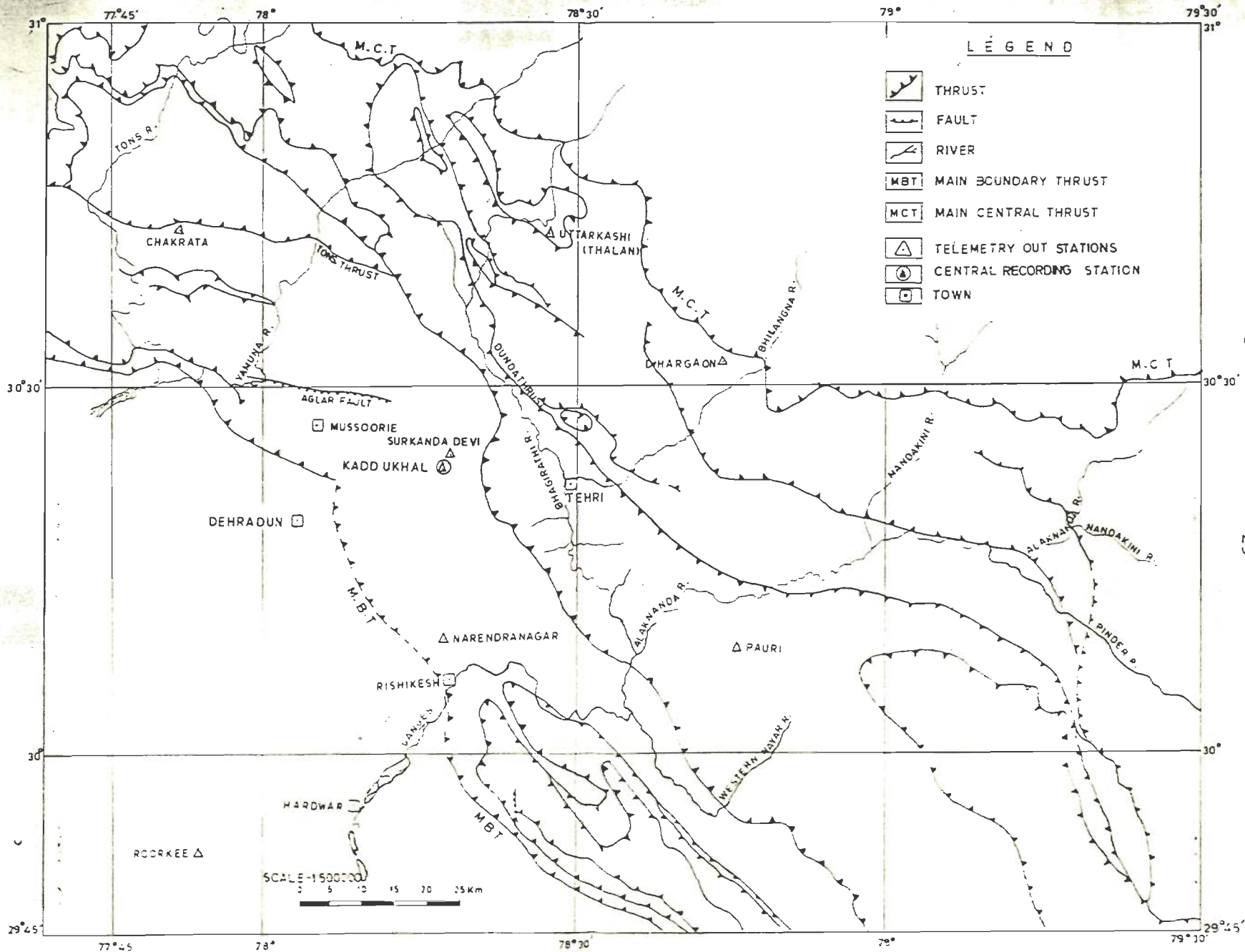


Fig. 2.1 - Tectonic map (Fuchs and Sinha, 1978) showing the locations of central recording station and outstations

TABLE 2.1 DESCRIPTION OF THE OUTSTATIONS

Sl. No.	Station Name	Latitude [N <sup>o</sup> ]	Longitude [E <sup>o</sup> ]	Height ( m )	Rock type
1.	NNR	30 10.06	78 17.38	1400	Quartzite [Padestral]
2.	POR	30 08.50	78 45.69	2200	Quartzite
3.	DHR	30 31.70	78 44.47	1800	Sandstone
4.	UTK	30 42.07	78 27.60	1700	Quartzite
5.	SUR	30 24.54	78 17.64	3030	Quartzite
6.	CHK	30 42.97	77 52.02	2500	Sandstone
7.	RRK	29 51.85	77 53.87	270	Alluvium [Padestral]

### 2.3.3 Description of the System

The principal components of a telemetered seismic station network can be categorized as: seismometer, signal conditioning device, signal transmission, recording media, common time base and power supply. The configuration of the radio link telemetered digital seismic array, TDSA, referred to in this study, is shown in the form of a block diagram in Fig 2.2. The transducer, a velocity sensor, is of short period ( $\sim 1$  sec) having a flat response in the frequency range DC-90 Hz, with a feed back damping. The feed back proportional to the ground velocity provides a marked reduction in instrumental noise and hence greater fidelity in measuring earthquake signals. The electrical signals in the frequency range DC-90 Hz at the outstations, are amplified and converted into a PCM bit stream through Auto Range Digital Modulator at a sampling rate of 360 samples/sec and then transmitted to the central receiving station through a high grade VHF transmitter with 2 watt RF output.

At the central receiving station there are as many receivers as the remote stations. The output from receivers is given as input to the multichannel line interface, which provides analog as well as parallel digital data for its recording on chart recorder or by a computer respectively. The digital output from each outstation is multiplexed into a computer digital interface by a control module which allows direct entry of digital data into Data Acquisition System (DAS). The DAS consists of a PDP



11/23 computer, a printer, a VDU, a Winchester disc drive and a computer compatible magnetic tape drive. Timing signals are then added to provide a common time base for all the seismometer stations from Omega face clock receiving signals from La Re Union transmitting station of the World Omega Standard Time. Through an event detection technique the event data is selected, formatted and stored on 1/2 inch nine track magnetic tapes.

The various units of the array consist of seismometer Mark III A, modulator, transmitter and antenna at each seismometer outstation and antenna, receiver, line interface unit (LIU), Winchester disc, magnetic tape drive, chart recorder, printer, VDU and clocks at the CRS. The basic Willmore adjustable period seismometer MK III manufactured by M/S Sensorics, U.K., is a velocity sensing device. The mass is a permanent magnet which is suspended on ligament springs giving frictionless axial movement by restraining it from movements in other planes. The output is derived from two coils fixed to the frame, one at each end of the mass. Auxiliary coils are provided for feed back and calibration. The natural period of oscillation of the mass is adjustable so that the instrument may be optimally matched to the required operation. The seismometer interfaces directly with the Auto Range Digital Modulator and this system includes feed back damping.

The Auto Range Digital Modulator samples the analog output from the seismometer at 360 Hz and each sample is converted into a digital bit stream using an ADC card. To achieve the

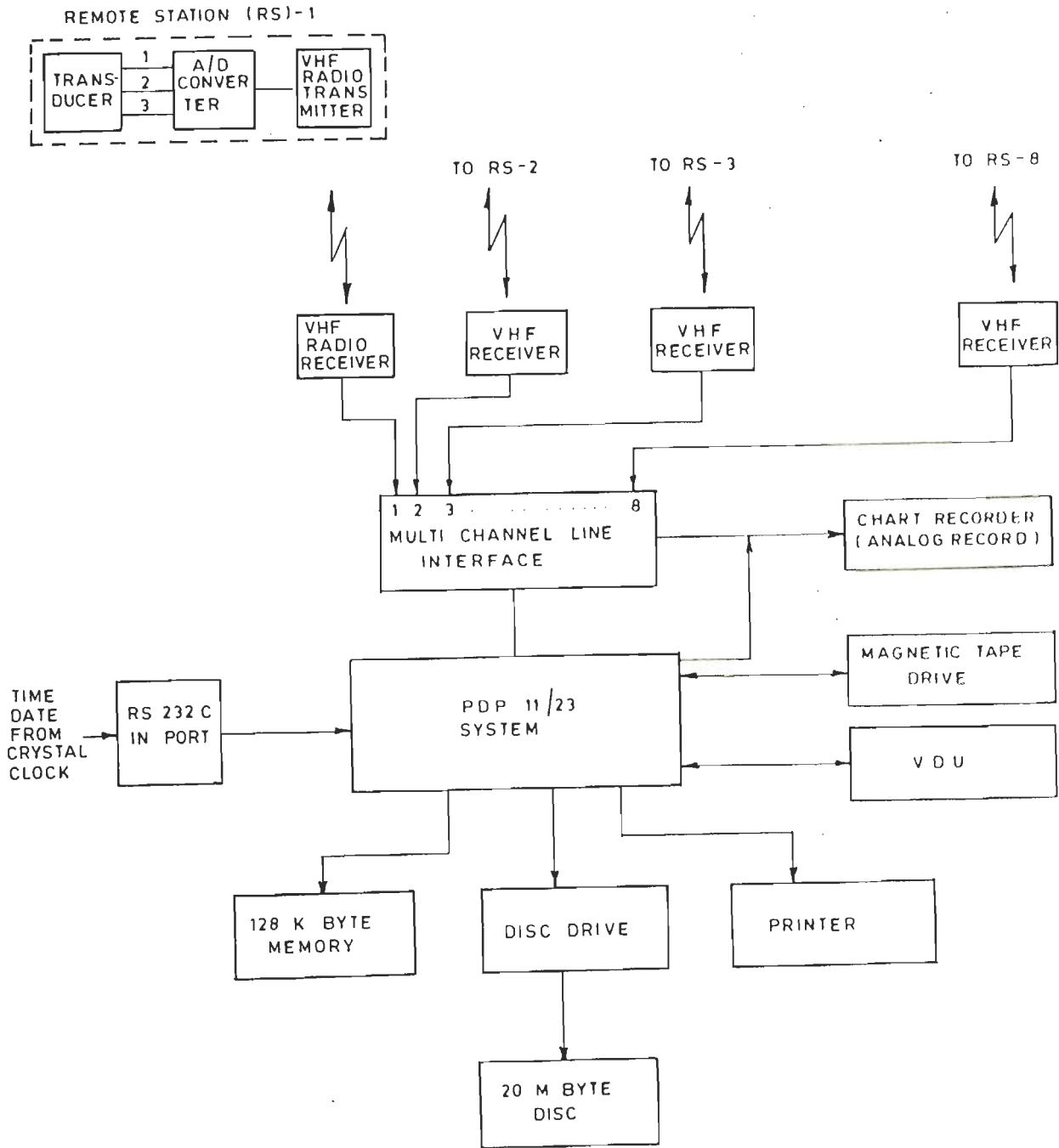


Fig. 2.2 - Block diagram of the configuration of the seismic telemetry system

dynamic range of 96 db ,the unit uses an auto range technique to produce 10 bit signal information and 2 bits of gain range , along with a parity bit. If the parity is not matched i.e, even parity in odd parity system or odd parity in even parity system, then the 16th bit of the word is set equal to one signifying the parity status of the word. Such 13 bit information is converted into PCM digital bit stream and is fed into the VHF transmitter.

Radio transmitter with 2 watt RF power transmits data from each seismometer outstation at 4800 bauds consisting of 4680 (13x360) bit of signal information and 120 synchronization bits, modulated over the allotted carrier frequency from the outstation to CRS. The outstations have a small current consumption of ~ 500 milliampere and the same is provided by a 12 volt battery trickle charged by a solar panel. The output of the transmitter is fed to an eight element Yagi Antenna and is received by the radio receivers at the central receiving station.

The output from the radio receivers is fed into the multichannel LIU. The LIU demodulates the incoming PCM bit stream and multiplexes it into 16 bit words incorporating 2 bits for component identification and 1 bit for synchronization between various channels (to differentiate between incoming data and invalid information) before transfer of data to the Winchester disc.

The VDU allows the operator to select the trigger parameters from a menu which control the operation of the trigger. In addition, the location of the site and its signal characteristics can be entered. This information will be recorded automatically on the tape when the system triggers.

Power requirements of the telemetry equipment at the central station is about 1800 watts average and 2000 watts peak. For the recording equipment power through A.C. mains is supplied. Data acquisition system has been described by Wason et al., 1986 and Sharma et al., 1987.

#### 2.3.4 Software for Data Acquisition

The software used for acquiring seismic data from the seismometer outstations consists of various programs in MACRO-11 and FORTRAN IV to be run in foreground and background. Data from the outstations is stored on the Winchester disc. The incoming data from the outstations through LIU is collected continuously and saved in a large file on the Winchester disc. This file is arranged in a circular manner so that the data may be saved continuously on the disc with the most recent data being saved, overwriting the oldest data, and the oldest data being discarded. Oldest data refers to saved outstation data that is typically 15-25 minutes old. The trigger algorithm for the DAS system uses the long term averaging and short term averaging technique operating individually on each of the selected

stations to determine if an event is to be recorded or discarded. The two running short and long term averages are computed for each station and their ratio when exceeds a prespecified value will put that station into a trigger mode. Such comparison is performed for each of the stations selected and whenever enough stations trigger within a specified time window, an event is deemed to have occurred and the system will then start saving event data. Whenever an event occurs, data from the trigger point of the event plus a predetermined amount of data before and after this time is recorded on to the magnetic tape for all the stations irrespective of the fact that a station has contributed to the trigger or not.

The software to control and transfer data from the trigger system uses the Digital Equipment real time Operating System RT11, which works as supervisor to the system, takes command from every component i.e., VDU, printer, chart recorder, magnetic tape drive etc. and hands it over to the modules. RT11 is used to load and control the data acquisition software and to provide file control facilities for utilities and data storage. The operating system is mapped on the highest memory available, then the SMS (Seismic Monitoring System) data acquisition system, SMS log file which is responsible for the hard copy on the line printer for the log of the events, and then vector area and hardware components towards low memory are mapped.

The application software for the system exists as a pair of self-contained modules each of which performs a specific function. The first is the main data acquisition module which collects data from the outstation and saves this data first on the Winchester disc and subsequently on to the magnetic tape. This module decides when to save data and when to discard it. The module saves the data whenever a predetermined number of stations exceed a specified level within a time window. This is deemed to be an event and data from the outstations will be recorded on to the magnetic tape. This module is called SMS.REL runs as high priority program, and is controlled by the system console VDU. The acquisition module operates in the foreground mode as a high priority module collecting data from the station inputs through LIU via receivers at the central station and directing this data to the main buffer on the Winchester disc. The second module receives event information from the acquisition module and controls the output of this information to the system printer. This module also controls output to the chart recorder when included. This module called SMSLOG.SAV operates as a low priority program and is controlled by the system keyboard/printer. The log module runs as a low priority background module and monitors the acquisition module for messages which are directed to the system printer.

#### 2.3.4.1 Station averaging

Long term and short term averaging of the incoming ground motion time histories data from each outstation are performed for two main reasons: firstly, to reduce acquisition of transient noise bursts upto desired level and secondly, to provide a method of monitoring data from the outstations in real time event recording. The system uses most recent data to maintain a running average of signal amplitudes for Long Term Averaging Period (LTAP) and Short Term Averaging Period (STAP). It is necessary to hold the values of the Short Term Average (STA) and Long Term Average (LTA) to which current data may be added to, and from which old and now redundant data may be removed. For this purpose a file is held on the Winchester disc for each of the long and short term averaging routines. These files are organized in circular buffer on the disc. The station data is collected at 360 sample/sec and a mechanism is provided to collect data at this rate and present it to the averaging routine at 10 Hz without losing the overall integrity of the incoming data. This is achieved by generating an interim sum consisting of 36 samples covering a 100 ms period in time. This interim value consists of a 32 bit (double word) unsigned integer and is the collective sum of the previous 36 samples. This double word value is saved in either the long or short term averaging file for subsequent use by the averaging routines. These interim sums are saved at 10 Hz for each of the stations and thus provides a running set of values that represent the sum of the data from

each station over a 100 ms period. Note that this sum is derived from each station data without regard to polarity.

#### 2.3.4.2 Event detection technique

The event detection technique uses the STA-LTA algorithm to detect the event in the incoming signals from the outstations. If the ratio STA/LTA exceeds the preset value at any instant of time then that particular station is said to be in the trigger mode otherwise the station is regarded as being in a normal or steady state. This comparison is performed every tenth of a second by adding in the latest 36 data samples and subtracting the oldest 36 data samples. This procedure is performed for each channel. When any station reaches a trigger state, the time window (TW) is started and if the number of trigger stations (NT) reaches the preselected value within the window then a system event trigger is flagged. The recording sequence is then initiated and the LTA value for each channel is held. The calculation continues using this LTA value and the updated STA value. When the signal amplitude has reduced in magnitude and the signals do not meet the set trigger criteria, data acquired on Winchester disc continues to be transferred to the magnetic tape from this program point until a period POSTEVP ( post event recording period) is completed and the system then automatically terminates the current data transfer and the LTA value is established. Fig 2.3 shows the parameters used in recording a triggered event. PREVP is the pre event period for which the data is recorded before the triggering



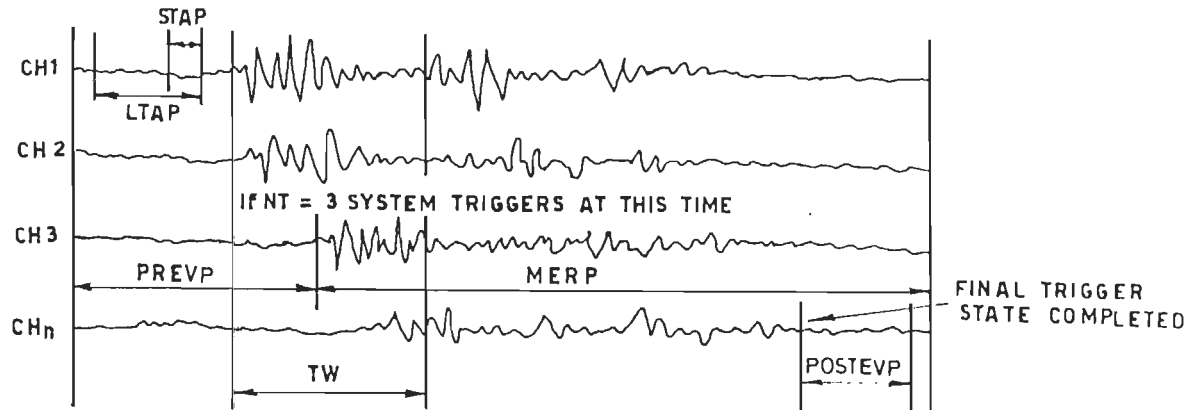


Fig.2.3 \_ Parameters for event Trigger and Recording

point of the first station. MERP is the maximum recording period after which the event recording is terminated.

#### 2.3.4.3 Saving event data on magnetic tapes

When the trigger criterion is met the data is saved in a separate area of the Winchester disc and is subsequently written to the magnetic tape and displayed on the chart recorder. In basic terms, data samples from the LIU are saved sequentially on a sample by sample basis. Each sample consists of one PDP word (two bytes). Each sample is made up of amplitude data, range bits, component identification bits, and error status. A sample from each station is taken at the acquisition frequency and stored on the tape in blocks. Each event is saved as a series of blocks on the magnetic tape and terminated with an end of file (EOF) mark. The date and time information of the first data sample of each block is written in the header section of the block. An event is saved on magnetic tape in three basic steps to provide a continuous data set covering a time interval spanning a period just before the event i.e., PREVP, the duration of the event and the period just after the event i.e., POSTEVP.

#### 2.3.4.4 Event data log

The event log is a log of individual station triggers caused by the increase in amplitudes arising due to some seismic activity or local noise. As a station exceeds its trigger level an entry is made in the event file which in turn is printed on

the system printer. The event log module also provides selection for the chart recorder replay. If parity bit is set in the signal information from an outstation channel the same is reported on the log after every hour. It should be noted that the post event time and the pre event time for the analog output of the event may be set different from that selected for the digital recording on magnetic tape. The times for the analog output are selected through the printer.

#### 2.3.4.5 Analog output of the event

The event data recorded on magnetic tapes by DAS can also be plotted on analog recorder side by side. The LIU is used to increase the signal voltage for proper analog recording of the signal on the chart recorder. In the 4 channel chart recorder on heat sensitive paper in TDSA, the time of the start of the event is also shown on the top of the trace in VELA uniform code. Each of the time or date nibbles is represented by a four bit cell containing a BCD value in the range of 00 to 99. A one or zero is represented by a different length code where 0.2 second represents 0, 0.5 seconds represents 1 and 0.8 second represents 59, 0 and 10 seconds markers. One minute code consists of the year, month, day, hour and last digit of the system banner. The plottings can be done on different speeds in the range from 5 mm/sec to 500 mm/min. The analog recording of the digital records of events acquired on magnetic tapes can also be replayed off-line. The program for this purpose is SMSR. But at

the time of off-line plotting in TDSA due to the system limitations, it will not acquire data from the outstations during such analog replay.

#### 2.3.4.6 PDP 11/23 data storage format

The PDP 11/23 based data acquisition system stores the selected events on the magnetic tapes at 1600 bpi. The word length is of 16 bits consisting of 2 bytes. The data is written in industrial compatible format. There is a header block written on to the magnetic tape containing the set up of the system when the tape was written followed by an end of file mark (EOF). Event data is then written on to magnetic tape in 4096 byte blocks. Events are separated by an EOF. The end of the last event is terminated with two EOF marks. EOF is a special non data block used to separate data fields.

The first block written on the magnetic tape in the configuration block of 4096 bytes contain the information about system parameters like STAP, LTAP, TR, TW, NT, PREVP, POSTEVP, MERP along with station parameters like latitude, longitude and trigger ratios etc. The end of configuration block is marked by EOF. Event data is recorded as a number of blocks terminated by EOF for each event. Each block has a 128 word (256 byte) preamble which contains time information for that particular block. The time code is inserted as the block is started so that the first data sample will correspond to the time encoded in the

data block. After this header, one word is stored for each station in turn upto the end of the block continuing onto the next block in sequence. The preamble contains the date written as BCD code, that is to say a 16 bit word will contain 4 decimal digits in the range 0-9. After 128 words one word data sample for each station is recorded. The station order of these samples are listed in the configuration block.

#### 2.3.4.7 Outstation data format

Station data is recorded on the magnetic tape in one word samples for each station in turn. A 13 bit sample containing the amplitude, sign, range and parity bits is transmitted at the rate of 4800 bits/sec to the CRS from each outstation. The other bits added by the LIU are component identification and the data not valid bit. Each of the outstations is acquiring data at 360 samples/sec and sending a continuous stream of digital data to the system. Now as each outstation is acquiring data independently, they will be running at slightly different frequencies dependent on their crystal tolerances. In effect each outstation will not be synchronized to each other or synchronized to the main system. To overcome this problem the system acquires data at a faster rate i.e., 362 samples/sec and records 2 samples per second approximately for which the data not valid bit (DNV) is set. The format of the 16-bit word recorded by DAS is given in Fig 2.4. ERR and DNV bits are for parity and data not valid. The CID (component identification) bits

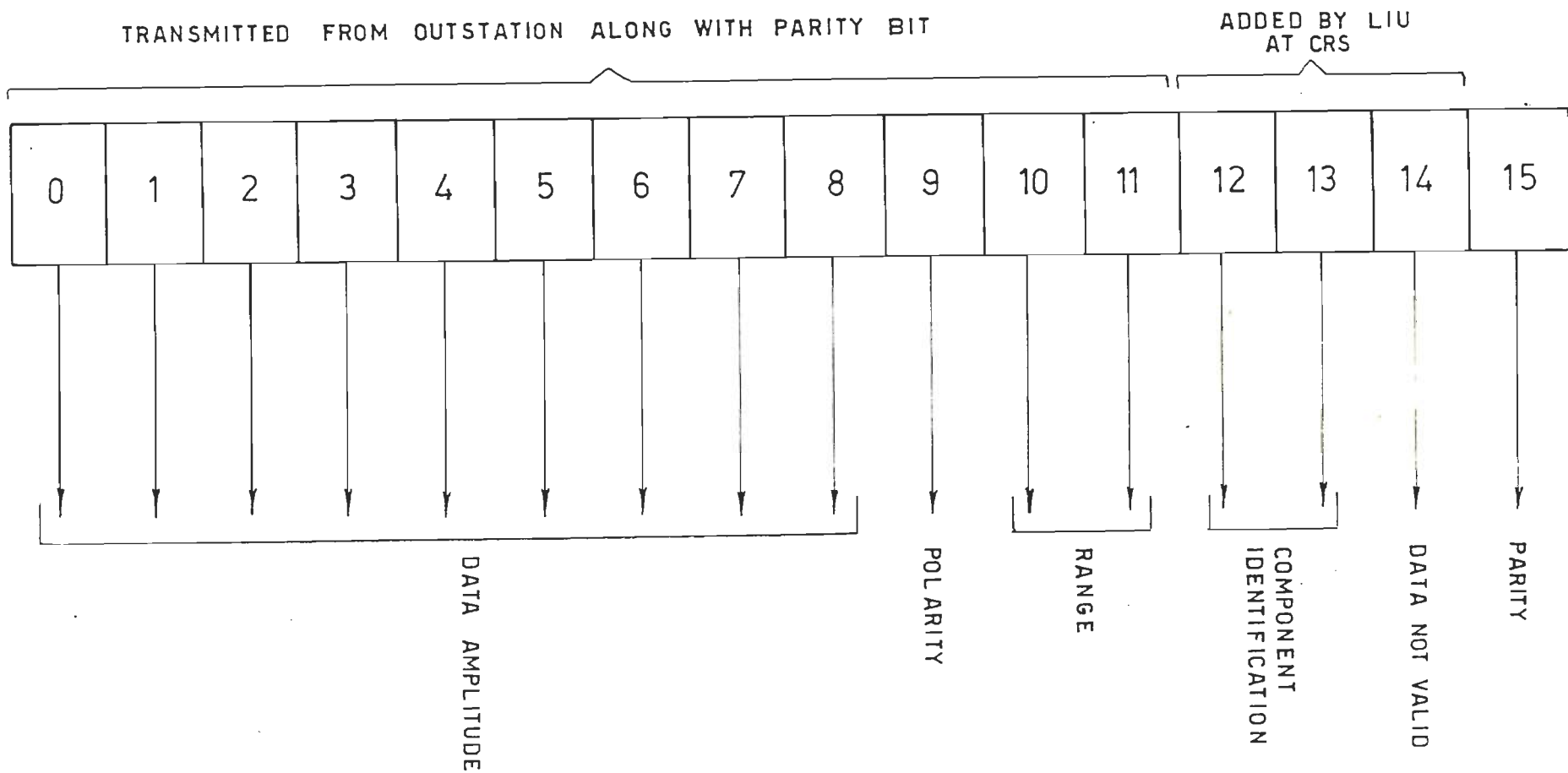


Fig. 2.4 - Bit structure of the 16 - Bit word recorded by Data Acquisition System

are for the component identification of the data recorded. The range bits are used to indicate the number of shifts to be applied to the data bits (0-8 bits) to obtain a 16 bit sample and give the channel a dynamic range of 96 dB. The polarity bit indicates the sign of the amplitude of the data. The least significant bit of this expanded word represents 10 micro volts giving an input range at the modulator input of  $\pm 327.68$  milli volts full scale.

## CHAPTER # 3

### DATA ACQUISITION AND PARAMETER SELECTION



---

## DATA ACQUISITION AND PARAMETER SELECTION

---

### 3.1 INTRODUCTION

TDSA is intended to record the local earthquakes using the event detection techniques as described in Chapter 2. The parameters viz, STAP, LTAP, TR, TW, NT and recording periods used in the trigger technique play an important role in event triggering and recording. The values of these parameters need to be selected for the area under investigation in order to acquire useful data on the local earthquake occurrence for (i) identifying active faults and earthquake precursors (ii) estimating earthquake risk, and (iii) studying the earthquake generating processes.

To acquire data on local earthquakes from an area through the event detection technique, the a priory knowledge of the type of source, the epicentral distances involved along with the depth of focus and frequency of occurrence of earthquakes is desired. The choice of LTAP, STAP and TR are governed by the

expected signal amplitudes in the ground motion time histories, the signal-to-noise ratio and the type of terrain in which the array is deployed. The terrain affects the quality of the data transmission due to line-of-sight conditions required for telemetry links and is an important factor in the selection of the parameters for the data acquisition. Similarly, TW is dependent on the station spacing which in turn is selected based on the geology and tectonics of the area. The recording periods i.e., PREVP, POSTEVP and MERP are related directly to the type of data to be recorded particularly the size of the earthquakes. PREVP depends on the amplitude data required to be recorded before the triggering point of the event at first station. In case of triggering due to S-arrival, the selection of PREVP depends on the epicentral distances to record the P-arrival. POSTEVP and MERP depends on the size of the earthquake to be recorded as these parameters would decide the termination point of recording of the time series. Therefore, a review of the present status of the knowledge with respect to seismicity, focal depth, velocity structure and focal mechanism of the Garhwal Himalaya region is presented in the following section.

### 3.2 PRESENT KNOWLEDGE ABOUT THE AREA

#### 3.2.1 Seismicity of the Area

Earthquake occurrence in the Himalaya has been portrayed by various investigators. A systematic study of the earthquake

occurrence was taken up along with the preparations of the Indian Standard recommendations for earthquake resistant design of structures (IS: 1893-1962) brought out in 1962 which incorporated a map showing epicenters of earthquakes in Himalaya and other parts of India and neighboring countries (46). For the Garhwal Himalaya, Agrawal and Kumar, 1982 on the basis of microearthquake recording done between 1974 to 1977 totaling up to 18 station months data from 5 locations reported that the activity varies from 1 to 4 events per day at various occupied sites, within the region around Tehri (2). The seismic activity was noted to be concentrated around 40 km North of Tehri and was interpreted by the authors related to Uttarkashi thrust. Very little activity had been found associated with Srinagar thrust. The MCT indicated sporadic activity and two clusters had been located along its length. MBT was found to be quiet during this period as no activity was picked up by these stations.

Gaur et al., 1985 analyzed records of 250 earthquakes from Garhwal-Kumaon region and concluded that earthquakes in the Himalaya occur in specific areas and belts (38). One such belt has been identified across the Yamuna river in this area. All but a few epicenter lie to the southwest of the surface trace of MCT in a zone with a width of 10-30 km.

Data recorded from three permanent observatories located at Narendranagar, Rudraparayang and Tehri during the period 1975-1984 exhibit a North-South clustering of the epicenters (3).

However, the pattern of earthquake occurrence shifts in the subsequent years revealing migratory character of the small size earthquakes. There are very few earthquake epicenters associated with MBT but a portion of MCT, near  $78.5^{\circ}\text{SE}$  and  $30.5^{\circ}\text{NW}$  is surrounded by a large number of earthquakes having magnitude between 1 and 3.

### 3.2.2 Focal Depths

In Garhwal Himalaya, the focal depths of microearthquakes as reported by many authors are generally less than 30 km. Focal depths estimated by Agrawal and Kumar, 1982 from data of 3 to 4 stations, show a range of 5 to 25 km (2). The evidences collected over the past 80 years from teleseismic and regional observations reveal that only shallow earthquakes occur in this part of the Himalaya. But the location accuracy for individual events is not good enough to assign them to specific geologic features. Gaur et al., 1985 after analysis of 250 earthquakes reported that most of the hypocenters located lie within an estimated depth of 10 km below the ground surface, the maximum estimated focal depth being about 32 km. However, focal depths exceeding 70 km in 20 cases have been reported (38). As none of the hypocenters located in this part using teleseismic data have been assigned depths in excess of 70 km., the cause of excessive depth estimates of locally recorded earthquakes must lie in the assumption of rather simple velocity model. Khattri, 1987 concluded from the microearthquake network data that the local

seismicity in Garhwal Himalaya is mostly confined to the upper 8 km of the crust (52). Agrawal et al., 1988 reported that most of the earthquakes in this region occur at depths less than 5 km. However, sometimes these depths are estimated to be as large as 80 km. The depth estimations based on three observation points are liable to be erroneous due to poor constraint over depth (3).

### 3.2.3 Velocity Structure

A number of authors have given seismic velocity models for the Himalaya region or its foot hills using the travel time curve method and data reported in seismological bulletins (49,97,100). Velocity values ranging from 5 to 6.2 km/sec for the P-wave in the upper crust have been obtained. Sarkar, 1983 estimated the compressional velocity in this part of the Himalaya as 5.41 km/sec, which is consistent with known values for metamorphic rocks which outcrop in the region (81). Chander et al., 1986 estimated P-wave velocity of 5.2 km/sec for upper crust in the vicinity of MCT as it lies well within the range of values for sedimentary and metamorphic rocks (41). The data used by Chander et al., 1986 consisted of the arrival times of P-waves recorded at five portable stations from nine earthquakes which occurred in the same region as considered by Sarkar, 1983. Agrawal et al., 1988 have used a velocity model in which P-wave velocity increases from 4.98 (surface) to 5.99 km/sec (at depth of 30 km) for Garhwal Himalaya region in which TDSA is deployed. For the present study, in the light of the above findings, the velocity

structure is taken to be 5.2 km/sec (upto 15 km) and 6.00 km/sec for the lower half space below 15 km (57).

### 3.2.4 Focal Mechanisms

Fitch, 1970 presented the focal mechanism solutions based on teleseismic and regional data for earthquakes in the Himalaya region (30). The results for the four earthquakes which occurred just east of Garhwal Himalaya considered by Fitch, 1970 supported the view that Indian lithospheric plate is under thrusting the Himalaya. Subsequently, many other investigators have presented such solutions for the Himalaya, but none of them referred particularly to the Garhwal Himalaya. Among earthquakes with available focal mechanism solutions, six occurring in the India Nepal border region east of the Garhwal Himalaya showed thrust faulting (14,70). Agrawal et al., 1988 reported the motion to be predominantly strike slip on both the nodal planes obtained from 38 earthquakes occurred in this region (3). The pattern of earthquake occurrence in 1984 supports strike slip dislocation in an East-West direction which is in line with the observations by Gaur et al., 1985.

Khattari et al., 1989 presented composite focal mechanism solution from 20 earthquakes. They have taken the NE dipping nodal plane with reverse fault motion as the fault plane (54). This is consistent with the view held by earlier workers (23,30) for earthquake to take the northerly dipping planes as the fault

plane. The composite solution indicating thrust faulting establishes that overall stress regime in the region is conducive to thrust or reverse fault earthquakes in the region occupied by TDSA.

### 3.3 SELECTION OF TRIGGER PARAMETERS FOR TDSA

The trigger criteria for the recording of the events based on the event detection technique is described in Chapter 2. The technique uses the STA/LTA ratio to detect change in the amplitude of the incoming time series of the ground motion within prescribed STAP over LTA expressing the background noise at any station. The parameters used for the acquisition of the data on the occurrence of local earthquakes in the region by TDSA are LTAP, STAP, NT, TR, TW, PREVP, POSTEVP and MERP (86,89). The following sub sections describe the selection of the values for these parameters for TDSA.

#### 3.3.1 Long Term Averaging Period

Long Term Averaging Period (LTAP) is the time duration over which a running average of amplitudes of the time series is taken to represent the background noise level of a particular station. The LTA is computed over the LTAP as given below :

$$LTA(i) = \frac{1}{T_L} \sum_{i=t-T_L}^t |x(i)| \quad (3.1)$$

where  $T_L$  is LTAP and  $i$  is the time index of the time series  $x(i)$ . LTA is the average over LTAP taken by averaging the preceding samples and  $t$  is the current time. Since LTAP is chosen usually much longer than the predominant period of the incoming signal, LTA represents the long term average of the signal level as detected by the seismometer (60). The minimum value of the period is selected to be the minimum time interval to represent the background noise level of the station. The selection of LTAP should take care of the transient noise bursts. The higher selection of the value is dependent on the memory and the computation power available with the system. Considering the seismicity of the area, as described in section 3.2.1, that another event has very low chances of occurrence within 60 sec of the previous event, the LTAP is selected to be 60 sec for TDSA.

### 3.3.2 Short Term Averaging Period

Similar to LTAP, Short Term Averaging Period (STAP) is the time interval over which the average of the amplitudes is taken to define the current signal amplitude. The STA is computed over this period as follows

$$STA(i) = \frac{1}{T_s} \sum_{i=t-T_s}^t |x(i)| \quad (3.2)$$



245711



where  $T_s$  is STAP. The STA is the representation of the current signal and it should reflect the changes in the signal at once. The selection of STAP depends on the background noise level of the particular station. STAP should be selected to take care of even a single pulse (wavelet) of the incoming signal. If the seismic signal is assumed to contain 30 Hz frequency, then the lowest choice of the STAP will be 0.033 sec. However, STAP should average out transient noise bursts and particularly single noise spikes due to environmental/electrical disturbances. But if during STAP of short duration such a spike is recorded then the STA will have very large value. To overcome this the selection of STAP is made on higher side to smooth out the single spike effects. As an example, the amplitude of the noise spikes is generally about 10,000 micro volts. Now, if the LTA is 10 micro volts at the station then one such noise spike will give STA of 842.5 for STAP of 0.033 sec at a sampling rate of 360 samples/sec. This will create confusion between the seismic arrival and the recording of the noise spike in the time series. Now, if STAP is considered to be 10 sec then the same spike will produce STA of 12.775 which is much lower than the previous value for STAP of 0.033 sec. The STAP value of 10 sec was adopted for TDSA after studying the of background noise level and seismic signal amplitudes along with the occurrence of noise spikes monitored during installation period.

### 3.3.3 Trigger Parameters

To detect any change in the amplitude of the ground motion time history of the station, event detection technique uses the STA/LTA ratio to represent the changes in the current signal with respect to the background noise level. For the purpose, a threshold value called Trigger Ratio, TR, is selected for the station, which when exceeded by STA/LTA ratio shows the arrival of the signal at the station. The selection of TR depends on the background noise level and the expected signal at the station from the seismic source to detect the earthquake. The minimum value of TR is 1 which means that there is no change in the incoming amplitudes of the time series. If STA/LTA exceeds 1, then the station show the increase in the amplitude of the time series at the particular instance. The higher side of the value of TR is chosen to reject some minimum increase in the amplitudes which may not be due to the seismic source. Also, the higher selection of TR takes care of the single noise spikes in the time series. For example, a 10,000 micro volt spike in 10 micro volt background noise level will produce STA value of 12.775 for 10 sec STAP and LTA value of 10.46 for 60 sec LTAP for a sampling rate of 360 samples/sec. The STA/LTA ratio will be 1.22. The TR value if selected for the station to be 1.23 will reject this noise spike for the triggering of the station. Of course, the seismic signal producing the STA/LTA ratio of 1.22 will also be rejected by this TR. TR value between the range of 1.2 to 2.5 were used for different stations in TDSA. These values are reset depending on

the weather conditions at the outstation and CRS which are responsible for the noise spikes due to environmental/electrical disturbances and hence increase the rate of the noise spikes in the time series. If any station is recording noise spikes continuously or at a very high rate of occurrence, TR equal to zero is set for the station until the station is checked and corrected for noise spikes. TR equal to zero disables the station to take part in the triggering algorithm but when other stations fulfill the trigger criterion then this station is also recorded along with the other stations on the magnetic tape. Higher value of TR is liable to miss recording of low magnitude events and the lower value leads to acquisition of transient noise bursts at the stations in turn posing the problems in data processing.

In order to record low magnitude local events within the array and reject transient noise bursts at particular station, trigger parameter NT (Number of stations to cause triggering of the system to record the time series) is selected. The trigger criterion makes use of NT to record the event if the TR is exceeded at least at NT number of stations. If a quiet site having very low background noise level is available, then the recording of the events is governed by the site by choosing NT equal to 1. The monitoring for the exceedance of TR is done for this station only and whenever trigger criteria is met, the data from all the stations is recorded on the magnetic tapes. To avoid recording of the transient noise bursts at single stations, the DAS should search for the same variation of the amplitudes

(corresponding to the specified TR at each station) at other stations simultaneously. The trigger parameter NT, therefore reduces the chances of recording of the noise bursts by observing the same change at some minimum number of stations within a chosen time window (TW) keeping in view the array geometry in relation to probable seismic source zones. The objective of the recording of the seismic event is the location of the source and for the purpose of computation of the epicenter the event should be recorded at least at three stations. In view of this the minimum value of NT is 3. The NT will govern the minimum magnitude to be recorded by DAS since the low magnitude earthquake may not be observed at many stations depending on the attenuation characteristics of the region. Since the attenuation characteristics of the region have not been studied yet, the value selected for the NT is 3 for TDSA.

Trigger Window (TW) is the time counted from the triggering of the first station, within which the stations are watched for their triggered state to bunch them for minimum number of stations (NT) to cause the recording. TW is dependent on the type of wave triggering the stations, the size of earthquakes and the geometry of the array. If  $D_{\max}$  is the maximum distance between any two recording stations in the array then TW may be computed as

$$TW = A \times D_{\max} / V \quad (3.3)$$

where  $V$  is the velocity of seismic waves (either P or S) and  $A$  is a constant representing the geometry of the array.  $TW$  should be selected as a minimum time of the seismic waves to reach from one source to at least  $NT$  number of stations to initiate the recording of the event. In case the station is triggered by S wave or later surface wave arrivals, larger  $TW$  is to be selected. The  $TW$  selected for TDSA is 30 sec.

### 3.3.4 Recording Periods

Sometimes, when the P-wave do not contain the requisite amplitude to trigger a station, the station is triggered by s-wave or later surface wave arrivals. If the recording of the event starts from the trigger point marked by the increase in the amplitudes due to S-wave, one may loose the data for the arrival of P-wave. To over come this problem the system records the data before the trigger point for a time period called PRE-Event Period (PREVP). The selection of PREVP depends on the range of epicentral distances of the events to be recorded. The aperture of the array is approximately 70 km, so the events within the array being of interest could vary upto S-P times of 20 sec or so. To be on the safer side the PREVP is selected to be 30 sec so as to discriminate the background noise before the P-arrival for further studies. For recording teleseismic events larger PREVP would be required which could be selected keeping in view the limitations of the DAS.

Similarly, an event ends when the trigger ratio falls below preset value. If NT is selected to be three and only three stations fulfill the trigger criterion, then it may be possible that the event may not be recorded for the full coda length if the STA/LTA ratio falls below the specified TR value at one or two stations. In this case the LTA value, at the instant specified TR is exceeded, is used to compute STA/LTA ratio during acquisition of the data for the event. The recording will be terminated much before the actual end of the event. For this purpose POSTEVP is selected to continue to acquire data to record the full event after the trigger ratio at any station out of NT becomes less than the specified TR value. POSTEVP for this array is selected to be 30 sec as the stations are closely spaced and differences in the coda lengths of the stations will not be large. Further the space on the magnetic tapes can be optimally used to record data for more events.

The last parameter is the Maximum Event Recording Period (MERP). This is the maximum time period for which the event will be recorded even if the trigger ratios have not been fallen below the threshold value. MERP is useful to terminate recording of noise due to environmental/electrical disturbances which increase the trigger ratio at every station and continue for longer time durations. The recording will be stopped after the MERP is exceeded. MERP selected for TDSA is 200 sec for optimum use of magnetic tapes for monitoring of local seismic events.

In the selection of STAP, LTAP, NT, TW and TR for different stations along with the recording periods many trials were made by computing the trigger parameters and the trigger times for the changes in signal level on different time series recorded by the system. The finally selected parameters along with their ranges for DAS are summarized in Table 3.1. Based on these parameters the data is acquired on the magnetic tapes. Since PDP 11/23 computer system is dedicated to data acquisition only, these tapes are transported to Roorkee and post processing of the data is done at Roorkee.

TABLE 3.1 RANGE AND SELECTED VALUES OF TRIGGER PARAMETERS

Trigger Parameter	Content	Range	Selected value
STAP	Short Term Ave Period	0.1 - 60sec	10 sec
LTAP	Long Term Ave Period	0.1 - 90sec	60 sec
NT	No. of Stn to Trigger	0 - 8	3
TW	Trigger Window	upto 90 sec	30 sec
TR	Trigger Ratio	0 - n	1.2 to 2.5*
PREVP	Pre Event Period	upto 90 sec	30 sec
POSTEVP	Post Event Period	upto 90 sec	30 sec
MERP	Max Event Rec Period	upto 15 min	200sec

\* - The Trigger Ratios are adjusted for stations depending on background noise and weather conditions.



# CHAPTER # 4

SOFTWARE DEVELOPED FOR  
DATA PROCESSING

---

SOFTWARE DEVELOPED FOR DATA PROCESSING

---

#### 4.1 INTRODUCTION

The TDSA deployed for the acquisition of data on local earthquakes in the Garhwal Himalaya region is a PDP 11/23 computer based system as described in section 2.3.3. Since PDP 11/23 computer is dedicated to data acquisition only, the post processing of the data had to be carried out on DEC 2050 computer system available at Roorkee. The first task therefore, was to make the data tapes recorded by DAS compatible to the DEC 2050 computer system. The software packages CHANGE/DUMPER available with DEC 2050 system could not be utilized for transfer of the data from the magnetic tapes to the hard disc of DEC 2050 computer system due to the reason that the data on magnetic tapes is written in Industrial Compatible format with blocks of 4096 bytes. However DUMPER can only be used to move the tape to its BOT mark. After mounting the tapes, the format and the record length are reset to Industrial Compatible format and 4096 respectively, and the data

is copied from the magnetic tapes to the hard disc of DEC 2050 by the simple copy command. One block of 4096 bytes on the tape is copied onto two pages of the hard disc of DEC 2050. The PDP 11/23 computer system is a 16 bit machine and the data needs to be read on the 36 bit DEC 2050 machine. To accomplish this, a software package TMD ( Transfer Magnetic tape Data) has been developed. After transfer of the data to hard disc of DEC 2050 system, TMD changes the format and demultiplexes the data into the date and time files and the seismogram files of the individual stations recorded by DAS. As most of the software and graphics packages for the processing of the time series are available on the PCs, the data files are transferred to the PCs using the standard software packages KERMIT/XTALK/PROCOMM. The following sections describe the development of the software at different stages for the post processing of the data recorded by DAS.

#### 4.2 SOFTWARE DEVELOPED FOR FORMAT CHANGE AND ARCHIVING

The magnetic tapes recorded on PDP 11/23 at the CRS containing events data are brought to Roorkee for the retrieval of the data from the tapes to the hard disc of DEC 2050 computer system at Roorkee University Regional Computer Center (RURCC). The data copied from the magnetic tapes on the hard disc is available in the binary form with 36 bit words. The 16 bits as initially written by the PDP 11/23 computer based DAS has to be retrieved as 36 bit DEC-2050 word. To accomplish this two words of 16 bit each are read from the hard disc as 36 bit single word of DEC

2050. These words are then split into two words of 16 bits by ignoring the extra 4 bits from the 36 bit word. This can be done by shifting the bits to right and left by taking modulo and divisions of the word. Program TMD is developed to accomplish this task (85). The source code of the program in FORTRAN 77 is given in Appendix I. The flow chart of the program is shown in Fig 4.1. The data is now available as 36 bit words containing 16 bit information. The information is still in the binary form.

In accordance with the magnetic tape format used in the PDP 11/23 system for data storage as given in Appendix II, the first file copied is the configuration block followed by event data in form of 4096 bytes blocks. The configuration block contains information on system configuration including station parameters, STAP, LTAP, TW, PREVP, POSTEVP, MERP and NT at the time of mounting the tape. This information can be reproduced in integer form for different stations by a separate software TMDC. The event is read block-wise and the information is retrieved according to the format of the blocks.

The next block recorded on the tape is the first block of the triggered time series recorded by DAS. The date and time information of the first sample recorded at each station in case of a triggered event(see Appendix II for its actual word location) is in Binary Coded Decimals (BCD) code. The time of the first sample recorded by each block is marked in 6th to 9th words of the header and is rounded off to the nearest 100th of a second. To

read and decode the date and time information of the first sample recorded at each station the subroutine SEREAL is called. The time of the first sample recorded in the second block is extrapolated by the software considering the total number of samples recorded in the first block for a particular station. For example, if there are five stations recorded by the system at any time, then each block will contain 384 samples from each station i.e., the data for 1.0666666 seconds of each station. To mark the time of the first data sample in a block, this time duration is added to the absolute time of the first sample recorded in the previous block. This time is rounded to 100th of a second which in turn give errors in matching the times with the amplitudes. To overcome this problem, the time of the first data sample recorded in the first block of the event is decoded and the timing for the remaining samples in the series are computed simply according to the sampling rate. The date and time information is read and decoded as follows:

Let  $M$  be the value of any word from 6th to 9th in the binary form of the header of each block containing date and time information. The modulo of  $M$  with  $2^n$  will give the values of the  $n$  bits towards the right. Similarly, the division by  $2^n$  will give the value of  $16-n$  bits towards the left of a 16 bit word. The information is decoded as

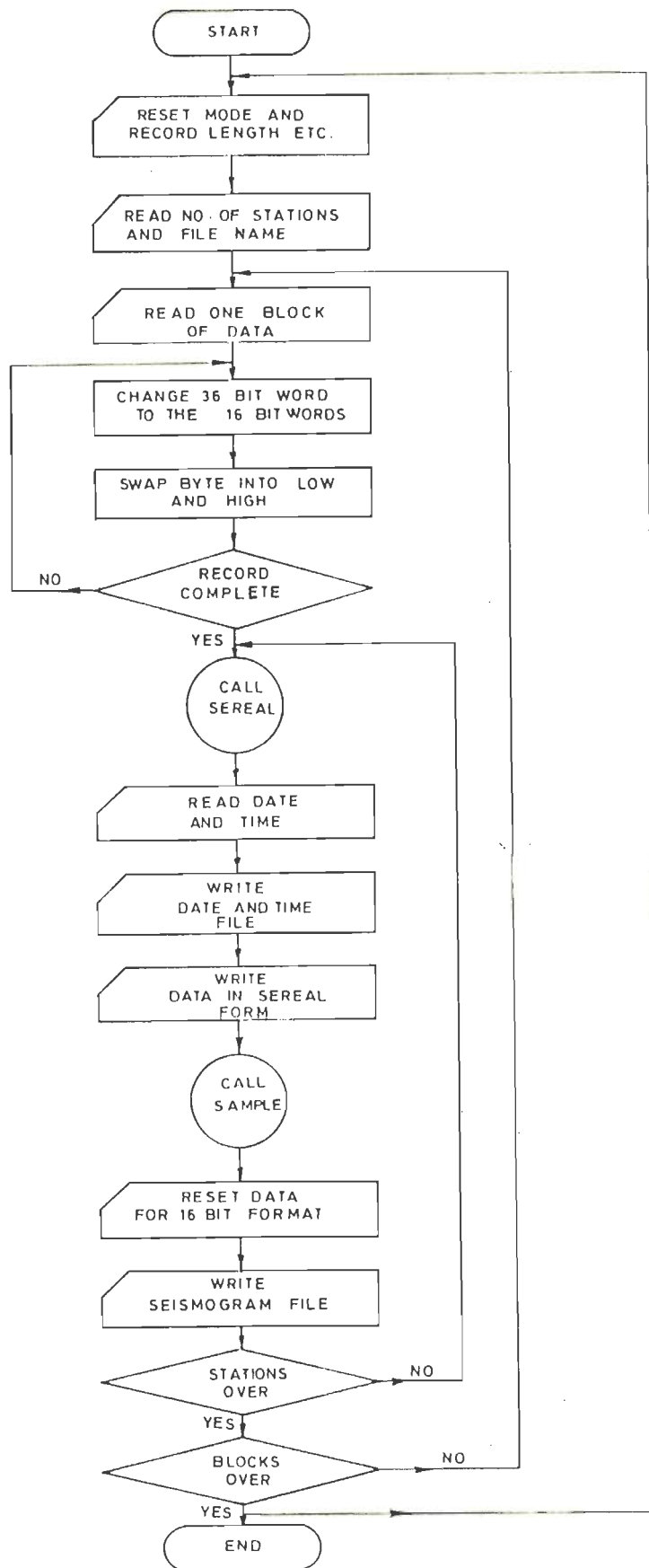


Fig. 4.1- Flow chart for software package TMD

$$LA=MOD(M, 16) \quad (4.1)$$

$$L1 = M/16 \quad (4.2)$$

$$LB=MOD(L1, 16) \quad (4.3)$$

$$L2=L1/16 \quad (4.4)$$

$$LC=MOD(L2, 16) \quad (4.5)$$

$$L3=L2/16 \quad (4.6)$$

$$LD=MOD(L3, 16) \quad (4.7)$$

$$NINT= LD*1000+LC*100+LB*10+LA \quad (4.8)$$

where NINT represents year ; month and day ; hour and minutes ; and seconds and 100th of a second ; for the words 6th to 9th, respectively, in integer form. These values are stored in a file DNT.DAT. According to tape format the event data starts from 129th word and each word afterwards is written as one sample for each station recorded up to 2048 words. The subroutine SEREAL which reads time only from first block also serialize the event data of the blocks for further use. The main program opens files S1.DAT to S8.DAT for the seismograms from 8 seismometer stations. Then the subroutine SAMPLE is called by the main program for each block. Each word of the event data containing information according to the outstation data format as given Fig 2.4, is decoded to reproduce the amplitudes of the series recorded at various stations. Thereafter, the words are copied to their respective files for the different stations by demultiplexing the series accordingly. One block consists of 1920 data words which can be divided fully by 1,2,3,4,5,6 and 8 that means the demultiplexing is easier when the number of stations recorded is from 1 to 8

except 7. So in every block the first word is recorded for the same station as in the first block. But if 7 stations are recorded then the first station recorded in each block is given in 48<sup>th</sup> to 79<sup>th</sup> word of the header of each block which is read to distribute the data among the different stations.

The following is the procedure to decode the 16 bit word information for amplitudes in micro volts of the ground motion time history at each station. Let M be any 16-bit word containing the information about amplitudes (0-8 bits), sign (10th bit), range (11th and 12th bit), component identification (13th and 14th bit), DNV (15th bit) and parity (16th bit). Firstly, the sign bit is checked for correcting the data for 1's compliment. The word is split into two parts of 9 and 7 bits each as follows

$$N = \text{MOD}(M, 512) \quad (4.9)$$

$$N1 = M/512 \quad (4.10)$$

where N and N1 are 9 and 7 bit words. The sign bit NS is given by

$$NS = \text{MOD}(N1, 2) \quad (4.11)$$

NS may be either 0 or 1. If it is 1 then the value is negative and complimented for one. 0 stands for a positive value.

Depending on NS the amplitude is complimented as

$$N = (511 - N). \quad (4.12)$$



The other information from N1 is decoded as follows:

$$N2=N1/2 \quad (4.13)$$

$$NR=MOD(N2,4) \quad (4.14)$$

$$N3=N2/4 \quad (4.15)$$

$$NC=MOD(N3,4) \quad (4.16)$$

$$N4=N3/4 \quad (4.17)$$

$$ND=MOD(N4,2) \quad (4.18)$$

$$NE=N4/2 \quad (4.19)$$

where NR, NC, ND and NE are range, component identification, data not valid and parity bits respectively. In case of errors in the data transmission the parity bit is set i.e.,  $NE = 1$ . In such a case the transmitted data is corrupted and its amplitude is unrealistic. As an approximation the amplitude of a corrupted sample is taken to be the same as the amplitude of the previous sample in which the parity bit is not set. Further, if ND is set then the corresponding data sample is ignored as it is the filling of the time series for the synchronization of the data between different stations and is superficial. This type of setting of the ND bit will occur after every 360 samples or so since the data is received at a higher rate of 362 samples/sec. To account for the range settings, the amplitude of a sample is multiplied by a factor of 1, 4, 16, or 64, if the range bits are 00, 01, 10 or 11, respectively. The data from one or more components operating at each outstation are identified by the value of NC bits. The component identification bits may have the settings 00, 01, 10, 11 which represent single component, north-south, vertical and east-west components of a 3-component station respectively.

Data samples after decoding according to the procedure explained above are stored in different files by executing the program TMD. Different files created for this purpose are as follows :

1. DNT.DAT

This file contains information about date and time of the first data sample recorded by the stations. This file also contains information about the number of stations for which the data is recorded and total number of data samples present in each station file.

2. S\*.DAT

These files contain the amplitudes of the ground motion in micro-volts for each station. The amplitudes can be expressed in terms of velocity ( m/sec) by multiplying each sample by the corresponding seismometer constant.

After the execution of TMD the files DNT.DAT and S\*.DAT are available. As the post processing of the recorded events is carried out on the PCs, the data from the hard disc of DEC 2050 is transferred to the personal computers and stored on floppy discs. However, the transfer rate of the data is quit low. For instance, a seismogram of 200 sec time span of a single station takes about 30 minutes to be transferred from the DEC system to the PC. The original magnetic tapes containing the triggered time series recorded by DAS are preserved for future use.

### 4.3 VISUAL ANALYSIS OF THE RECORDED DATA

#### 4.3.1 Procedure

By visual analysis here we mean interactive process of displaying recorded event data on PC screen and marking the various parameters of the trace, viz, P- and S-onset times, maximum peak amplitude, up/down motion of the first arrival and coda duration of the seismic event. The data already archived on the floppy diskettes using TMD is used for visual analysis. The time series is plotted on the screen of the PC and is searched for the seismic event. The time series is visually examined for the coda shape and other characteristics of the seismogram like the exponential decay, the signatures of P- and S-arrivals and the general shape of the seismogram. A time series which do not fulfill the above criteria for a seismic event is declared as false alarm and hence is rejected. All the time series recorded at various stations for each triggered event are looked simultaneously to match the features of different seismic wave arrivals. If needed, a time series may be displayed with a lower sampling rate depending on the total number of samples using the software SMRT. This is being done to save the time used for plotting large number of samples. Secondly, the seismograms containing large number of samples could not be copied on a single floppy while transferring the data from DEC to PC. The sampling rate may be decreased by selecting the alternate samples for 180 Hz, or every 3rd and 4th sample for 120 Hz and 90 Hz, respectively. This type of reduction of sampling rate acts as a

low pass filter and reduces the data without any loss of information in the interested frequency band. The false alarms present in the triggered recorded time series are rejected at this stage and the seismic events are archived for further analysis. The software GRD is developed to change the format accordingly to plot the file on the screen of the PC. Fig 4.2 shows the full plot of a seismic event which was recorded at Surkanda, Narendranagar and Dhargaon stations on 25-11-88. Fig 4.3 shows the example of a false alarm recorded on the same date. The characteristic difference between a false alarm and a seismic event as explained earlier can be seen very clearly from the two plots. Sometimes noise spikes may get recorded in the data due to environmental/electrical disturbances. The amplitudes of such noise spikes are generally of the order of 10,000 micro volts and during plot of a time series the other part of the data gets suppressed to accommodate the maximum/minimum amplitudes present. It becomes difficult to recognize the characteristics of a seismic event from such plots (Fig 4.4 a ). In such cases two approaches can be followed ; either the time series is replotted by expanding the scale on the vertical axis (Fig 4.4 b), or the noise spikes are substituted by the average trend before plotting(Fig 4.4 c). For such type of problem the software PRICT is developed which identifies the amplitudes which are not considered as relevant to the time series and replaces them by the present trend of the time series.

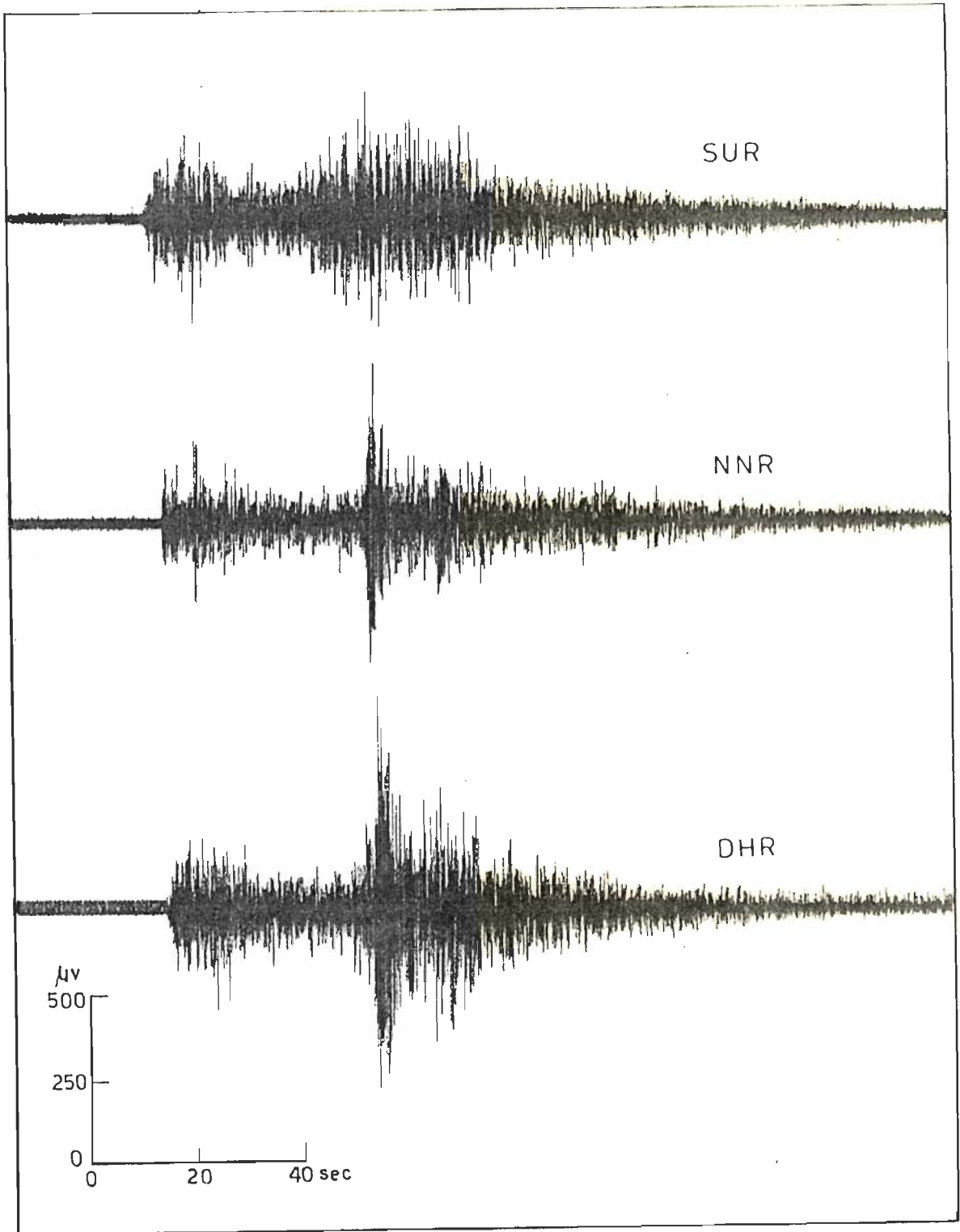


Fig. 4.2 - Plot of ground motion time histories of the seismic event recorded by DAS on 25-11-88 at three stations

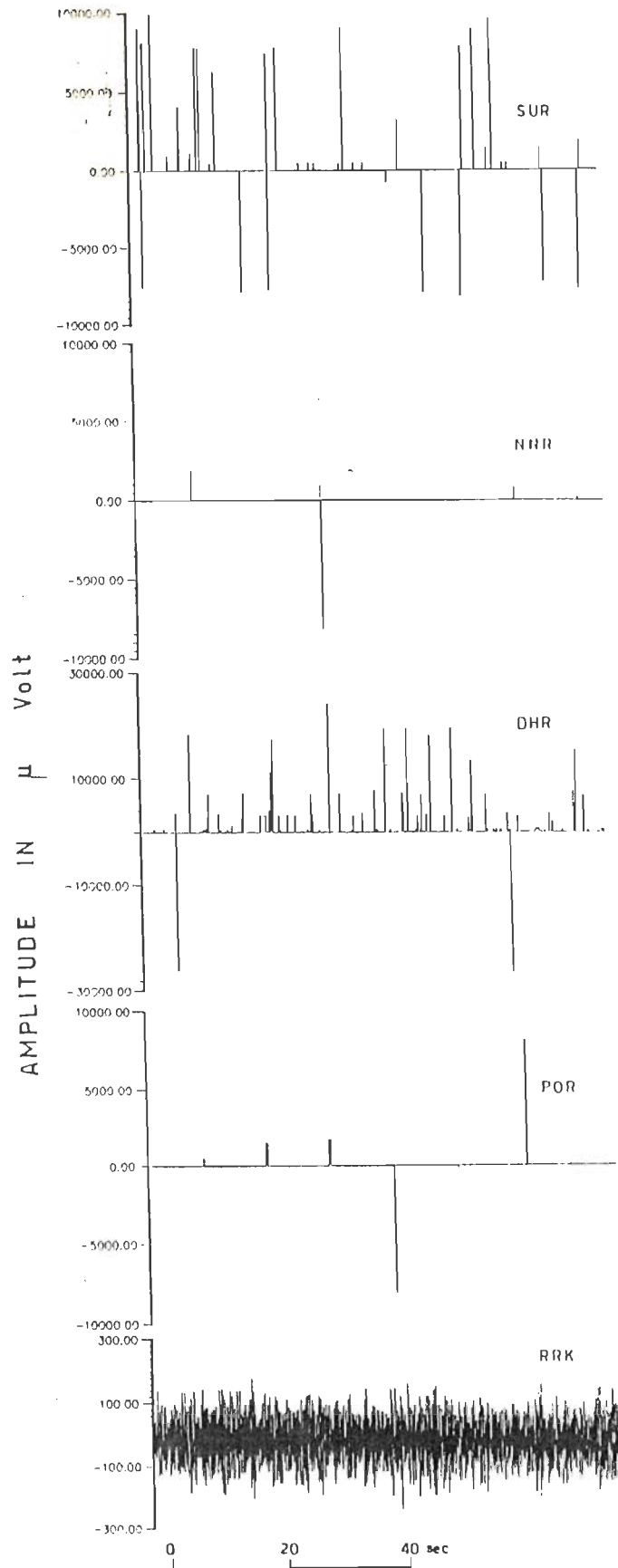
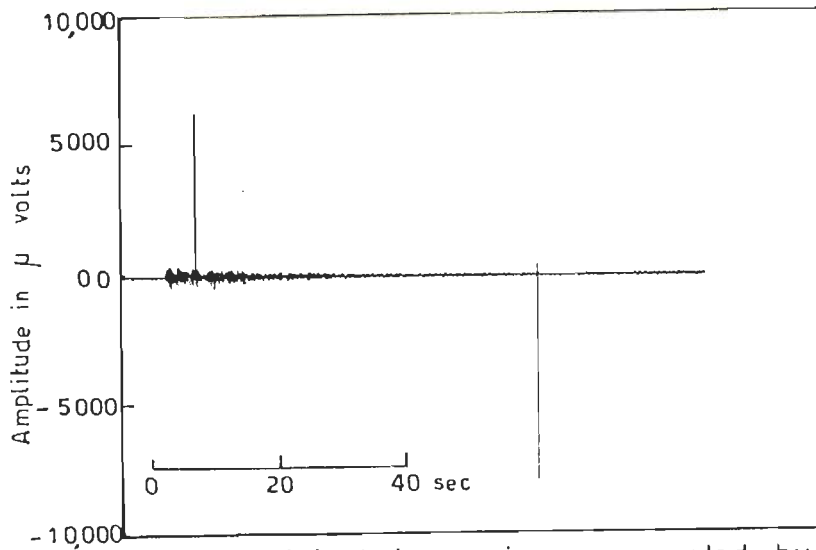
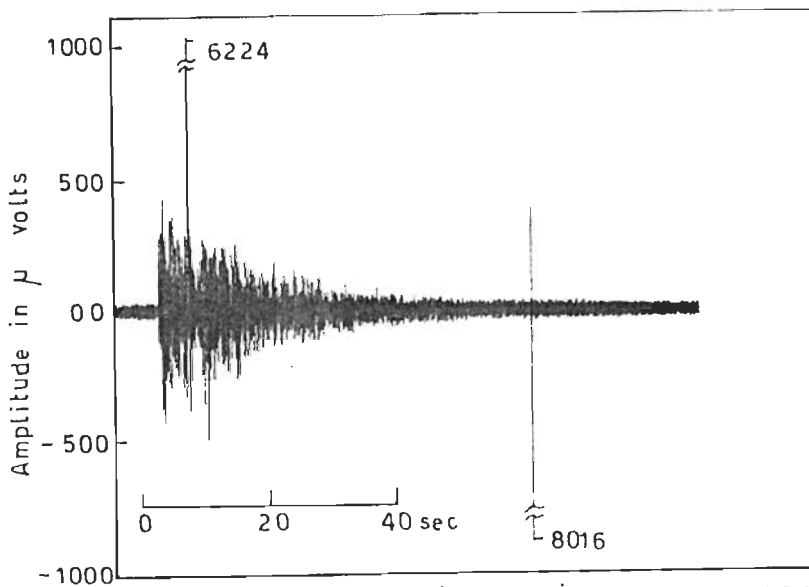


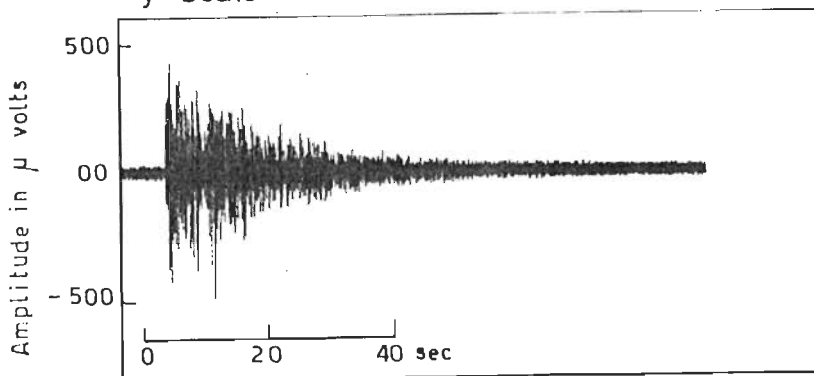
Fig. 4.3 - Plot of a false alarm recorded by DAS at five stations



(a) Plot of original time series as recorded by DAS having two noise spikes



(b) Plot of the same time series on an expanded y-scale



(c) Plot of the same time series after replacement of noise spikes by average trend

Fig. 4.4 - Example of post processing of the seismogram recorded at Surkanda station on 12-4-89

After a time series is verified to be a seismic event, the time series are plotted station wise to mark P- and S-onset times, up/down motion of the first arrival, maximum peak amplitude recorded in micro volts and coda length in respect of each station. Fig 4.5 shows plots of a seismic event taking expanded X- and Y-axis to obtain these parameters more clearly on the screen of the PC. Fig 4.6 shows the accuracy attained in picking the P-onset time by visual analysis on the screen of the PC. In Fig 4.6 (a) the seismograms for the event are plotted as if they are recorded on the analog recorder at the speed of 60 mm/min in which case the accuracy in marking the onset times of the seismic phases is known to be of the order of 0.1 sec. The portion containing the P-onset are plotted in Fig 4.6 (b) on the right side of the seismograms on an expanded X-axis. In these plots one can easily mark the P-onset up to the particular sample. The resolution of the data is 2.77 milli sec in case of 360 samples/sec and 11.1 milli sec for 90 samples/sec.

#### 4.3.2 Filtering Process

Present day measuring techniques in any technical or scientific field, unfortunately, do not provide noise free observational data. Therefore, it is very likely that when starting to evaluate these observations one shall confront with the signal-noise separation problem in all its complexities and thus one may resort to some filtering of the data. The term filter is used to characterize a system which can perform an



effective prescribed separation of the desired information carried by the signal from the unwanted portion called noise. Secondly, sometimes it is very necessary to check the time series in different frequency windows to discriminate the seismic phase arrivals otherwise masked by the background noise. If the time series is passed through required frequency filters then the characteristics can be more clearly inspected. The filters are applied to remove the DC bias and the high frequency content out of the time series, using low pass and high pass single pole filters in time domain. The technique of filtering is taken to be the simple filtering applied in the time domain and the selection of the filter coefficient is based on the objective that the response of the filter has no sharp fall off.

There are many types of filtering process available in the literature for the time and frequency domains. The choice of the filter from vast available filters depends on the objectives. In the present study the filters are selected such that, if needed, they can be adopted for real time processing which rejects the choice of frequency domain filtering. Secondly, the computation time of the filter should be less which compels us to use single pole low pass filters. The most general form of the first order digital filter is defined by a difference equation (72) of the form

$$y(i) = \sum_{k=0}^m b_k x(i-k) - a_1 y(i-1) \quad (4.20)$$

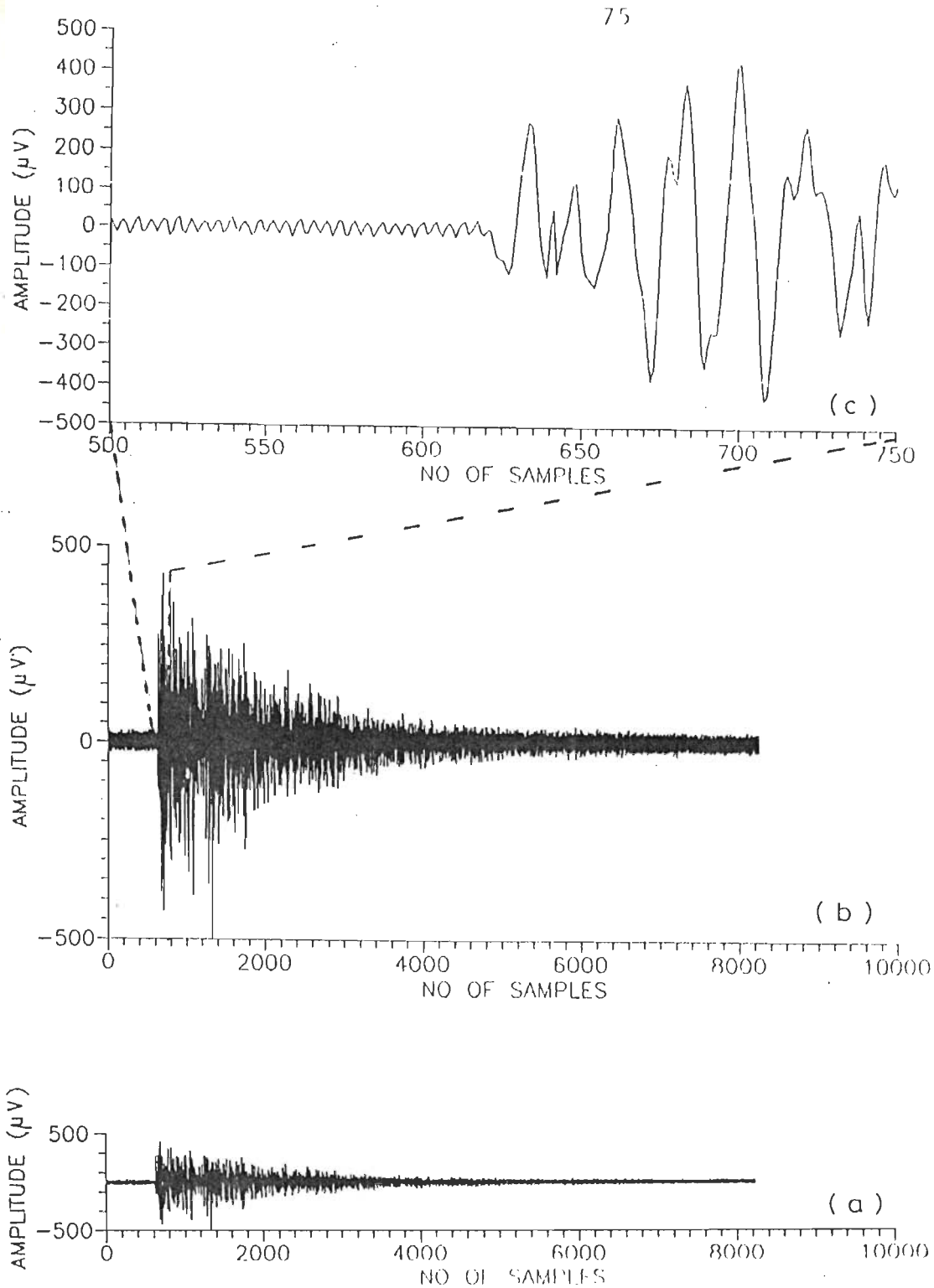


Fig.4.5\_ Procedure of digital processing of the seismogram recorded by DAS at a station to mark characteristic parameters of the seismic event

- (a) Plot of the full seismogram ,
- (b) Plot of the original seismogram taking expanded y-axis
- (c) Plot of a segment containing P-arrival on expanded x- and y-axis

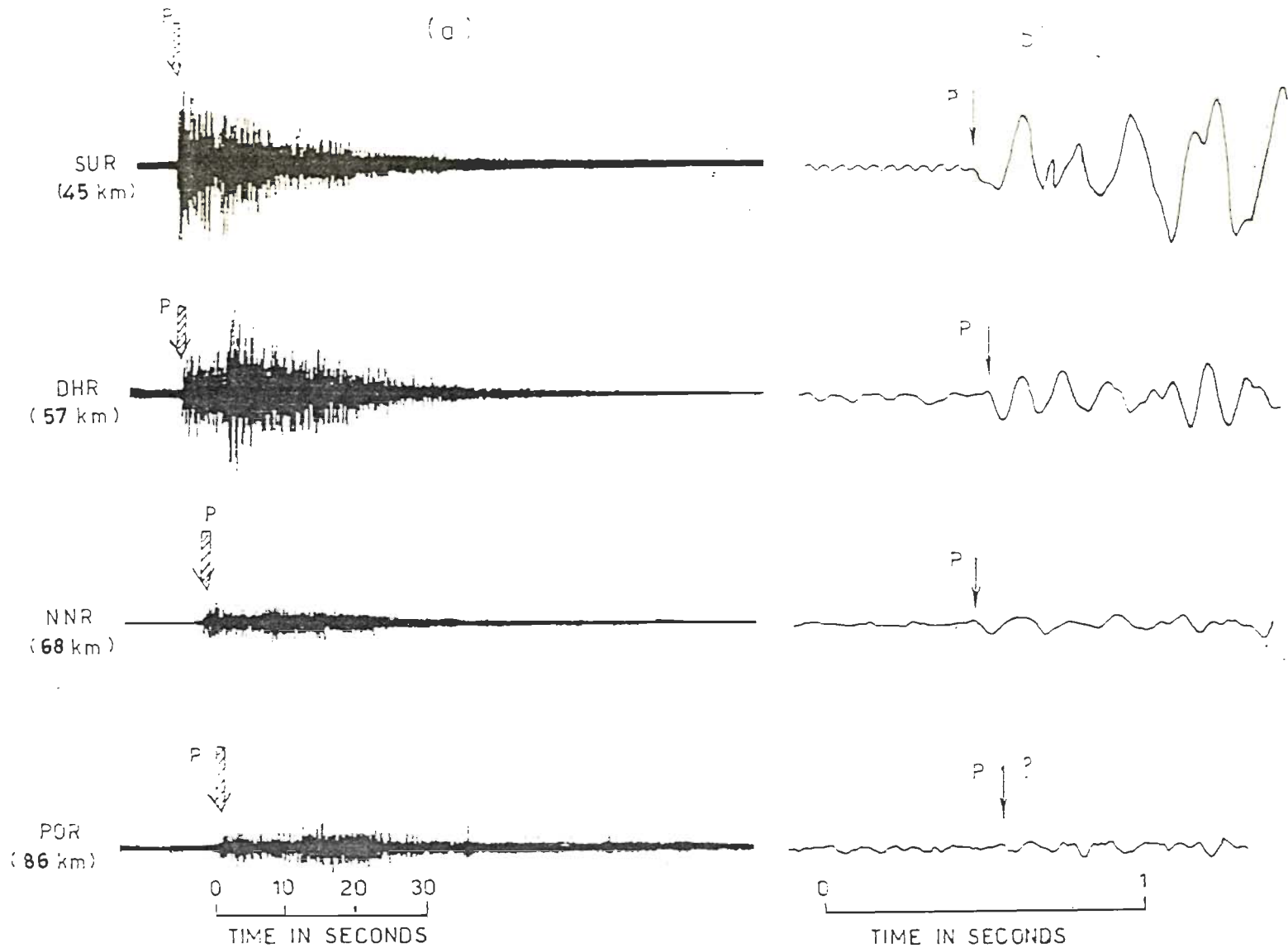


Fig.4.6\_ Example of a microearthquake ( $M_L=3.0$ ) recorded by DAS. The accuracy for P-phase onset as in (a) marked with  $\Downarrow$  increases in (b) with  $\downarrow$  mark. The epicentral distances are given in paranthesis

The current output  $y(i)$  of the filter is defined by combining linearly  $m$  past inputs  $x(i)$ , the current input  $x(i)$  and the single past output  $y(i-1)$ . This is a first order filter because a single previous output (time a constant) is subtracted from the combined input to form the new output values. In general, it is the number of such previous output terms employed in the calculations that determines the order of the filter(72). The coefficients for important types of this filter are given in Table 4.1.

As indicated in Table 4.1 the low pass filter which is of prime importance in our case has the form

$$y(i) = (1-\alpha) x(i) + \alpha y(i-1) \quad (4.21)$$

The standard tools for analyzing filters are the transfer function and its gain and phase. For the computation of transfer function, let us define Fourier transform in discretized form (72) as follows.

$$Y(f) = T \sum_{i=-\infty}^{\infty} y(i) \exp(-j2\pi f i T) \quad (4.22)$$

where  $T$  is the sampling rate. Substituting for  $y(i)$  from equation (4.21), we get

$$Y(f) = T \sum_{i=-\infty}^{\infty} [(1-\alpha)x(i) + \alpha y(i-1)] \exp(-j2\pi f i T) \quad (4.23)$$

$$\begin{aligned}
&= (1-\alpha)T \sum_{i=-\infty}^{\infty} x(i) \exp(-j2\pi f iT) \\
&\quad + \alpha T \sum_{l=-\infty}^{\infty} y(l-1) \exp(-j2\pi f l T) \quad (4.24)
\end{aligned}$$

The first term on the r.h.s. in the above equation represents the Fourier transform of  $x(i)$  i.e.,

$$(1-\alpha) \sum_{l=-\infty}^{\infty} x(l) \exp(-j2\pi f l T) = (1-\alpha)X(f) \quad (4.25)$$

The second term, on substituting  $p=l-1$ , can be rewritten as

$$\begin{aligned}
&\alpha T \sum_{l=-\infty}^{\infty} y(l-1) \exp(-j2\pi f l T) \\
&= \alpha T \sum_{p=-\infty}^{\infty} y(p) \exp(-j2\pi f (p+1) T) \\
&= \alpha \exp(-j2\pi f T) T \sum_{p=-\infty}^{\infty} y(p) \exp(-j2\pi f p T) \\
&= \alpha \exp(-j2\pi f T) Y(f) \quad (4.26)
\end{aligned}$$

By making the change of variable it is possible to factor out an exponential term and end up with the product of an exponential and the Fourier transform of  $y(i)$ ; it does not matter whether the dummy variable in the definition of  $y(i)$  is  $i$  or  $p$ .

If all these results are collected, the Fourier transform of equation (4.21) becomes

TABLE 4.1 COEFFICIENTS FOR DIFFERENT TYPES OF FIRST ORDER DIGITAL FILTERS ( $0 < \alpha < 1$ )

Type of filter	$b_0$	$b_1$	$a_1$
Integrator	$T^*$	0	-1
Differentiator	$1/T$	$-1/T$	0
Low pass filter	$(1-\alpha)$	0	$-\alpha$
High pass filter	$(1-\alpha)$	0	$\alpha$

\* - T represents sampling interval

$$Y(f) = (1-\alpha)X(f) + \alpha \exp(-j2\pi fT)Y(f) \quad (4.27)$$

which on simplification yields

$$H(f) = \frac{Y(f)}{X(f)} = \frac{(1-\alpha)}{(1-\alpha \exp(-j2\pi fT))} \quad (4.28)$$

or,

$$H(f) = \frac{(1-\alpha)}{(1-\alpha \cos 2\pi fT) + j\alpha \sin 2\pi fT} \quad (4.29)$$

Thus the gain of the filter is

$$\begin{aligned} |H(f)| &= \left[ \frac{(1-\alpha)^2}{(1-\alpha \cos 2\pi fT)^2 + (\alpha \sin 2\pi fT)^2} \right]^{1/2} \\ &= \frac{1-\alpha}{(1-2\alpha \cos 2\pi fT + \alpha^2)^{1/2}} \end{aligned} \quad (4.30)$$

The gain of this filter is computed for several values of  $\alpha$  and plots are given in Fig 4.7.

Note that  $|H(0)|=1$  for all values of  $\alpha$ . The coefficient  $a_0=(1-\alpha)$  was selected solely for the purpose of normalizing the gain of the filter at 0 Hz to unity. The impulse response function  $h(i)$  for this filter could be formed by taking the inverse Fourier transform of  $H(f)$  and is given by

$$h(i) = \int_{-F}^F H(f) \exp(j2\pi f iT) df$$

$$= \int_{-F}^F \frac{(1-\alpha)\exp(j2\pi f1T)}{1-\alpha \exp(-j2\pi fT)} df \quad (4.31)$$

Rather than performing this nontrivial integration it is possible to find  $h(i)$  as the response to the sequence  $1/T, 0, 0, 0, \dots$ . By definition

$$h(i)=0 \text{ for } i < 0$$

Then the response is computed as

$$h(0) = \frac{1-\alpha}{T} + 0$$

$$h(1) = (1-\alpha)0 + \alpha \frac{1-\alpha}{T} = \alpha \frac{1-\alpha}{T}$$

$$h(2) = (1-\alpha)0 + \alpha \left( \alpha \frac{1-\alpha}{T} \right) = \alpha^2 \frac{1-\alpha}{T}$$

⋮

⋮

$$i\text{th term, } h(i) = \alpha^i \frac{1-\alpha}{T}$$

From the above, we may write the impulse response as

$$h(i) = \alpha^i \frac{1-\alpha}{T} \quad (4.32)$$



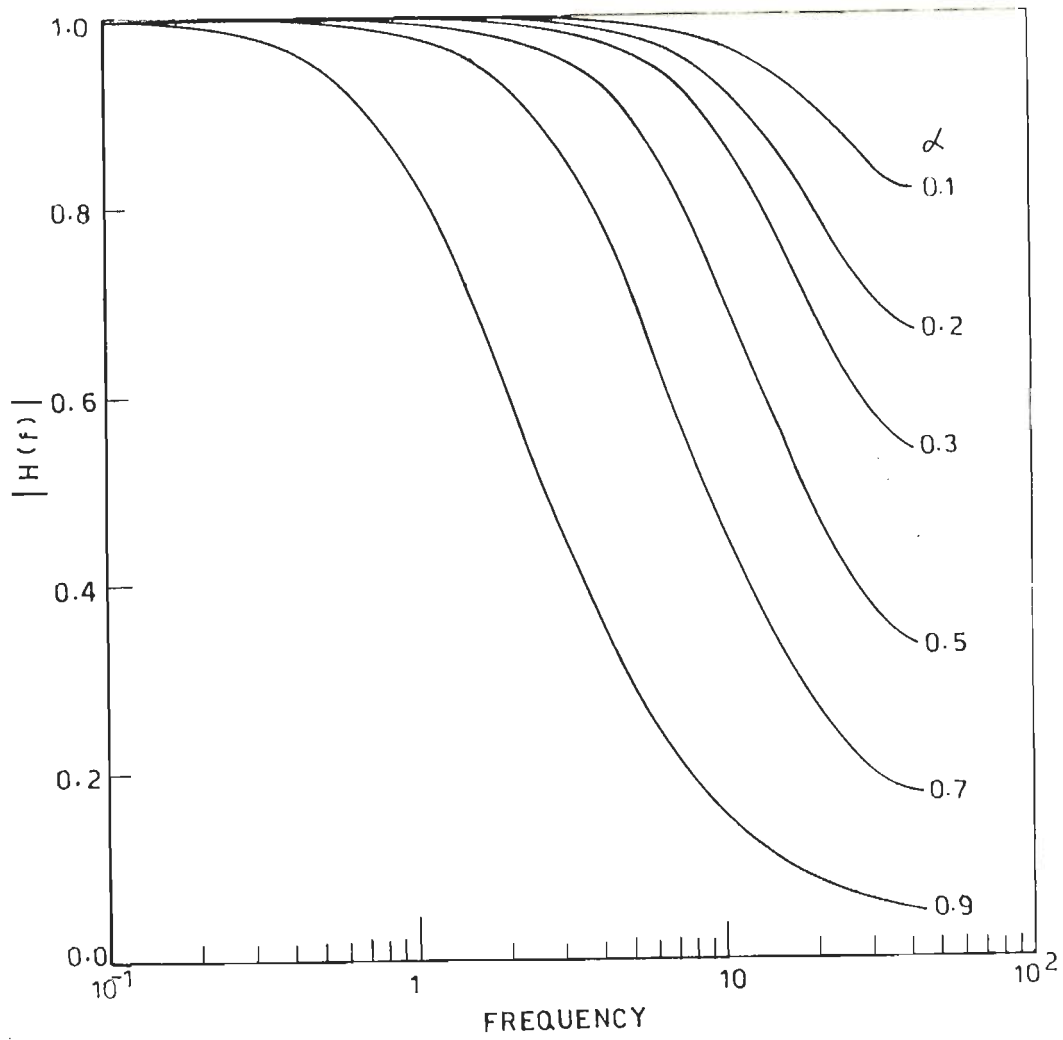
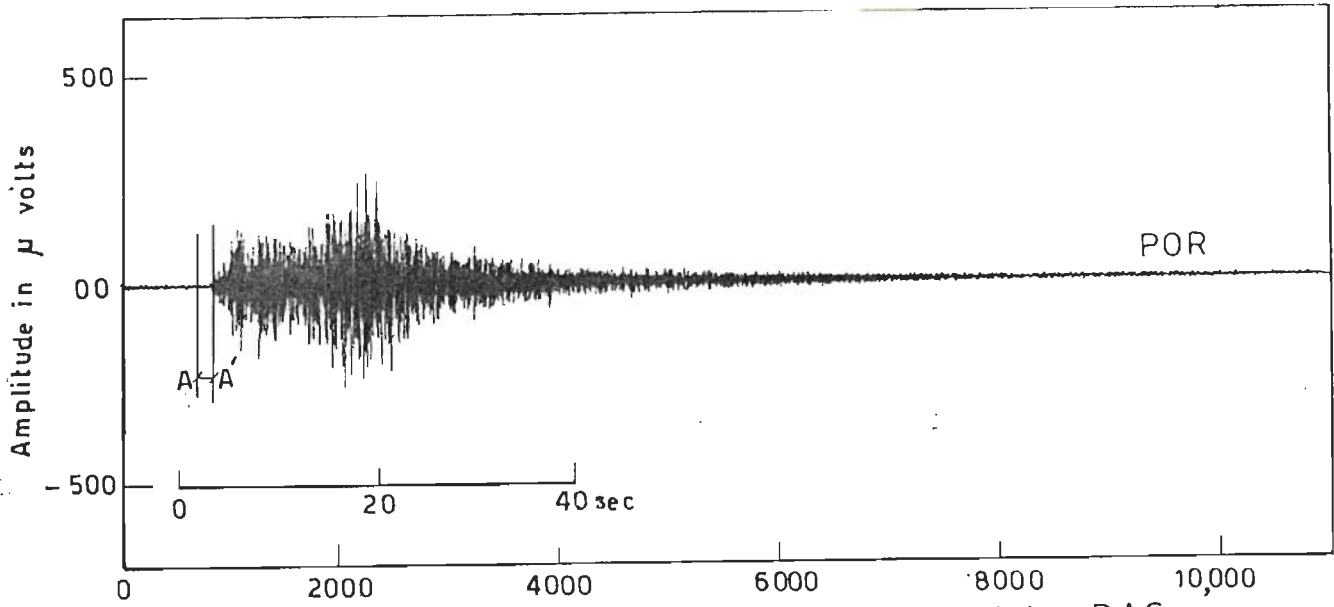


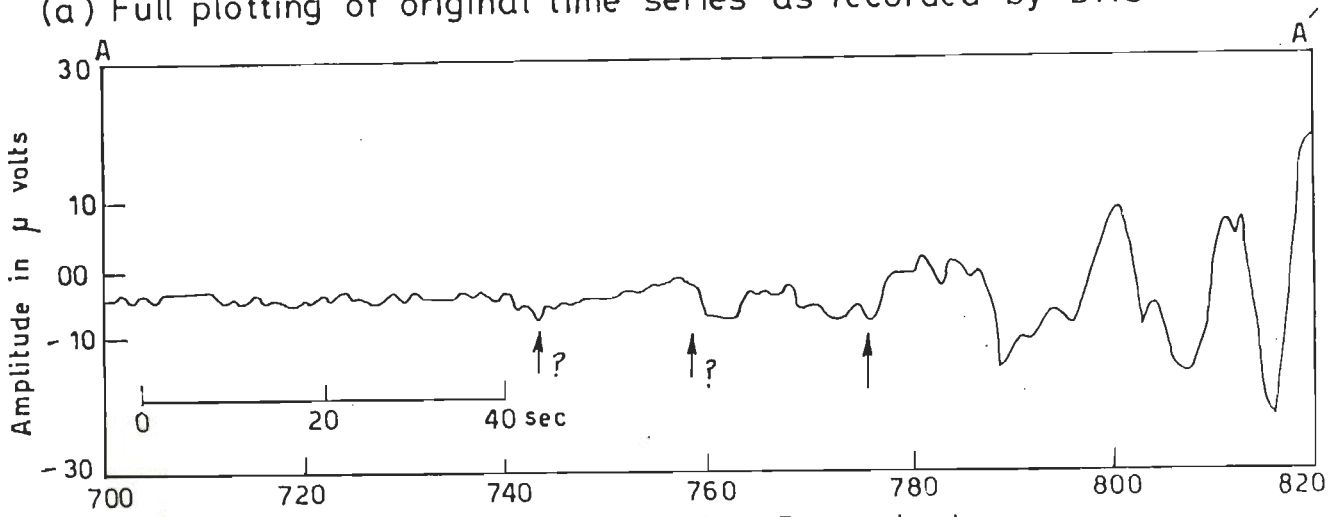
Fig. 4.7 - Gain of low pass filter for different  $\alpha$

The reason for  $\alpha$  being limited to the range  $0 < \alpha < 1$  becomes clear when this expression is examined. For  $\alpha$  in that range,  $h(i)$  is geometrically decreasing with respect to  $i$ , for  $\alpha > 1$  it is geometrically increasing. For  $\alpha = 2$ , the impulse response increases tremendously up to the size beyond the capacity of any finite arithmetic device to contain it, which results in overflow. It may be noted that this is an example of instability in a digital filter.

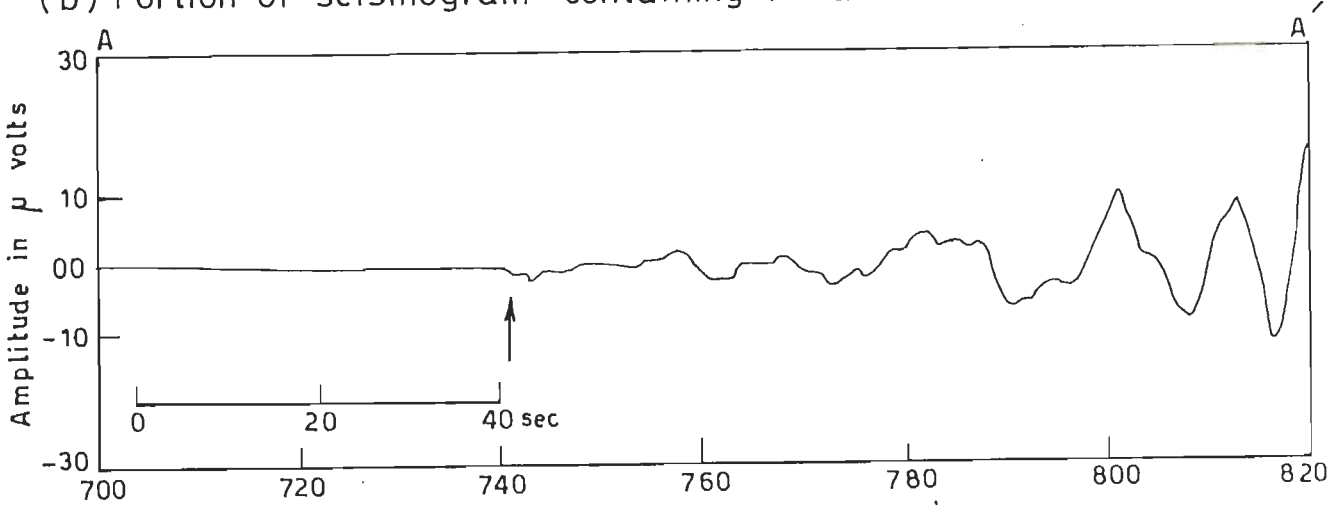
The usefulness of the filtering process is illustrated in Fig 4.8. Fig 4.8 (a) is the plot of the time series of an seismic event dated 02-04-89 recorded at Pauri station. The portion AA' consisting of samples from 700 to 820 at a lower rate of 90 samples/sec is shown in expanded form in Fig 4.8 (b). The filtered output of these samples obtained using the filter as given in equation (4.21) with  $\alpha = 0.3$ , i.e., low pass filter up to 15 hz, along with the DC removal, is shown in Fig 4.8 (c). The onset of the seismic phase arrival can be marked more accurately in the filtered series in comparison to the original time series. This establishes the utility of filtering process in the post processing of the seismograms recorded by DAS.



(a) Full plotting of original time series as recorded by DAS



(b) Portion of seismogram containing P-arrival



(c) Filtered time series containing P-arrival

Fig. 4.8 \_Example of post processing of the seismogram recorded at POR (PAURI) station on 02-04-89

# CHAPTER # 5

## PHASE PICKER

---

## PHASE PICKERS

---

### 5.1 INTRODUCTION

The phase pickers are defined as the devices used to scan seismic traces for searching different seismic phase arrivals which are required by a seismologist in order to determine hypocentral location and other parameters describing the earthquake source. However, a distinction should be made between 'event detectors' and 'phase pickers'. For event detectors a relatively imprecise estimation of the P-onset time suffices, whereas in phase pickers, timing precision is comparable to that of hand pick made from films/interactive cathode ray tube. A picker should time a seismic phase arrival with a precision of no worse than a few hundredths of a second, whereas a detector usually is allowed at least a second of leeway or more. A phase picker not only performs the function of an event detector i.e., recognition of a seismic phase arrival in the presence of background noise but also obtains precise estimates for the onset

times of the seismic phases. To pick a phase in a seismic event, the background noise and the signal characteristics of a seismic event should be studied. The background noise is typically of low amplitude and high frequency content having appearance as quite periodic and/or random. Because of instrumental noise and cultural activities, transient signals having a broad range of amplitude and frequency are often present. Depending on the size of the event, teleseismic amplitudes can range from barely perceptible to those which may go out of the dynamic range of the instrument. Their predominant periods are typically a few seconds. Similarly, the amplitudes of regional events can range from barely perceptible to large, but their predominant periods are less than those of the teleseismic events. Local events are often characterized by impulsive onset and high frequency waves. The envelope of the local earthquake signals has typically exponentially decaying tail. Another characteristic of all seismic signals is that the predominant period generally increases with time from the onset of the first arrival. On the other hand, a transient noise signal of instrumental or cultural origin often has the same predominant period throughout its duration (60). TDSA is deployed for monitoring of local events which in general can be characterized by their impulsive onsets, high frequency content and exponentially decaying envelope.

## 5.2 PHASE PICKING ALGORITHMS - A REVIEW

Since seismic signals are now often recorded in digital mode and manual analysis of a large number of seismograms is a time consuming task, several phase picking algorithms have been developed in the past decade which allow an automated determination of P-phase onset times (5,6,8,9,12,28,93,94). For several years scientists have been involved in research programs to evaluate and develop efficient and more accurate phase pickers which are necessarily evolved from the event detectors. For precise timing, the picker must search for a rapid change of amplitude or dominant frequency as apparent in the seismic series. The phase picker algorithms are applied in time as well as in frequency domains. The following sections presents a comprehensive review of the phase picker algorithms in both the domains.

### 5.2.1 Time Domain Algorithms

Basically all time domain algorithms consider the amplitudes of incoming time series and modify them to enhance the signal to noise (S/N) ratio corresponding to a seismic phase arrival. The concept of Characteristic Function (CF) which is the modified time series is very common in designing the phase picker algorithm. The arrival of a seismic phase in the time series is indicated by a change in the amplitude and/or frequency content of the time series. The change in the amplitude is used by the STA-LTA triggering techniques to mark the seismic phase arrivals.

Thereafter, some of the algorithms enter into tests designed to confirm the incoming signal as seismic event and then to record the full coda of the seismic event by running some extra tests made for the purpose.

#### 5.2.1.1 Logical structure

As explained above, the phase picker algorithms are having strikingly similar logical structure to mark, confirm and record the seismic events from an array. To start with, a simple logical structure, in general, is taken as shown in Fig 5.1. The first block in the figure is the input section after which the filters are applied to remove the unwanted portion of the time series. The time series is then modified to generate CF in the third block which is examined for changes in the amplitudes occurring due to a seismic phase arrival. STA and LTA are then computed on the CF and their ratio is compared with some threshold value. The STA and LTA may also be computed over the original time series  $x(i)$ . If the ratio  $STA/LTA$  exceeds the threshold value then the event is declared at that particular channel and some tests are performed on the time series to confirm it for the seismic event. If the time series passes the tests then the end criterion is tested to record the end of the event for the full coda length. If the end criterion is not passed then the algorithm resumes the further computation of STA and LTA. These criteria are designed for a single channel and, generally, are performed on all the channels in an array which may incorporate some more tests. The



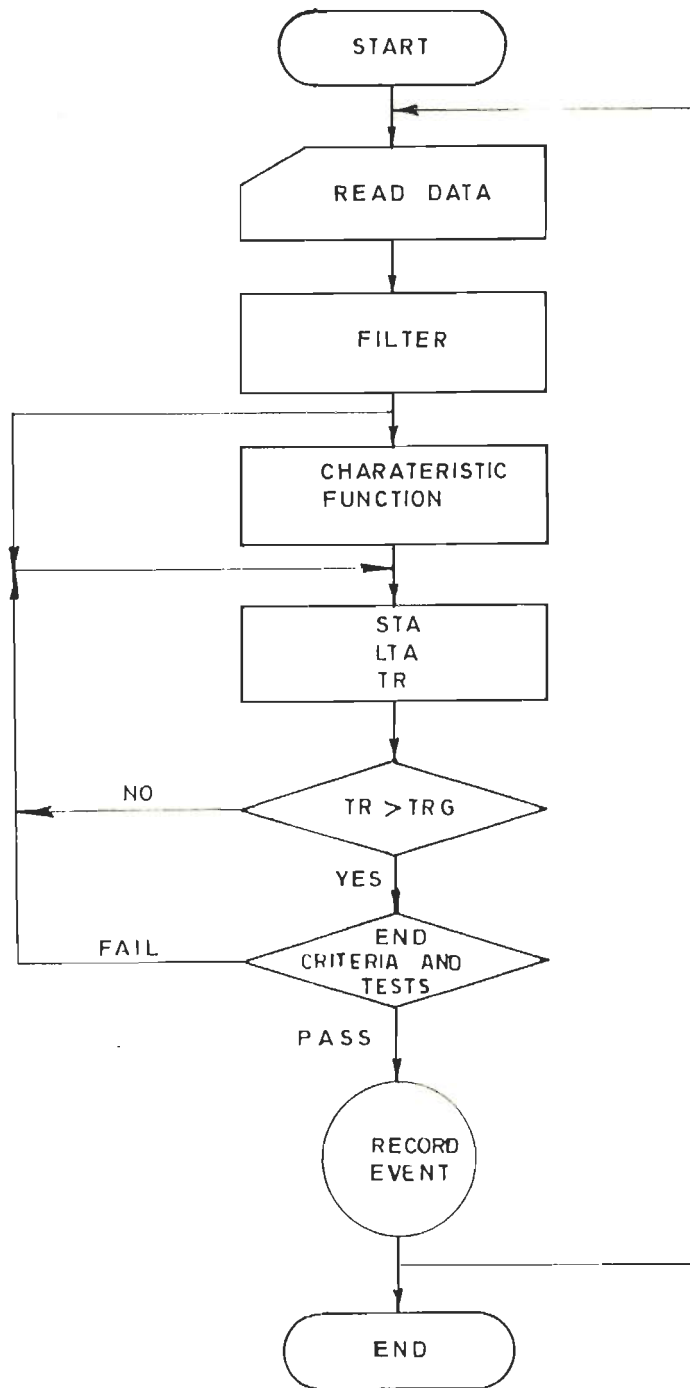


Fig. 5.1\_ Generalised logical structure for a phase picker

following is the description of each section of the block diagram (Fig 5.1).

The concept of Characteristic Function (CF) is useful in designing an algorithm for timing seismic phase arrivals. The incoming signal in digital form is seldom used directly and is usually transformed into one or more time series that are more suitable for determining the seismic phase arrivals. The transformed series is referred to here as CF.

The input time series is so transformed into CF as to enhance the amplitude in the interested frequency range i.e., the signal from a seismic event, and also to suppress the amplitudes of the noise. The result of a phase picking algorithm will depend very significantly on the CF used in the algorithm. The arrival of a seismic phase is indicated by a change in the frequency content or amplitude or both in the time series and thus the CF must respond to the changes in the amplitude and/or frequency content arising due to the presence of a seismic phase as rapidly as possible and ideally should enhance these changes. The simplest CF may be taken just the absolute value of the input time series  $x(i)$ . Some other similar simple CF's could be taken as  $(x(i))^2$ ,  $(x(i)-x(i-1))$ ,  $(x(i)-x(i-1))^2$  or their linear combinations as used by different workers (Fig 5.2)

The next section in Fig 5.1 is of averages taken over the time series for some time interval  $t$ . To exploit the

characteristics of microearthquakes, the concept of LTA and STA of incoming signal amplitude as defined in equation (3.1) and (3.2) respectively, has been used by a number of authors (5,7,8,28,95). Typically STA is taken over 1 sec or less permitting a quick response to changes in the signal level to characterize the onset of an earthquake. Similarly, LTA represents the background noise level of the channel and is usually taken over much longer time interval than the predominant period of the incoming signal.

After the computation of LTA and STA, using equation (3.1) and (3.2), their ratio is computed to detect the changes in the incoming signal. If the ratio exceeds a preset threshold value, a tentative event is declared. Some pickers invoke additional criteria for confirmation of an event at this point while others apply additional tests at a later stage. In an array comprising of many channels, the triggering technique is applied for all the channels simultaneously. If there are more than say  $n$ , stations triggering within some time interval, an event is declared and then the recording of the incoming data is started for all channels of the array.

The methodology that leads to a decision to stop recording a detected event and return to the search mode for the next event is referred to as the end criteria. Usually, the end of an event is not empirically the time of signal level reaching cut off threshold level (i.e., background noise level). The end of the earthquake may be defined as that time when the signal last

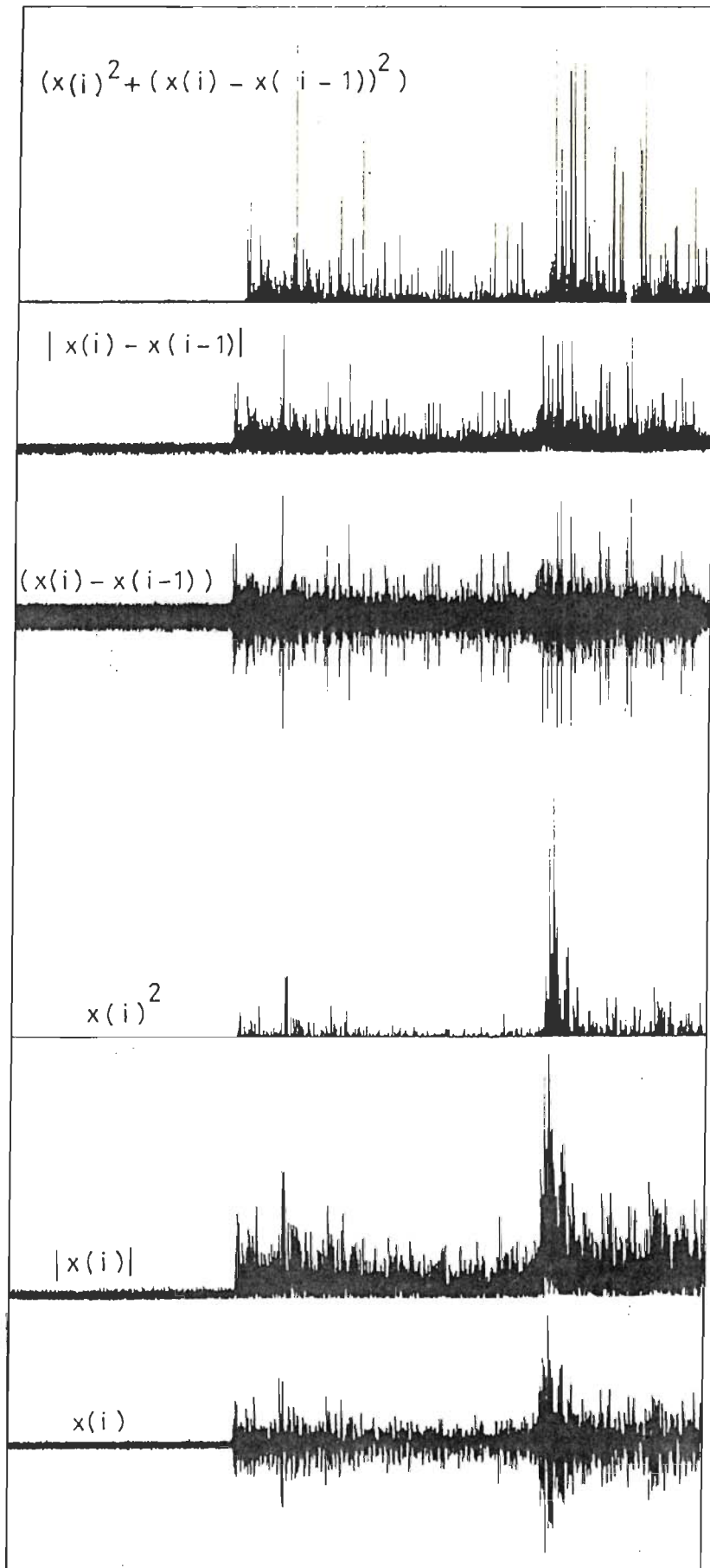


Fig.5.2\_ Different types of characteristic functions  
(Plotted on different vertical scales)

crossed below the cut off threshold level and remained within it for some minimum time. Since an earthquake may occur within the coda portion of another earthquake, especially during an aftershock sequence or swarm, the event detection algorithm must be able to handle such cases. Every end criteria should be sensitive enough to yield accurate estimates of the coda length.

#### 5.2.1.2 Different time domain algorithms

The following is the description of some of the important event detectors implemented in time domain.

Stewart et al., 1971 used a small digital computer to implement a real time detection and processing system for the USGS Central California microearthquakes network (95). The input time series  $x(i)$ , with 50 samples/sec, is modified to construct the CF as

$$CF(i) = |x(i) - x(i-1)| \quad (5.1)$$

The two averages  $S$  and  $L$  are computed on this CF as

$$S(i) = S(i-1) + (CF(i) - S(i-1))/t_1 \quad (5.2)$$

$$L(i) = L(i-1) + (CF(i) - L(i-1))/t_2 \quad (5.3)$$

where  $t_1$  and  $t_2$  are 0.2 sec and 5 sec time durations respectively.

The parameters  $TR_1$  and  $TR_2$  are used to detect and confirm the onset of the first seismic arrival and are computed as

$$TR_1(i) = CF(i)/L(i) \quad (5.4)$$

$$TR_2(i) = S(i)/L(i) \quad (5.5)$$

The event is detected when  $TR_1$  exceeds a preset threshold level and is confirmed as seismic arrival when  $TR_2$  exceeds its preset threshold level within 1 sec after  $TR_1$ . The time series is only recorded when it passes  $TR_1$  and  $TR_2$  stages on some minimum number of channels within some time interval.

Crampin and Fyfe, 1974 referred equation (5.1) as the one sample mechanism  $CF_1(i)$  (28). They also computed a 4- and 8-sample mechanism on the time series with 25 samples/sec as

$$CF_4(i) = |x(i) - x(i-4)| \quad (5.6)$$

$$CF_8(i) = |x(i) - x(i-8)| \quad (5.7)$$

For each channel  $CF_1$ ,  $CF_4$  and  $CF_8$  are checked in sequence against their preset threshold levels. If any of these mechanisms exceed preset levels then this channel is said to be in trigger state. An event is declared if at least three channels are triggered within a small time interval. For each channel, the time of its first trigger is taken to be the first P-arrival time. In the off line processing system described by Crampin and Fyfe, 1974, the detected event is saved by writing the digitized data onto a digital tape for further processing. Each detected event was saved for at least 80 sec, beyond which the data is saved in blocks of

20 sec until the total number of triggering channels fall below some preset minimum.

Stevenson, 1976 devised two averages S and L on the original time series  $x(i)$  with 100 samples/sec as follows :

$$S = (1/(m-1)) \sum_{i=m-n+1}^m x(i) \quad ; \quad m=5 \quad (5.8)$$

$$L = (1/(n-1)) \sum_{i=1}^n x(i) \quad ; \quad n=50 \quad (5.9)$$

Then, the parameters  $TR_1$  and  $TR_2$  are computed as

$$TR_1 = x(i) / L \quad (5.10)$$

$$TR_2 = S / L \quad (5.11)$$

If  $TR_1 \geq 2$  and  $TR_2 \geq 2$  or if  $TR_1 > 2$  for either of the previous samples and  $TR_2 > 2$ , then the channel is triggered and the seismic phase is picked (93). The function  $TR_1$  is more sensitive than  $TR_2$  to sudden changes in the signal level. This picker algorithm is a modification of Stewart et al., 1971 work. The main dissimilarity is that Stewart et al., 1971 used the first difference  $x(i)-x(i-1)$  rather than the original series  $x(i)$ .

Stewart, 1977 adopted a little different approach to detect the less impulsive P-arrivals in the time series (94). If  $D(i)$  represents the first difference as

$$D(i)=x(i)-x(i-1) \quad (5.12)$$

Then CF is designed as

$$CF(i) = \begin{cases} D(i) & \text{if } g(i) \neq g(i-1) \\ D(i) & \text{if } g(i) = g(i-1) \text{ and } J(i) = 8 \\ D(i) + D(i-1) & \text{if } g(i) = g(i-1) \text{ and } J(i) \neq 8 \end{cases} \quad (5.13)$$

where

$$g(i) = \begin{cases} +1, & \text{if } D(i) \text{ is positive or zero} \\ -1, & \text{if } D(i) \text{ is negative} \end{cases} \quad (5.14)$$

and

$$J(i) = \left| \sum_{k=i-7}^i g(k) \right| \quad (5.15)$$

This technique transfers the incoming signal in such a way that (i) the oscillatory nature of the signal is preserved, (ii) the direction of the first motion is preserved, (iii) the frequency components of the signal below that for the local events, especially the diurnal and longer term drift are reduced, and (iv) slightly emergent onsets have a chance to be detected. Using  $CF(i)$  as defined in equation (5.13) its average value  $\overline{CF(i)}$ , for a preset time interval is computed and when  $|CF(i)/\overline{CF(i)}|$  exceeds a preset value, event is declared. The algorithm held on to a trigger state for 0.5 sec in each case and then examines it for frequency, amplitude and S/N ratio which could qualify the trigger as a seismic event. Stewart, 1977 developed cutoff criteria when the signal remains below the background noise level for at least 2



sec. If these criteria are passed, the system enters into coda processing mode in which the coda duration, maximum amplitude and approximate average frequency are determined. If the criteria are not met, the surveillance mode is immediately resumed.

Allen, 1978 devised a CF sensitive to variation in signal amplitude and its first derivative (5). In examining the CF for picking a seismic phase arrival, the picker algorithm compares the current value of the series of the record to the predicted value. The predicted value is usually taken as some form of the average absolute value of the function. The CF is defined as

$$CF(i) = R(i)^2 + \beta_2 (R(i) - R(i-1))^2 \quad (5.16)$$

where  $\beta_2$  is a weighting constant. The modified signal amplitude,  $R(i)$  (filtered to remove DC offset), is defined as

$$R(i) = \beta_1 R(i-1) + (x(i) - x(i-1)) \quad (5.17)$$

where  $\beta_1$  again is a weighting constant. Using this CF, STA and LTA are computed similar to Stewart et al., 1971 as follows

$$STA(i) = STA(i-1) + \beta_3 [CF(i) - STA(i-1)] \quad (5.18)$$

$$LTA(i) = LTA(i-1) + \beta_4 [CF(i) - LTA(i-1)] \quad (5.19)$$

where  $\beta_3$  and  $\beta_4$  are constants with values ranging from 0.2 to 0.8 and 0.005 to 0.05, respectively. Equation (5.18) and (5.19) are

essentially single pole low pass filters governed by  $\beta_3$  and  $\beta_4$ . If  $STA(i)/LTA(i)$  exceeds a preset threshold level then an event is declared. The first P-arrival is determined by the intersection of the slope of the modified signal amplitude  $R(i)$  with its zero level. Allen, 1978 used a particular end criterion in view of the seismicity of the area to record all the events. If the time differences between occurrence of two events is small, then the previous event is cut off as soon as possible to begin recording of the second event. This criterion terminates the signal well before the end of the earthquake coda. The continuation of the event recording depends on the LTA computed in a particular manner on CF and the number of zero crossing etc. The time series is checked for the minimum number of the peaks after the P-onset, the frequency dispersion and the shape of the coda. If these tests are passed, then the time series is recorded as seismic event.

McEvelly and Major, 1982 designed the algorithm with the following features : (i) the time series is digitized at the rate of 100 samples/sec with 12 bit resolution (ii) the mean is removed from the time series  $x(i)$ , (iii) a new time series  $CF(i)$  is formed as

$$CF(i) = (1/n) \sum_{k=i-n}^i x(k) \quad (5.20)$$

with  $n$  equal to previous 16 or 32 points, (iv) LTA of 4096 points and STA of 16 points are taken over  $CF(i)$ , and (v) if STA exceeds LTA by a specified constant, then a trigger point is found

otherwise the algorithm waits for a new digitizing point and the sequence starts all over again (63).

Baer and Kradolfer, 1987 has modified Allen's, 1978 work by taking CF in the form of a envelope function as given by

$$E(i)^2 = R(i)^2 + R(i)^2 / \omega(i)^2 \quad (5.21)$$

where

$$R(i) = R(i) - R(i-1) \quad (5.22)$$

The instantaneous frequency  $\omega(i)$  is approximated by the ratio of the sum of  $R(i)$ 's and its first difference up to the present sample from the beginning of the record (12). Then another function is created from  $E(i)$  as

$$SF(i) = E(i)^4 \quad (5.23)$$

whose signal to noise behavior is much more distinct and then the CF is computed as

$$CF(i) = (SF(i) - \overline{SF(i)}) / S(i) \quad (5.24)$$

where  $\overline{SF(i)}$  is the average SF, and  $S(i)$  is its variance taken from the beginning of the series to the present point. When the CF value increases above 10, the channel comes in trigger state and the pick flag is set.  $S(i)$  is continuously updated till CF is

less than 20 to allow for the variation of the noise level. A declared event is confirmed as seismic event only if CF remains in trigger state continuously for a preset time interval otherwise the pick flag is cleared. Their method for determining precise arrival times for a single trace yields excellent results for local, regional and teleseismic events.

Anderson, 1978 proposed a different method to compute the CF. The DC bias is removed from the incoming time series and a moving average of the absolute values of the modified signal amplitude is defined as

$$R(i) = (1/(n+1)) \sum_{i=k-n}^k x(i) \quad (5.25)$$

where the length of the time window is  $n\Delta t$ ,  $\Delta t$  being the digitizing interval (9). The  $R(i)$  is used to compute the threshold level. The CF is obtained by saving zero crossing points and points corresponding to the maximum amplitude only (either positive or negative). This CF removes the high frequency content from the time series but the oscillatory character of the signal is still preserved. It consists of a series of serrations each of which is referred to as a blip. If the duration of the blip exceeds 0.06 sec and the normalized amplitude exceeds a preset threshold level then the tentative P-arrival is marked. If the tentative P-arrival is not confirmed which is done by searching for coda of the event, then the next blip is examined. If coda is found, the event is confirmed as seismic event and recorded.

### 5.2.2 Frequency Domain Algorithms

The waveform of a seismic event differs with that of background noise not only in the amplitudes distribution but also in the frequency content. By using a detector based on a transform of the data into a frequency domain, changes in the amplitude and frequency can be sensed for determining the occurrence of a seismic event by marking the first seismic arrival in the incoming time series. The precision in timing the phases dictates that the very powerful frequency domain methods available to detectors are not immediately applicable to pickers (6). In frequency domain analysis, a section of record is examined for the presence of a specified spectral distribution which indicates seismic energy in that section of record. The power of the method to detect and resolve the specified spectral distribution in the presence of masking noise is dependent on the length of the window, but the timing precision, the ability to specify at exactly which sample the seismic energy first appears, is inversely proportional to this window (6).

Goforth and Herrin, 1981 made first use of the Walsh transform by the development of an automatic seismic signal detection algorithm (40). The Walsh transform goes into sequency domain which is more general, of which frequency is a member. Since the amplitude of a Walsh function is either +1 or -1, the Walsh transform can be accomplished in a computer with a series of shifts and fixed point additions. The detection threshold, which

is computed from the distribution of previous 512 sums of the absolute values of the time series is defined by

$$\text{Threshold} = V_{50} + K ( V_{75} - V_{50} ) \quad (5.26)$$

where  $V_{50}$  is the median of the distribution of previous 512 values,  $V_{75}$  is the 75th percentile of the distribution of the previous values and  $K$  is an arbitrary constant set by the operator. If the current value of the sum of the absolute values of the Walsh coefficients exceeds the threshold, a signal is detected. If it does not exceed the threshold, the sum of the values is ranked among the previous 512 values and the oldest values are discarded. Michael et al., 1982 also made use of the Walsh transform and based the decision of marking the seismic arrival on a matrix computed from the Walsh transform of the data (64). This allows them to detect changes in the amplitudes of the waveform as well as frequency shifts.

In the present work we have considered only the time domain algorithm and further details of the frequency domain algorithm can be seen in the work by Goforth and Herrin, 1981 and Michael et al., 1982.

### 5.3 PHASE PICKER DEVELOPED

This section describes the phase picker developed under this study along with its implementation in the form of computer

program. The development of the phase picker was necessitated due to the simple event detection technique being used by the DAS to acquire digital data on earthquake occurrence from TDSA, which generates voluminous data by recording higher number of false alarms along with the seismic events. Since manual analysis of the data is a time consuming job, an endeavor is made to automate the data processing by developing a phase picker. The phase picker should, firstly, select the seismic events out of the data recorded by DAS using simple event detection technique and secondly, it should mark the P-arrivals with good accuracy and then confirm the time series as seismic event.

The phase picker developed incorporates, briefly, the DC offset removal from the incoming time series, modification of this time series into CF to enhance the changes in the time series arising due to the incoming seismic phases, STA-LTA algorithm to detect these changes to mark the onset time of the P-arrival, end criterion to mark the end of the coda of the event and confirmatory tests to confirm the time series as seismic event. Firstly, the DC offset and very low frequency content (approx. 0.1 Hz) is removed from the time series. This time series is then modified to CF to enhance the changes in the time series arising due to the seismic phase arrivals. The CF enhance the amplitude as well as the frequency changes. Since the frequency content of seismic waves is different compared to that of background noise, the STA is computed in such a way as to filter out the frequency content of the background noise. Similarly, the LTA is the the

representation of the background noise and the signal content (as in STA) are removed from the LTA so as to increase the S/N ratio. If the STA/LTA exceeds above some threshold value, the event is declared and end criterion is then tested to mark the end of the coda of the event. The part of the time series between P-onset and the end of the event is tested by two confirmatory tests which check the frequency dispersion ( Test I) of the time series and the coda slope ( Test II) to confirm the time series as seismic event. Once the P-arrivals are marked from all the stations, Test III checks the arrival times. The following is the detailed description of the phase picking algorithm.

### 5.3.1 Automatic Phase Picker Algorithm (APP)

The input time series  $x(i)$  i.e., the ground motion time history of an outstation is passed through standard filters to remove DC bias and low frequency noise. The program does not look back in time and uses only a limited amount of memory both for program instructions and for array scratch pad storage needed during elimination of DC bias.

A single pole, high pass filter with constant  $\beta_1$  controlling its response is implemented in time domain as follows

$$R(i) = \beta_1 * R(i-1) + x(i) \quad (5.27)$$



where  $R(i)$  is the modified time series with out DC bias and

$$\overset{o}{x(i)} = x(i) - x(i-1)$$

Initial conditions are

$$x(i) = 0, \quad i \leq 0$$

$$R(i) = 0, \quad i \leq 0$$

Taking the Fourier transform of the above equation (5.27) as discussed in previous sections ( see equations (4.20) to (4.30)), we obtain the gain of the filter as

$$|H(f)| = \frac{(2-2\cos 2\pi fT)^{1/2}}{(1+\beta_1^2 - 2\beta_1 \cos 2\pi fT)^{1/2}} \quad (5.28)$$

As the high pass characteristics to remove DC bias require

$$H(f) = 0 \quad \text{at } f = 0$$

$$H(f) \neq 0 \quad \text{at } f \neq 0$$

we would require  $\beta_1$  to be close to unity, but not equal to 1 i.e., the all pass filter. Therefore, we choose the value  $\beta_1 = 0.995$  as is clear from the response of the filter as shown in Fig. 5.3.

After the removal of the DC bias and the very low frequency content, the next step is to compute the CF from this modified time series  $R(i)$ . Various forms of CF's are considered to enhance the S/N ratio and it is finally seen that a CF

constructed as the sum of the squares of the  $R(i)$  and its first difference yields higher S/N ratio (refer Fig 5.2). The CF, therefore, is defined as follows

$$CF(i) = R(i)^2 + \overset{\circ}{R(i)}^2 \quad (5.29)$$

where  $\overset{\circ}{R(i)} = R(i) - R(i-1)$

The change in amplitude of the time series is taken care by the first term and the frequency changes are sensed by the second term of the equation (5.29). This type of CF is chosen because of the trade off between the accuracy of the P-onset to be picked and the computation time.

The next part of the picker developed is based on the simple STA-LTA algorithm. Better performance of the averaging techniques can be made if the filtering process is also involved while taking the averages. In order to enhance the S/N ratio, STA and LTA should filter out their respective noises. Averaging techniques are used to distinguish the background noise with the incoming signals. The averages, LTA representing the background noise level and STA representing the incoming signal, are taken such as to filter out those frequency contents which are not of interest.

The STA and LTA can be computed incorporating the requisite filters. The technique for the computation of STA and LTA is the same. In the equation (4.20) if the output  $y(i)$  is

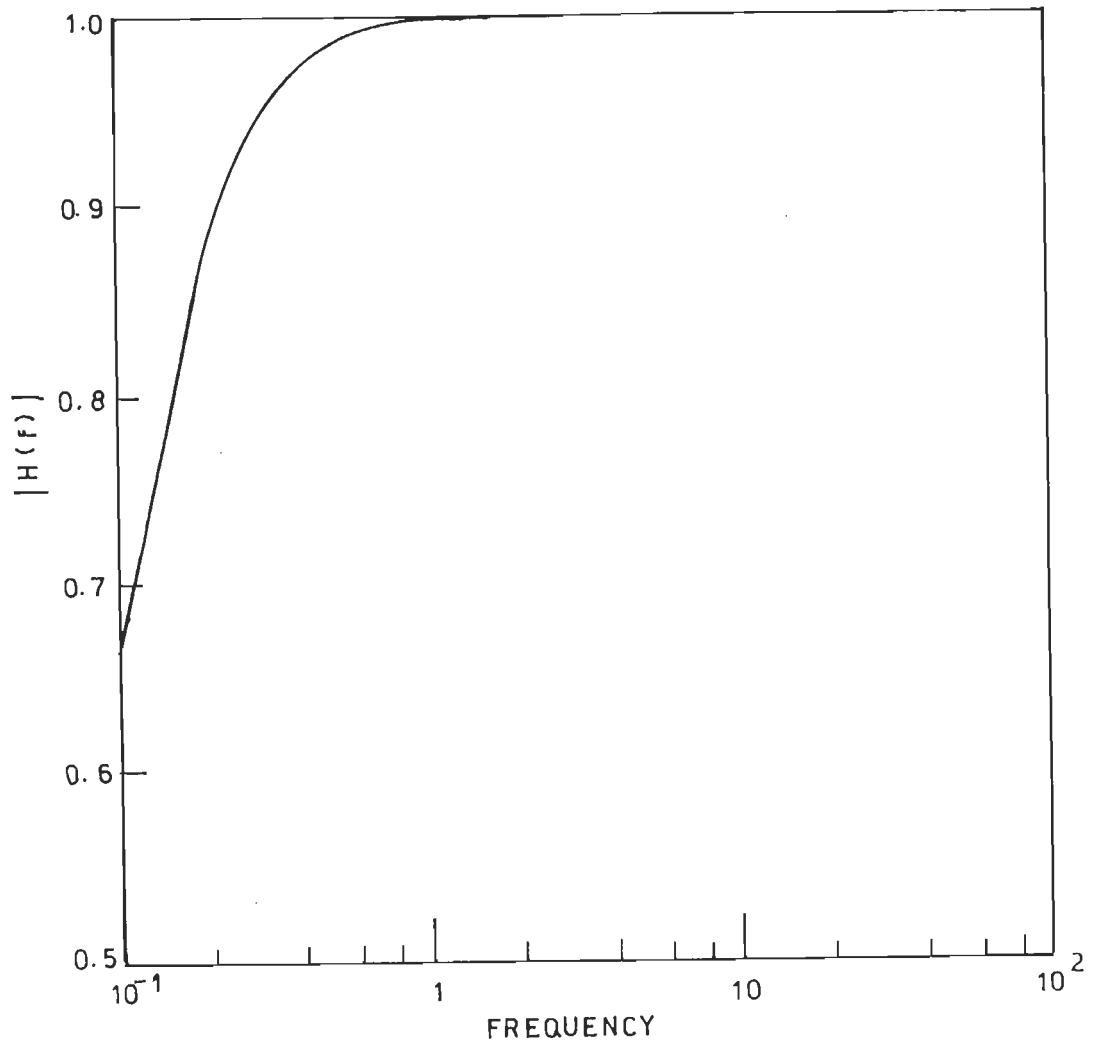


Fig. 5.3\_ Gain of high pass filter with  $\beta_1 = 0.995$

replaced by STA(i) and the input x(i) by CF(i), then it takes the form as

$$STA(i) = \sum_{k=0}^m b_k CF(i-k) - a_1 STA(i-1) \quad (5.30)$$

As the low frequencies have to be retained, we select the low pass filter from Table 4.1 by putting  $b_0$  as  $(1-\alpha)$ ,  $b_1$  as 0 and  $a_1$  as  $-\alpha$  in the above equation. Then

$$STA(i) = (1-\alpha) CF(i) + \alpha STA(i-1) \quad (5.31)$$

Similarly for the LTA, we have

$$LTA(i) = (1-\alpha) CF(i) + \alpha LTA(i-1) \quad (5.32)$$

Now by choosing the value of  $\alpha$  in equation (5.31) and (5.32), the STA and LTA are taken as averages over the CF including the filtering process to filter out their respective noises. The choice of  $\alpha$  depends on the seismic signal expected so as to filter out the noise outside the range of interested frequencies while computing STA. In case of LTA,  $\alpha$  is selected to filter out all the noise and the average should represent the zero level which in turn increases the S/N ratio tremendously while computing the trigger ratio (STA/LTA). This averaging technique is essentially integrating the signal using low pass filters of single pole implemented in time domain. The design of STA and LTA now, becomes the design of single pole, low pass

filters with different time constants signifying the range of frequency of interest for that particular average. The LTA is representative of the background noise level and can be called as a predicting factor for the incoming signal. The STA is sensitive to rapid changes in the CF and thereby aid in accurate timing of the seismic phases. The gain of the filter, therefore, using equation (4.30) is given by

$$|H(f)| = \frac{1-\alpha}{(1-2\alpha \cos 2\pi fT + \alpha^2)^{1/2}} \quad (5.33)$$

The constant  $\alpha$  is chosen as 0.33 and 0.992 for STA and LTA respectively. The response of the filter is shown in Fig 5.4 and Fig 5.5.

The P-onset time is marked by comparison of the ratio of STA/LTA by a threshold, which is fixed by the operator in the initial interaction with the program. When STA/LTA ratio exceeds the threshold, an event is declared and the program searches for the preceding zero crossing of the modified time series  $R(i)$ . The zero crossing time is recorded as the P-onset time. The first motion is marked by the sign of the maximum amplitude between the P-onset and the subsequent zero crossing. The P-onset time, maximum amplitude and first motion information is stored in a pair of scratch pads for later use by the analysis routine.

A phase picker must apply some criteria to confirm triggered events as seismic events. In the present algorithm,

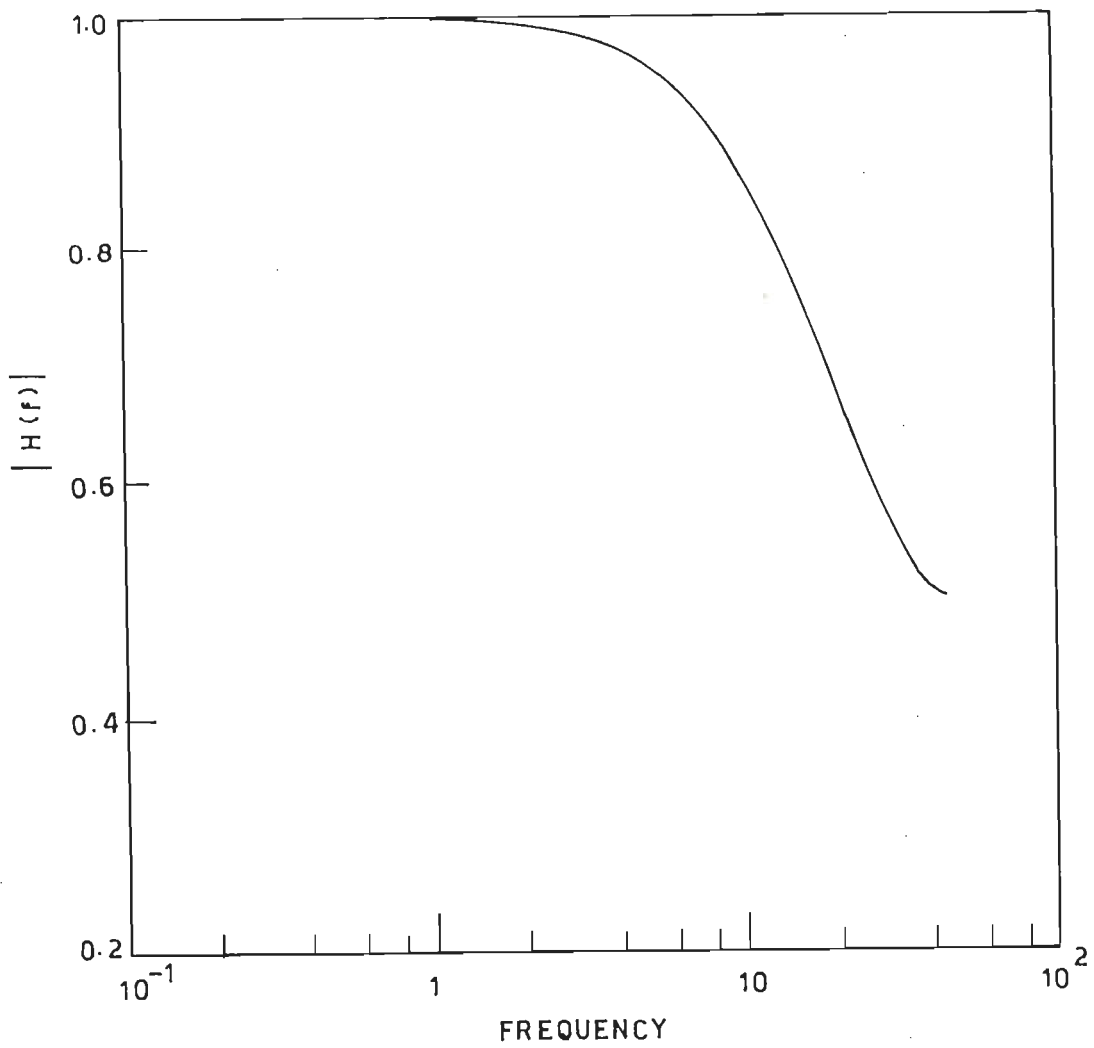


Fig. 5.4 - Gain of low pass filter with  $\alpha = 0.33$  used for STA

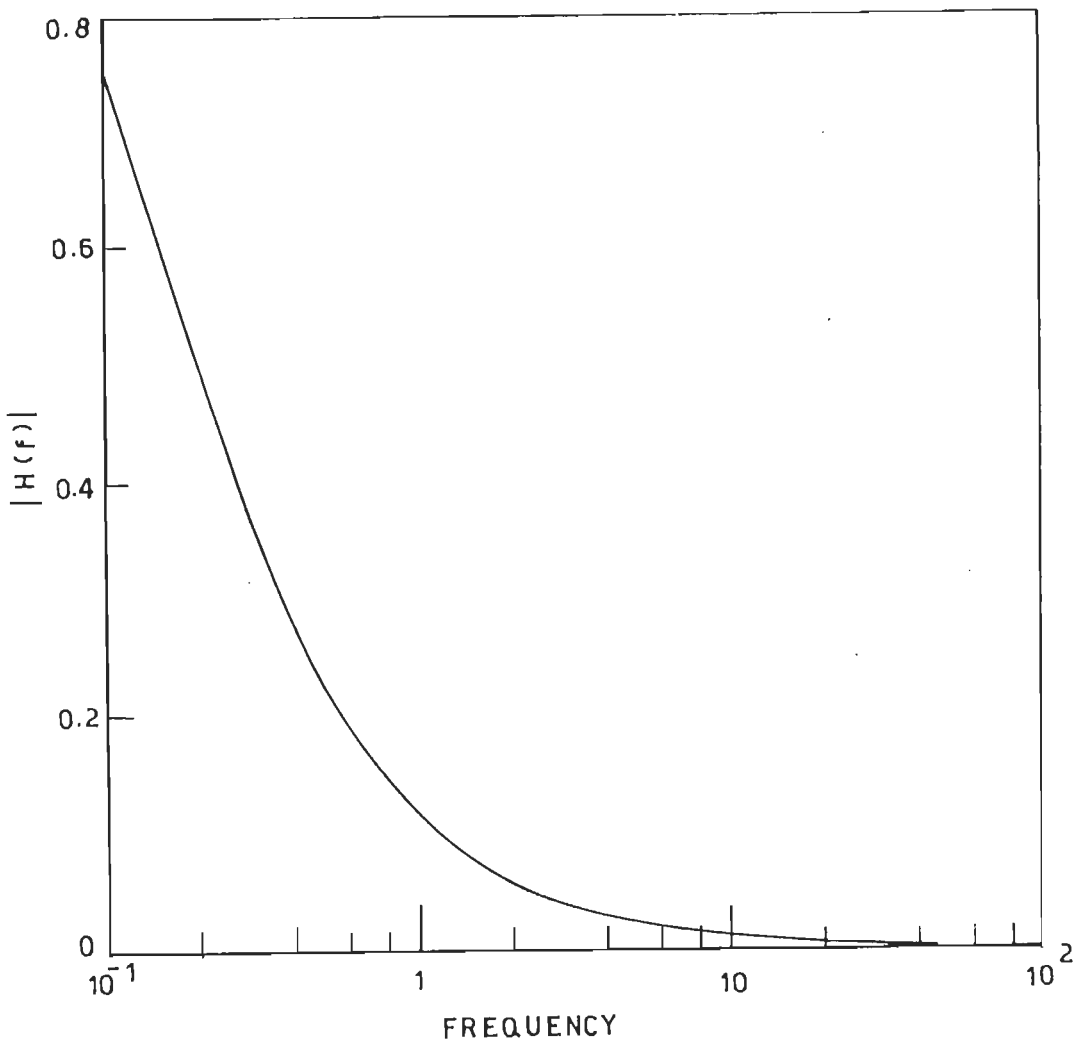


Fig.5.5\_ Gain of low pass filter with  $\alpha = 0.992$  used for LTA

three criteria have been used which must be met in the case of a seismic event. The first criteria is the frequency test in which a dispersion of the frequency is computed. A key procedure (subroutine) divides the observed coda into half second intervals and counts the number of peaks in each interval, storing the numbers in short scratch pad array. The mean frequency of the seismic signal is computed. The measure of frequency during the event is computed by calculating the standard deviation. For example, cultural noise such as passing traffic will typically be monochromatic compared to earthquakes. If the dispersion is more than a prefixed threshold then the event is passed as seismic event otherwise the program ask for another event to be processed.

The second criteria is based on the shape of the observed coda of the event. This procedure quantifies the shape of the observed coda in terms of relative steepness of onsets and decays in the envelop shape. The procedure selects the largest peak in each half second interval and compares it with the largest in the following interval. The difference between the peak amplitude is squared and added to the variable "POS" if the envelop is increasing and to 'NEG' if the envelop is decreasing. When the entire coda has been processed the number SHAPE is computed as

$$\text{SHAPE} = (\text{POS}/\text{NEG})^{1/2} \quad (5.34)$$

Earthquakes with steep onsets and slow decays tend to produce values of the parameter SHAPE around one or greater, whereas noise



bursts tend to have values of this ratio less than one. If this test is passed then the event is confirmed as seismic event and the package enters into the checking of P-onset times marked at different stations.

The third confirmatory test which is run after marking P-onset times at each station, is the difference of the arrival times of the P-phases picked at different stations. This test is made after the picking of the seismic phases from all the stations and thus this test is made for the array and not for a particular station or a single channel. The difference of the arrival times of a seismic phase at two stations should obviously, be not greater than the total travel time of the seismic phase picked by the algorithm, between the two stations.

The event is checked for its minimum duration so as to reject transient spikes by comparing the number of zero crossings with a threshold signifying the length of the event.

We have used a simple end criterion considering that after the end of the event the background noise level normally is the same as before the start of the event. So whenever the signal level (an average over a small interval of time) is equivalent to the noise level average, the end of the event is declared. Since the data is collected already by a trigger event detection technique, the end of the event if not found by APP, is taken to be the end of the recorded event data.

### 5.5.2 Dynamic Threshold

The algorithm developed in the previous section is based on the threshold value which have to be set empirically by studying the background noise and the type of earthquakes (teleseismic, regional or local). Depending on the trigger threshold, the seismic events may be rejected if the threshold is chosen to be on the higher side and on the second hand if we choose the TR to be low, most of the false alarms can be judged as seismic events.

To overcome this difficulty APP can be easily modified to include some of the statistical analysis on the time series. The raw data is the same as that in the previous section up to the input to the characteristic function. But if we see equation (5.29), it is one of the form of envelop function of a time series if second term on right hand side is multiplied by the instantaneous frequency  $\omega(i)$  of the time series. To calculate the instantaneous frequency in such an analysis work is a lengthy process, and this is not suitable to be incorporated in on-line data processing. As an alternative one can approximate  $\omega(i)$  by (Baer and Kradolfer, 1987)

$$\omega(i) = (\Sigma R(i)^2 / \Sigma R(i)^2)^{1/2} \quad (5.35)$$

If we put the value of  $\omega(i)$  in equation (5.29), the characteristic function becomes

$$CF(i) = R(i)^2 + ((\sum R(i)^2) / (\sum R(i)^2)) R(i)^2 \quad (5.36)$$

To average out the background noise level, the technique of Baer and Kradolfer, 1987 is used to define the characteristic function as follows

$$MCF(i) = (SF(i) - \overline{SF(i)}) / S(i) \quad (5.37)$$

where

$$SF(i) = CF(i)^2$$

and  $\overline{SF(i)}$  and  $S(i)$  are the average and variance of  $SF(i)$ . When the MCF increases above a preset threshold, the pick flag is set. Variance of the series is further updated if CF is less than double of the preset threshold to allow the variation of the noise level.

The false alarms are rejected by checking the up time of the event which is 1 sec for which the pick flag should remain set otherwise the pick flag is cleared. As the characteristic function is not smooth due to the variation in frequencies in the incoming signal and other complications in the time series, the CF may drop below the threshold level for very short time intervals which results in premature termination of a phase detection. To overcome this problem if MCF drops below the threshold for less than 0.2 sec the pick flag is not cleared. Other criterion for testing the time series for seismic event and recording technique of phase list is the same as that of APP.

### 5.3.3 APP Computer Program

The computer program, developed in TURBO PASCAL (Ver 5.0), is in interactive mode which asks for the information about input data file name, the sampling rate of time series in the data file, threshold value of STA/LTA ratio to pick up the P-onset time (87). The program gives the output in form of P-onset time, UP/DOWN motion, maximum peak amplitude and coda length. The program contains 13 procedures (subroutines) to accomplish various tasks. The procedures setvedio, putstring, putprompt, getstring, setpromptstring are being used to facilitate the input data to the program. Some of the procedures in the program are not directly related to the phase picking algorithm but are designed to make the program as user friendly. The procedure getreal and getpromptedreal are used to read the input data. The procedures P3 and P4 are used to compute CF, STA, LTA and to verify the presence of zero crossings. The peak index is updated by procedure P0. The procedure frequency and coda slope are used to test the time series for seismic event. Procedure convert is used to change the format of the input file if it is not stored in free format. The flow chart of the program APP is given in Fig 5.6 which is self explanatory. The listing of the source code of the program is given in Appendix I.

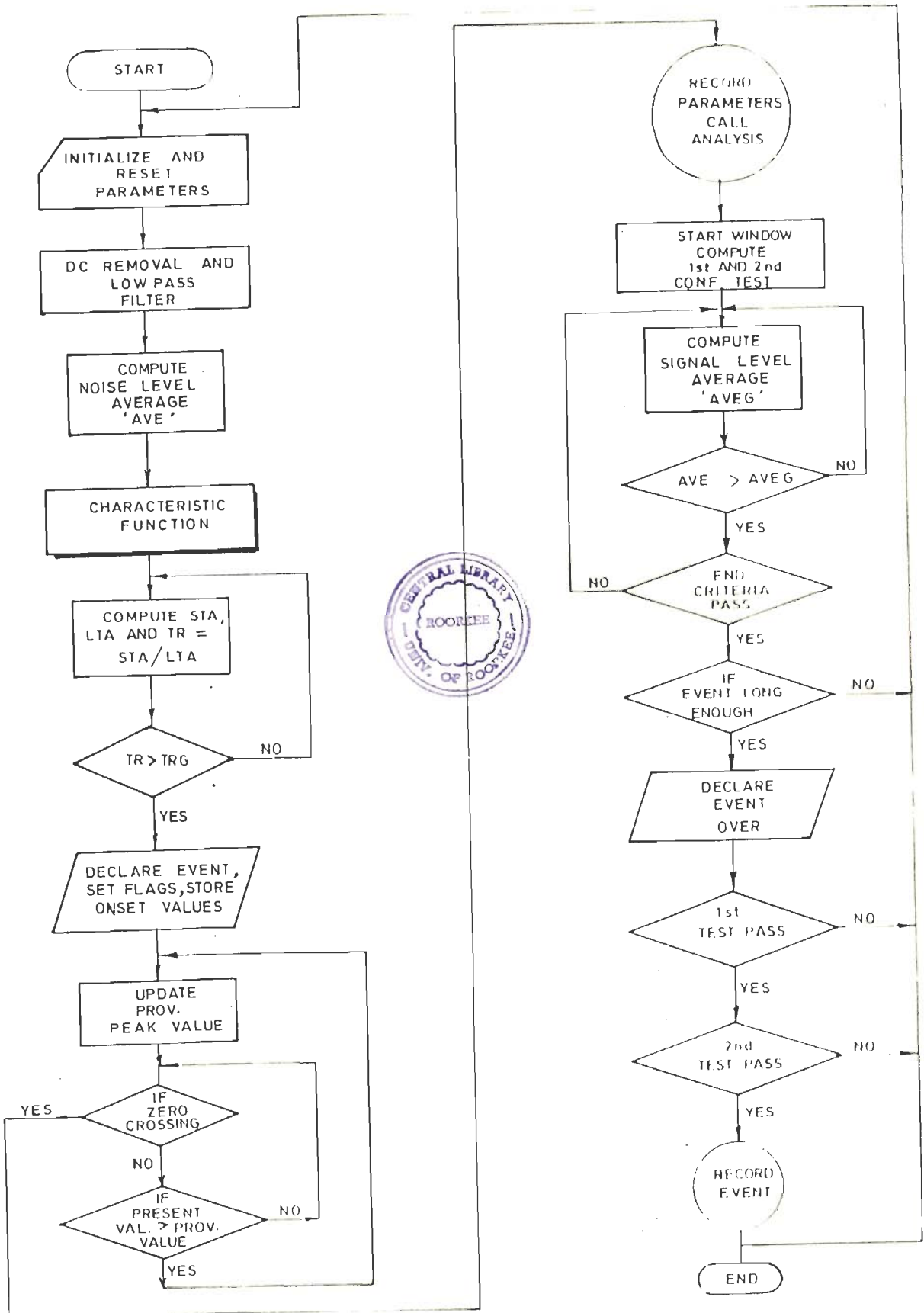


Fig.5.6 \_ Flow chart of software package for Automatic Phase picker

# CHAPTER # 6

## RESULTS AND DISCUSSIONS

---

## RESULTS AND DISCUSSIONS

---

### 6.1 INTRODUCTION

This chapter contains the results obtained from the analysis of the data recorded between 13-02-89 to 07-05-89 by TDSA and a discussion of the results with respect to the present geological and tectonic environment of the region. The telemetered data has been acquired according to the data acquisition procedures as discussed in Chapter 4 and using the minimum triggering at three stations. The post processing of the data has been done according to the data processing procedures using the software available and developed specially for the purpose explained earlier. This being the first telemetered digital seismic array installed in the Himalaya, the aim of the present study has been to develop the procedures and methodology for the processing of the data acquired from TDSA on a routine basis to identify the seismic events and to compute the onset times of first arrivals of seismic waves, direction first motion, maximum peak amplitude, coda length and frequency decay pattern in respect

of each seismic event. This information is then used to determine the hypocentral parameters and magnitude of each event and a composite fault plane solution. Further, the existing formulations are used to compute the source parameters e.g., seismic moment, stress drop, source dimension, slip and energy released pertaining to each event. Least squares linear regression analysis have been used to determine the form of empirical relationships between the magnitude and different source parameters. The results obtained are interpreted to understand the phenomenon of earthquake occurrence in the Garhwal Himalaya.

## 6.2 DATA SET

The values of trigger parameters are selected to record local seismic activity taking into account the various characteristics of the region as discussed in Chapter 3. Based on these parameter values selected for this region, the digital events data on local seismic activity has been acquired during the period 13.02.1989 to 07.05.1989 on magnetic tapes (2400 ft. half inch 9 track magnetic tapes). Data of one seismic event recorded during the installation and testing phase is also included. Due to the high altitude of the CRS it experiences heavy snowfall in the winter season resulting into shutdown of DAS during that period. Further the array is located in a rough terrain, the power supply to the system has had frequent breakdowns directly affecting the data acquisition. As the data could only be acquired for intermittent periods the small number of seismic events recorded by DAS and analysed in this study can be construed at best a



sample of the seismicity of the region. A total of 530 events triggered at 3 or more stations have been recorded by DAS for a total run time of 781 hours during this period.

### 6.3 RETRIEVAL OF THE DATA

The data tapes are brought to Roorkee from the CRS to Roorkee for the retrieval and post processing of the recorded data. The magnetic tapes containing the data in binary mode and Industrial Compatible Format are copied to the hard disc of DEC 2050. Using the event log and the map of the tape obtained from PDP 11/23 computer system, the number of triggered time series are cross checked as one block of 4096 bytes is copied onto two pages of the hard disc of DEC 2050. After copying the time series the program TMDC is run to check the date and time of the event which is available in the event log made at the time of recording of the time series as discussed in the section 4.2.

The data transferred to the hard disc of DEC 2050 in binary mode and Industrial Compatible format is converted into the integer form using TMD software program as described in section 4.2. The data is stored in the form of files, namely, date and time file i.e., DNT.DAT and seismogram files i.e., S1.DAT to S8.DAT. The data files are transferred to PC from DEC 2050 system using XTALK/KERMIT/PROCOMM standard programs at baud rate of 4800 bits/sec and stored on floppies. Due to high sampling rate, the volume of data for a seismogram from one station for a particular event could not be copied on a single floppy. In view of the large

volume of data, some of the data processing procedures are performed by taking only 90 samples/sec from the recorded data which does not deteriorate the information required for such an analysis.

#### 6.4 VISUAL ANALYSIS OF THE DATA

The procedures for the visual analysis of the data are discussed in section 4.3. The full seismogram of an event is plotted on the screen of the PC to search for the characteristics of a seismic event. For the seismic events, onset times of P- and S-arrivals are determined as discussed in chapter 4. In cases, when the onsets of P- and S-phases are not easily seen, the seismograms are plotted in parts for better resolution. To look at the seismogram in different frequency windows, digital filtering is done using the filters as developed and discussed in section 4.3.2. The filters are mainly applied for DC offset removal and low pass filtering of the time series with a cut off around 15Hz or as required in particular cases. All the 530 triggered events are visually examined for seismic events and associated parameters like P- and S-arrival times, up/down motion of the first arrival, maximum trace amplitude and coda length of the event. Out of 530 triggered events only 18 events are found to be the seismic events based on the coda shape and other characteristic features of the seismograms. All the remaining 512 triggered events are found to contain noise spikes due to environmental/electrical disturbances. Most of the triggered events detected by the trigger event detection technique are characterised by high amplitude

noise spikes due to above reasons; followed by a constant amplitude which shows that they are not arising from any seismic source. The maximum value of such type of constant amplitudes recorded in the time series is generally about 10,000 micro volts. More than seventy percent of the events are recorded due to presence of one or two peaks of maximum amplitude due to which the STA increases tremendously giving rise to higher trigger ratio, and there by the incoming time series triggers the system and is recorded by DAS.

In order to check the validity of the triggered event data as recorded by the DAS, the digital data acquired by the system from one station (NNR) is compared with the corresponding analog records of the Benioff Seismograph installed at the same station. This Benioff seismograph and Willmore seismometers of this array are installed on the same platform in this observatory. Fig 6.1 shows a comparison of the records from the two systems for the event which occurred on 29-03-89. The ground motion recorded by TDSA at Narendranagar observatory in digital form have been plotted on the same scale as if it is recorded on Benioff seismograph and is compared with the corresponding record of the Benioff seismograph of the same date and time.

The P- and S- arrival times, direction of the particle motion of the first arrival, S-P time, maximum trace amplitude recorded and coda length, wherever possible, have been determined for the 18 seismic events by visual analysis of the digital seismograms plotted on the screen of the PC and are listed in Table 6.1.

## 6.5 AUTOMATIC ANALYSIS BY PHASE PICKER

All the 530 triggered events recorded by TDSA have also been analysed using automatic phase picker software (APP). The program APP is run for all the recorded time series from each station for all triggered event. APP has picked 403 P-phases from 178 events and rejected 1680 time series from 352 triggered events as false alarms. After picking the P-phases, the confirmatory tests are run to confirm the time series as seismic event. The time series from individual stations are passed through confirmatory test I (i.e., frequency dispersion test) and test II (coda shape test). When all the stations of recording an event are checked for these tests, the P-arrival times from all the stations are then checked simultaneously for confirmatory test III (i.e., difference in P-arrival times test). The events for which APP has picked P-phase only at one station are rejected as false alarm by this test. The events for which P-phases are passed by test I and II for at least two stations, are tested for the difference of P-arrival times for all possible pairs of stations. If any one pair has passed test III the corresponding event is declared as seismic event.

Fig 6.2 shows the frequency dispersion values obtained from 173 time series by the APP. The values marked as (O) of 70 time series are from 18 seismic events and the values marked as ( $\Delta$ ) are of 78 noise bursts from 42 triggered events which are passed as likely seismic events by the confirmatory test I. Rest

DATE \_ 29.3.89.      TIME 10:59:18.00

BY BENIOFF SEISMOGRAPH

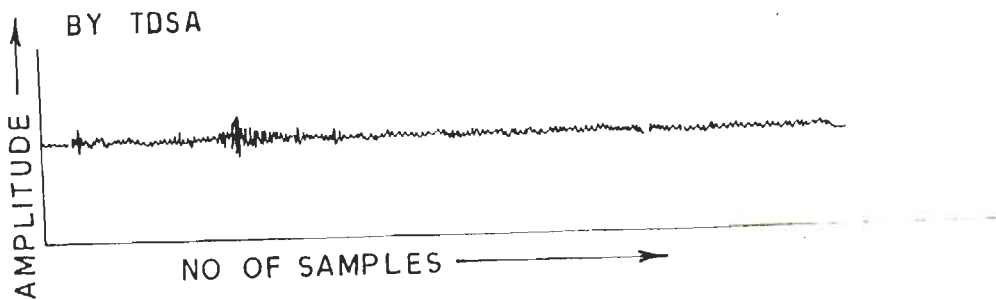


Fig. 6.1\_ Comparison of records for Narandranagar observatory obtained by Banioff Seismograph and TDSA for the same event

TABLE 6.1 RESULTS OF VISUAL ANALYSIS OF TRIGGERED EVENTS  
RECORDED BY TDSA. ONLY THE SEISMIC EVENTS ARE TABULATED

Sl No.	DATE	STN	P ONSET			S-P (SEC)	MAX AMPL ( $\mu$ VOLT)	FIRST MOTION (U/D)	CODA LENGTH (SEC)
			ARRIVAL TIME (H) (M) (S)						
1.	25.11.89	SUR	05:37:29.911			23.6	563	D	143.30
		NNR	05:37:32.744			22.1	1209	U	148.00
		POR	05:37:32.811			24.0	861	D	150.60
2.	08.03.89	SUR	11:36:43.533			-	423	U	-
		NNR	11:36:45.866			-	172	U	-
		DHR	11:36:46.833			-	160	U	-
		POR	11:36:50.100			-	52	D	-
3.	16.03.89	SUR	22:06:39.444			-	469	D	126.66
		NNR	22:06:42.466			-	421	U	146.66
		DHR	22:06:42.411			-	513	D	135.55
		POR	22:06:45.877			-	251	U	143.33
4.	29.03.89	SUR	10:59:21.933			-	413	U	58.88
		NNR	10:59:24.222			6.1	175	D	71.00
		DIIR	10:59:21.933			-	314	U	63.00
		POR	10:59:20.233			-	1208	D	72.00
5.	30.03.89	SUR	03:04:48.025			-	1200	U	-
		NNR	03:04:50.816			-	623	D	-
		DHR	03:04:52.247			-	885	D	-
		POR	03:04:54.469			-	317	U	-
6.	02.04.89	SUR	10:39:17.900			-	253	D	81.67
		NNR	-			-	-	-	-
		DIIR	10:39:08.644			-	503	D	92.00
		POR	10:39:07.933			-	470	U	82.20
		RRK	10:39:09.544			-	-	-	86.00
7.	04.04.89	SUR	01:12:51.808			-	1505	U	-
		NNR	01:12:50.822			-	581	D	-
		DHR	01:12:47.655			-	813	D	-
		POR	01:12:45.461			-	2014	U	-
		RRK	-			-	-	-	-
8.	09.04.89	SUR	08:03:55.944			-	364	U	-
		NNR	08:03:55.766			-	110	U	-
		DIIR	-			-	-	-	-
		POR	08:03:50.177			-	235	D	-
9.	11.04.89	SUR	09:36:42.388			-	206	U	-
		NNR	09:36:45.222			7.2	213	U	-
		DHR	09:36:41.333			-	-	-	-
		POR	09:36:42.755			-	140	U	-

TABLE 6.1 CONTINUED

Sl No.	DATE	STN	P ONSET			S-P (SEC)	MAX AMPL ( $\mu$ VOLT)	FIRST MOTION (U/D)	CODA LENGTH (SEC)
			ARRIVAL TIME (H) (M) (S)						
10.	11.04.89	SUR	10:55:47.361			2.4	209	D	-
		NNR	10:55:47.486			-	155	D	-
		DHR	10:55:53.027			5.4	180	U	-
		POR	10:55:52.611			4.9	110	U	-
		RRK	-			-	-	-	-
11.	12.04.89	SUR	17:39:30.000			-	860	D	54.50
		NNR	17:39:35.366			-	217	D	71.00
		DHR	17:39:31.366			-	922	U	58.00
		POR	17:39:31.266			-	225	U	-
		RRK	-			-	-	-	-
12.	16.04.89	SUR	-			-	-	-	-
		NNR	02:07:70.577			5.2	516	-	-
		DHR	02:07:64.466			3.1	820	-	-
		POR	02:07:64.466			-	523	-	-
		RRK	-			-	-	-	-
13.	19.04.89	SUR	04:38:71.688			12.1	207	U	76.67
		NNR	04:38:69.433			12.6	195	U	57.78
		DHR	-			-	-	-	-
		POR	04:38:57.644			8.6	1550	D	30.22
		RRK	-			-	-	-	-
14.	22.04.89	SUR	21:40:52.444			-	1573	D	91.80
		NNR	21:40:57.100			-	1251	U	85.00
		DHR	21:40:54.322			-	929	D	99.00
		POR	21:40:60.700			-	1024	U	77.00
		RRK	-			-	-	-	-
15.	23.04.89	SUR	11:42:38.944			-	76	-	-
		NNR	11:42:42.266			-	71	-	-
		DHR	11:42:39.655			-	-	-	-
		POR	11:42:44.488			-	30	-	-
		RRK	11:42:34.500			-	-	-	-
16.	03.05.89	SUR	11:26:65.922			9.6	42	U	92.23
		NNR	11:26:62.988			-	228	D	109.55
		DHR	11:26:57.300			-	310	U	98.44
		POR	11:26:57.366			6.3	256	U	110.64
		RRK	-			-	-	-	-
17.	03.05.89	SUR	21:15:35.800			-	15	U	34.00
		NNR	21:15:34.933			3.7	217	D	55.97
		DHR	21:15:29.066			-	126	U	62.92
		POR	21:15:29.500			-	135	D	71.46
		RRK	-			-	-	-	-
18.	04.05.89	SUR	-			-	-	-	-
		NNR	01:33:37.500			-	68	U	34.55
		DHR	01:33:36.188			-	21	U	36.23
		POR	01:33:49.400			8.1	43	D	-

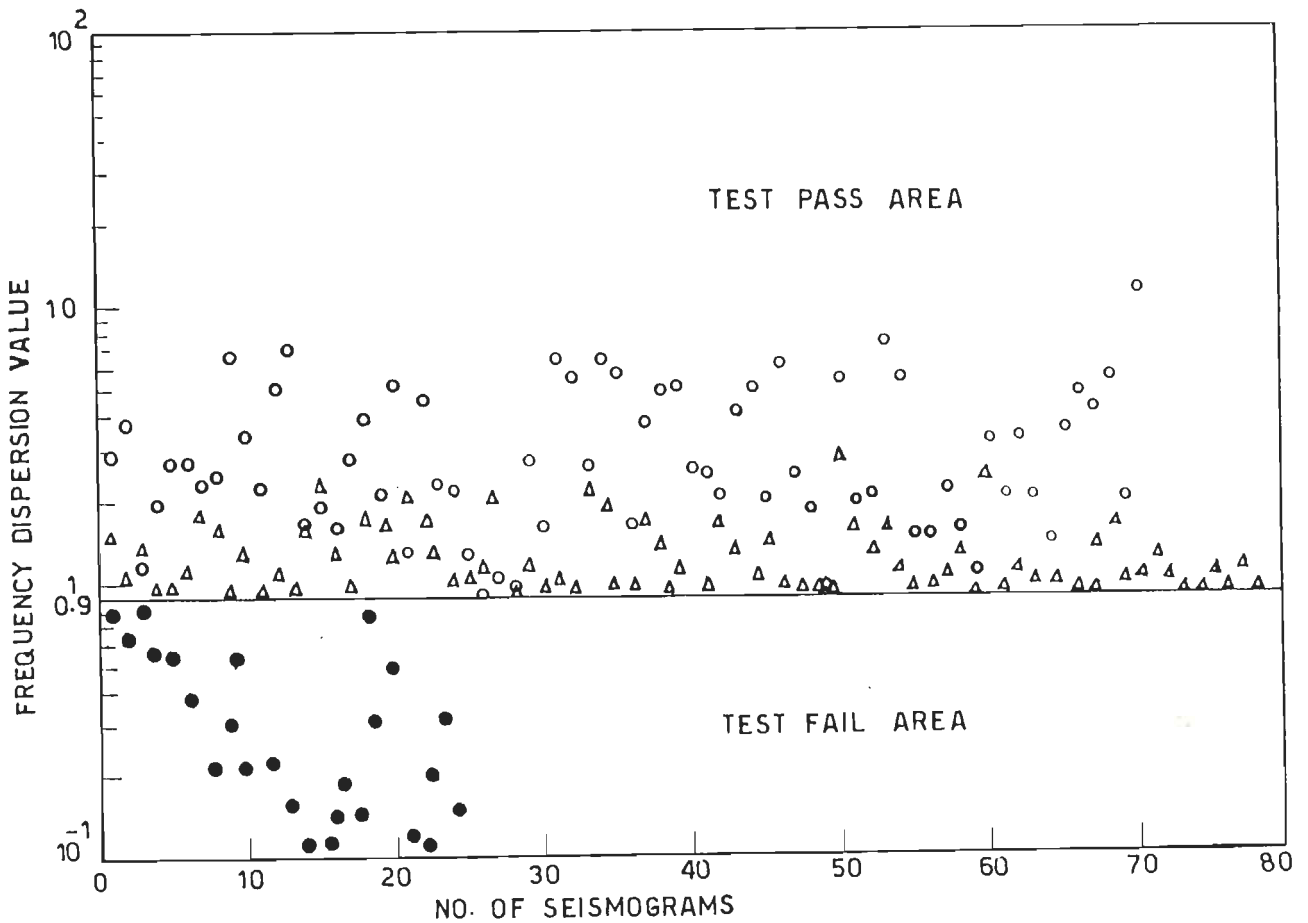


Fig. 6.2 - Frequency dispersion values of time series obtained using APP. The time series corresponding values marked as (o) and ( $\Delta$ ) are passed by this test as seismic event whereas those corresponding to values marked as ( $\bullet$ ) are rejected as false alarms



255 time series from 118 triggered events are rejected as false alarm from this test. Out of 255 triggered time series, only 25 frequency dispersion values are plotted (●) having values between  $10^{-1}$  and 0.9 in the test fail area and other 230 time series having values between  $10^{-1}$  and  $10^{-3}$  are not shown in the Fig. and all are taken as false alarms. The horizontal line drawn through the value 0.9 could be taken as the threshold below which is called the test fail area and the trigger time series whose frequency dispersion values fall in this zone are taken to be as false alarms. The threshold value is chosen on the lower side with the view that none of the seismic event is excluded irrespective of the larger number of false alarms being passed as likely seismic events at this stage.

The second confirmatory test is the coda shape test as explained in section 5.3.2. This test is applied to all the 148 time series passed by test I as likely seismic events. Fig 6.3 shows the plot of coda shape values obtained from 120 triggered time series. The values marked as (○) for 70 time series are from 18 seismic events, the values marked as (Δ) are from 15 time series corresponding to noise bursts from 13 triggered events which are passed as likely seismic events by this test. The 35 values marked as (●) are rejected as false alarms from this test. Other 28 coda shape values having the range between  $10^{-1}$  to  $10^{-5}$ , which are not plotted in the Fig., are also rejected as false alarms by this test. The coda shape value equal to 0.9 is taken as the cutoff value for this test and if the coda shape value is  $\geq$

0.9, the event is passed as seismic event. As in the first test, the bias is for not rejecting any seismic event as false alarm.

The third confirmatory test is the difference of the P-onset times picked up by APP. The difference between the P-onset times at two stations can obviously be maximum equal to the time of reaching of P-wave from first station to the second station or vice versa. The difference of the P-onset times picked up by the phase picker algorithm is compared to that of P-wave travel time between the two stations considering the average velocity of P-wave to be 5.2 km/sec. This test will also reject those time series for which, somehow, the P-phase is not recorded and the time series is either triggered due to S-wave or any later phase arrival. Fourteen triggered events (including one seismic event dated 16-04 89) passed by test I and test II both as likely seismic events are rejected under test III. These 14 rejected events also include one seismic event which occurred on 16-04-89 (confirmed as seismic event by visual analysis). For this seismic event, the P-phase is only picked at two stations and the difference of the P-arrival times between these two stations is found to be more than that the time required for a P-wave to reach from one station to the second. This time series was rechecked by plotting the seismograms from these two stations and it was noticed that a noise spike is misinterpreted as P-phase by APP and the time series is passed as seismic event because of the seismic signals being recorded just after the noise spike. The results obtained through APP in form of P-arrival times, direction of first motion and coda length are tabulated in Table 6.2. Since the

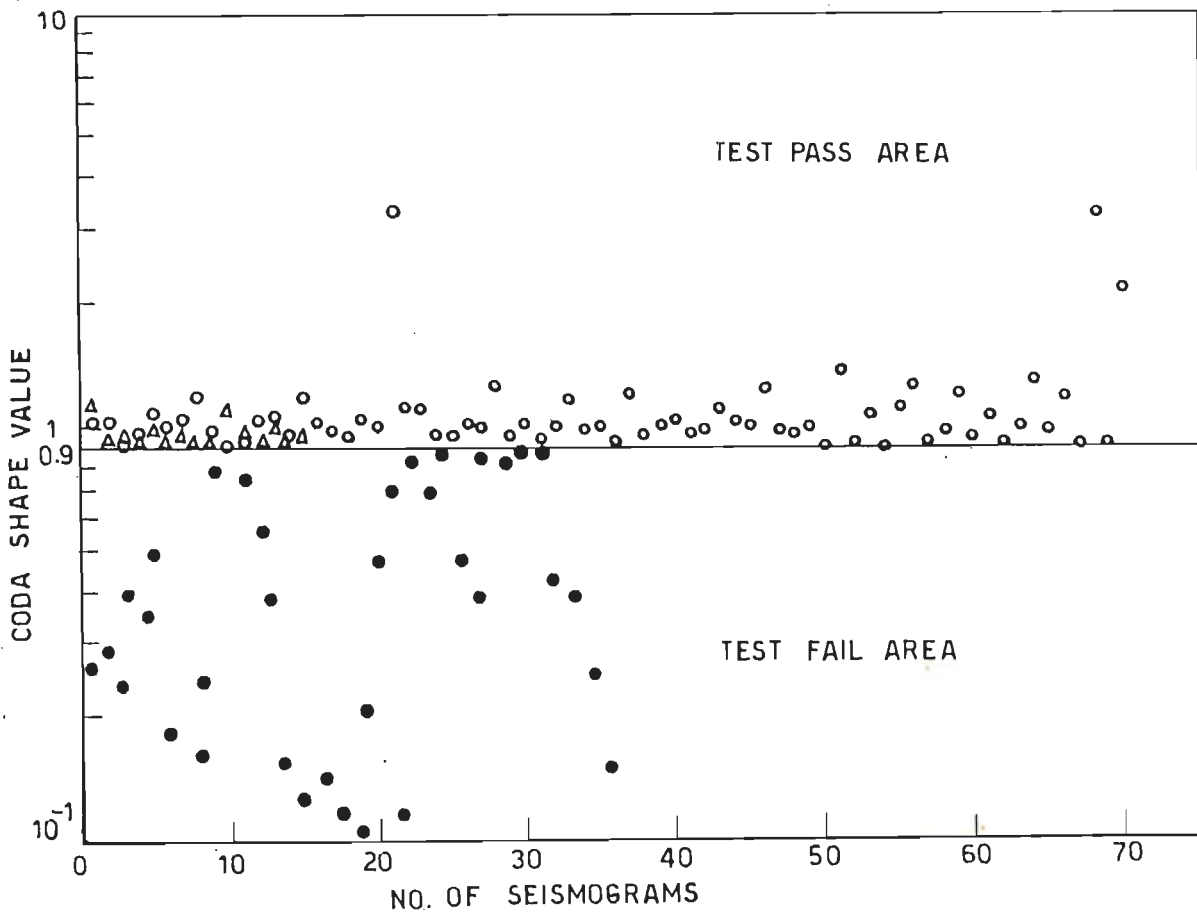


Fig. 6.3 - Coda shape values of time series obtained by APP. The values marked as (o) and ( $\Delta$ ) are passed as seismic events while the value marked as ( $\bullet$ ) are rejected as false alarms

TABLE 6.2 RESULTS OF AUTOMATIC ANALYSIS OF TRIGGERED EVENTS RECORDED BY TDSA. '\*' SHOWS THE CODA LENGTH IS TAKEN TO BE THE END OF THE RECORD.

SL. NO	DATE	STN.	P ARRIVAL TIME			MAX AMPL ( $\mu$ VOLT)	FIRST MOTION (U/D)	CODA LENGTH (SEC)
			(H)	(M)	(S)			
1.	25.11.88	SUR	05:37:29.977			563	D	135.40
		NNR	05:37:32.744			1209	U	140.70
		POR	05:37:32.811			861	D	150.60
2.	08.03.89	SUR	11:36:43.533			423	U	*
		NNR	11:36:45.911			172	U	*
		DHR	11:36:46.833			160	U	*
		POR	11:36:50.266			52	D	*
3.	16.03.89	SUR	22:06:39.444			469	D	107.60
		NNR	22:06:42.466			421	U	*
		DHR	22:06:42.388			513	D	135.54
		POR	22:06:45.877			251	D	139.10
4.	29.03.89	SUR	10:59:21.933			413	D	43.66
		NNR	10:59:24.255			175	U	69.20
		DHR	10:59:21.911			314	U	*
		POR	10:59:20.233			1208	D	72.00
5.	30.03.89	SUR	03:04:47.788			1200	U	*
		NNR	03:04:50.594			623	D	*
		DHR	03:04:51.913			885	D	*
		POR	03:04:54.469			317	U	*
6.	02.04.89	SUR	10:39:17.90			253	D	53.70
		NNR	10:39:10.30			337	D	*
		DIIR	10:39:9.544			503	D	*
		POR	10:39:8.300			470	U	73.30
		RRK	10:39:9.544			467	U	68.75
7.	04.04.89	SUR	01:12:51.808			1505	D	*
		NNR	01:12:50.822			581	U	*
		DIIR	01:12:47.655			813	U	*
		POR	01:12:45.461			2014	U	*
		RRK	01:12:43.405			929	D	*
8.	09.04.89	SUR	08:03:55.944			364	U	53.00
		NNR	08:03:55.766			110	U	*
		DIIR	-			-	-	-
		POR	08:03:50.177			235	D	72.65
9.	11.04.89	SUR	09:36:42.333			206	U	83.00
		NNR	09:36:45.577			213	U	79.20
		DHR	09:36:40.377			332	D	*
		POR	09:36:43.455			140	D	*
		RRK	09:36:39.688			224	U	*

TABLE 6.2 CONTINUED

SL. NO	DATE	STN.	ARRIVAL TIME			MAX AMPL ( $\mu$ VOLT)	FIRST MOTION (U/D)	CODA LENGTH (SEC)
			(H)	(M)	(S)			
10.	11.04.89	SUR	10:55:	47.	361	209	D	66.35
		NNR	10:55:	47.	486	155	D	54.20
		DHR	10:55:	53.	027	180	U	*
		POR	10:55:	53.	013	110	U	*
11.	12.04.89	SUR	17:39:	30.	000	860	D	*
		NNR	17:39:	35.	433	217	D	67.20
		DHR	17:39:	31.	366	922	U	43.50
		POR	17:39:	31.	266	225	U	*
12.	19.04.89	RRK	17:39:	31.	866	312	U	*
		SUR	04:38:	72.	233	207	U	48.30
		NNR	04:38:	69.	433	195	U	43.22
		DHR	-	-	-	-	-	-
13.	22.04.89	POR	04:38:	57.	644	1550	D	23.11
		SUR	21:40:	52.	444	1573	D	71.00
		NNR	21:40:	57.	522	1251	U	79.10
		DHR	21:40:	54.	322	929	D	83.00
14.	23.04.89	POR	21:40:	60.	766	1024	U	*
		RRK	21:40:	57.	333	1065	U	58.20
		SUR	11:42:	40.	255	76	U	*
		NNR	11:42:	43.	022	71	D	*
15.	03.05.89	DHR	11:42:	39.	655	65	U	*
		POR	-	-	-	-	-	-
		RRK	11:42:	34.	500	47	U	*
		SUR	-	-	-	-	-	-
16.	03.05.89	NNR	11:26:	62.	977	228	D	63.40
		DHR	11:26:	57.	677	310	U	55.00
		POR	11:26:	58.	033	256	D	73.00
		SUR	21:15:	35.	733	15	D	23.00
17.	04.05.89	NNR	21:15:	34.	933	217	U	36.11
		DHR	21:15:	29.	066	126	D	46.00
		POR	21:15:	29.	500	135	D	37.32
		SUR	-	-	-	-	-	-
		NNR	01:33:	37.	500	68	U	*
		DHR	01:33:	37.	066	21	U	31.20
		POR	01:33:	49.	400	43	D	23.00

data is recorded through event detector used in TDSA, the end of the event, if not marked by APP, is taken to be the end of the recorded data marked as (\*) in the Table 6.2.

In off-line processing, the picking of P-phase by APP is dependent on the threshold value to be fixed by the operator in advance. The phase picker algorithm (APP) described above uses a preset value of the STA/LTA ratio supplied by the seismologist to decide the triggering of individual channels and to record the triggered events. Thus, the triggered events recorded are directly dependent on this ratio. If the threshold value is chosen to be high, some of the seismic events might get rejected. On the other hand, if the threshold value is chosen to be low then APP may record higher number of false alarms, which in turn increase the processing time of the data to select the seismic events. This optimization of threshold value is not needed if instead of a fixed value we use dynamic threshold as described in Chapter 5. In this case the CF used is different to that used in APP and the CF is selected in such a way that it takes care of the background noise. The results of the phase picker algorithm using dynamic threshold are comparable to that of the APP using static threshold value. The only difference in these two algorithms in on-line processing is that of the CPU time used and the memory space which are higher in case of the algorithm using dynamic threshold in comparison to APP. As the present algorithm is developed keeping in mind that the same shall be used in a real time data acquisition system, so the phase picking algorithm with the static threshold value is preferred here.

## 6.6 VISUAL Vs AUTOMATIC ANALYSIS

Evaluation of performance of the automatic phase picking algorithm using direct comparison of automatic picks and the picks from the visual analysis are presented in this section. Visual analysis, as described in section 4.3.1 is the picking of P- or S-phase from the screen of a PC, in which case one can go to the particular sample of P- and S-phase onset of the seismic wave. However, the accuracy in marking the correct onsets, in general, will depend on the seismologist's decision to mark the correct sample and also the sampling rate at which the ground motion is digitized. This accuracy, of course, is much higher than the accuracy achieved in the conventional phase pickings from analog seismogram recorded by drum recorders or pen recorders having very low speed. In conventional phase picking, in general, the resolution is of the order of 0.1 sec, whereas in the visual phase picking on a PC the resolution goes up to 0.01 sec when the sampling rate is 90 samples/sec and is as high as 2.77 milli sec in case of 360 samples/sec. The block diagram for the analysis of data by visual analysis and phase picker techniques is shown in Fig 6.4. The events recorded by DAS are analysed in the beginning using both the techniques as shown in the Fig and when a certain level of confidence is acquired then the processing may be done only by automatic mode i.e., by phase picker. Once the phase list is worked out, the event is located and the source parameters are computed using frequency domain analysis.

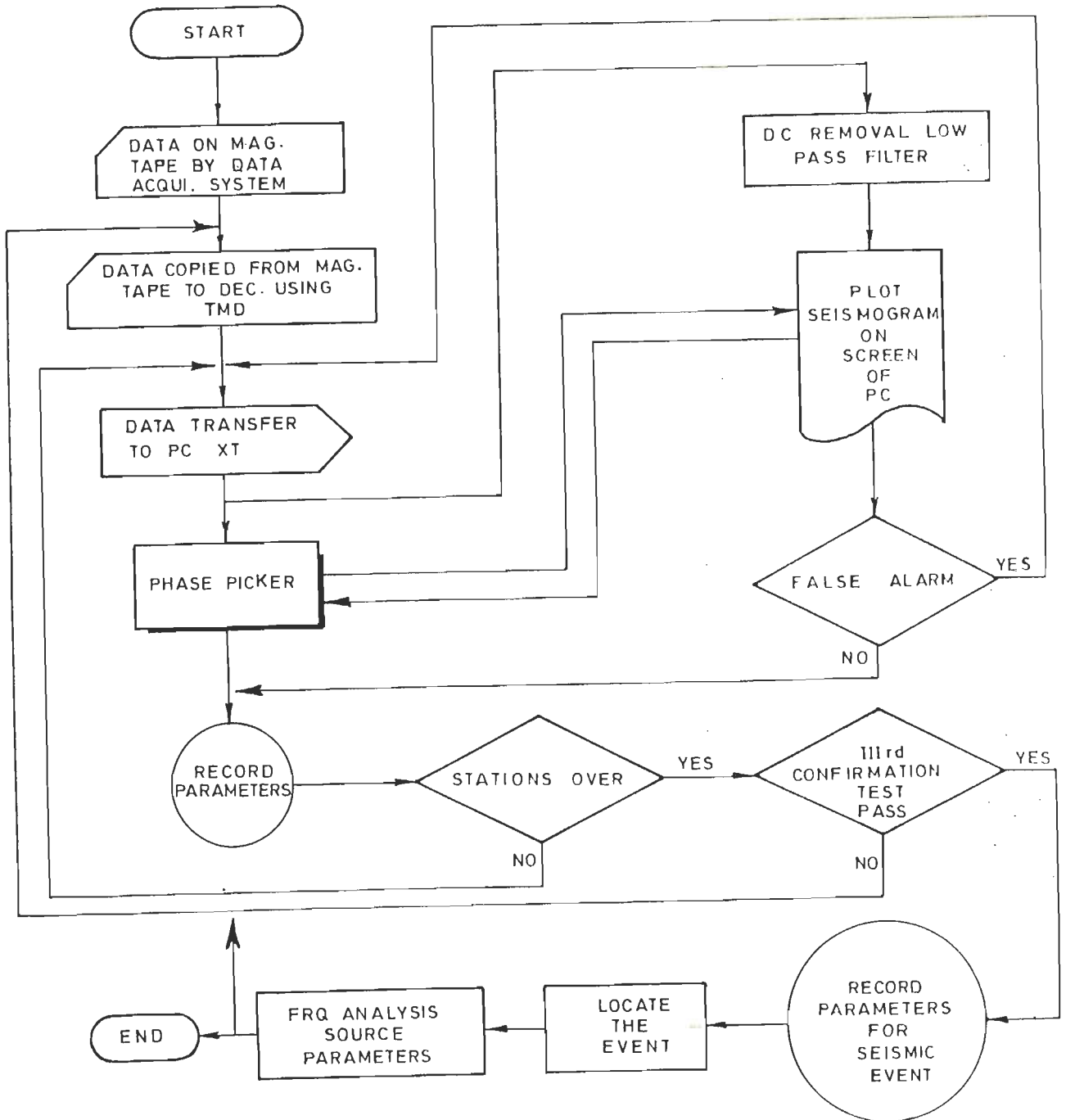


Fig. 6.4 - Block diagram showing procedures laid down for data processing using visual analysis and phase pickers



The arrival times as determined by visual analysis and APP do match except in few cases and their differences are summarized in Table 6.3. The APP has marked exactly the same sample of the P-onset as picked by the visual analysis in 36 seismograms out of 63 seismograms. There are 19 seismograms in which the difference in P-onset times as marked by APP and visual analysis is less than 0.5 sec. In 7 cases, the difference is between 0.5 and 1.0 sec and only in one case the difference is more than 1 sec. There are 5 seismograms in which APP has marked the P-onset whereas it was not marked by visual analysis. On the other hand, there are 5 such seismograms including two from the seismic event dated 16-04-89 in which the P-onset was marked by visual analysis and the same could not be picked by APP. Fig 6.5 shows, as an example, the event dated 12.04.89 displaying 1 second data on the screen. The vertical lines are drawn at the corresponding samples at which the visual analysis (V) and the phase picker (P), have marked the arrival of P-phase. The difference between the picks by the two procedures are very small as can be seen from the Fig . In case of the seismogram at the station RRK, the P-phase being embedded in the background noise could not be marked by visual analysis, but P-onset has been picked by APP.

The triggered events data was also analysed by two other phase picker algorithms given by Stewart, 1971 and Allen, 1978. The quantitative comparison of marking the triggered events as seismic events is given in Fig 6.6 giving the final results as produced by the three phase picking algorithms in comparison to

the visual analysis. Table 6.4 shows the number of P-phases picked by Stewart, 1971, Allen, 1978 and APP at different stages of confirmation of triggered events as seismic events. If Test III is applied to Stewart, 1971 and Allen, 1978, then 150 and 26 seismic events are confirmed by these algorithms, respectively. The first Test is applied in case of APP and Allen, 1978 after the P-phases picked by the algorithm have passed the 'minimum duration' criteria of seismic event.

## 6.7 FURTHER ANALYSIS OF THE RECORDED DATA

### 6.7.1 Location and Magnitude of the Events

In order to determine the hypocentral locations and to compute the magnitude of the seismic events, the available procedures and programs have been used. All the seismic events as picked up by the visual analysis and the phase picker are located using the HYP071 computer program developed by Lee and Lahr, 1975. The velocity structure for the Garhwal Himalaya region given by Chander et al., 1983 and Kumar et al., 1987 as described in section 3.2.3 is taken. The hypocentral parameters determined using the P- and S- arrivals from three or more stations as computed by visual analysis (V) are tabulated in Table 6.5. The hypocentral parameters determined using the P-arrivals as picked by APP (A) are also tabulated in Table 6.5 for comparison. The hypocentral locations obtained by these two procedures (O - APP ; ● - Visual analysis) are marked in the tectonic map of the region in Fig 6.7. The comparison shows very small variation in the

TABLE 6.3 COMPARISON OF THE P-ONSET TIMES (VISUAL - AUTOMATIC)  
AS OBTAINED FROM VISUAL AND AUTOMATIC ANALYSES

SL NO	DATE	DIFFERENCE IN P ONSET TIME IN SEC				
		SUR	NNR	DHR	POR	RRK
1	25-11-88	-0.066	0.000	-	0.000	-
2	08-03-89	0.000	-0.044	0.000	-0.166	-
3	16-03-89	0.000	0.000	0.022	0.000	-
4	29-03-89	0.000	-0.033	0.022	0.000	-
5	30-03-89	0.237	0.222	0.334	0.000	-
6	02-04-89	0.000	-	-0.900	-0.367	0.000
7	04-04-89	0.000	0.000	0.000	0.000	-
8	09-04-89	0.000	0.000	-	0.000	-
9	11-04-89	0.055	-0.355	0.956	-0.700	-
10	11-04-89	0.000	0.000	0.000	-0.403	-
11	12-04-89	0.000	-0.066	0.000	0.000	-
12	19-04-89	-0.544	0.000	-	0.000	-
13	22-04-89	0.000	-0.422	0.000	-0.067	-
14	23-04-89	-1.311	-0.756	0.000	-	0.000
15	03-05-89	-	0.011	-0.377	-0.667	-
16	03-05-89	0.066	0.000	0.000	0.000	-
17	04-05-89	-	0.000	-0.878	0.000	-

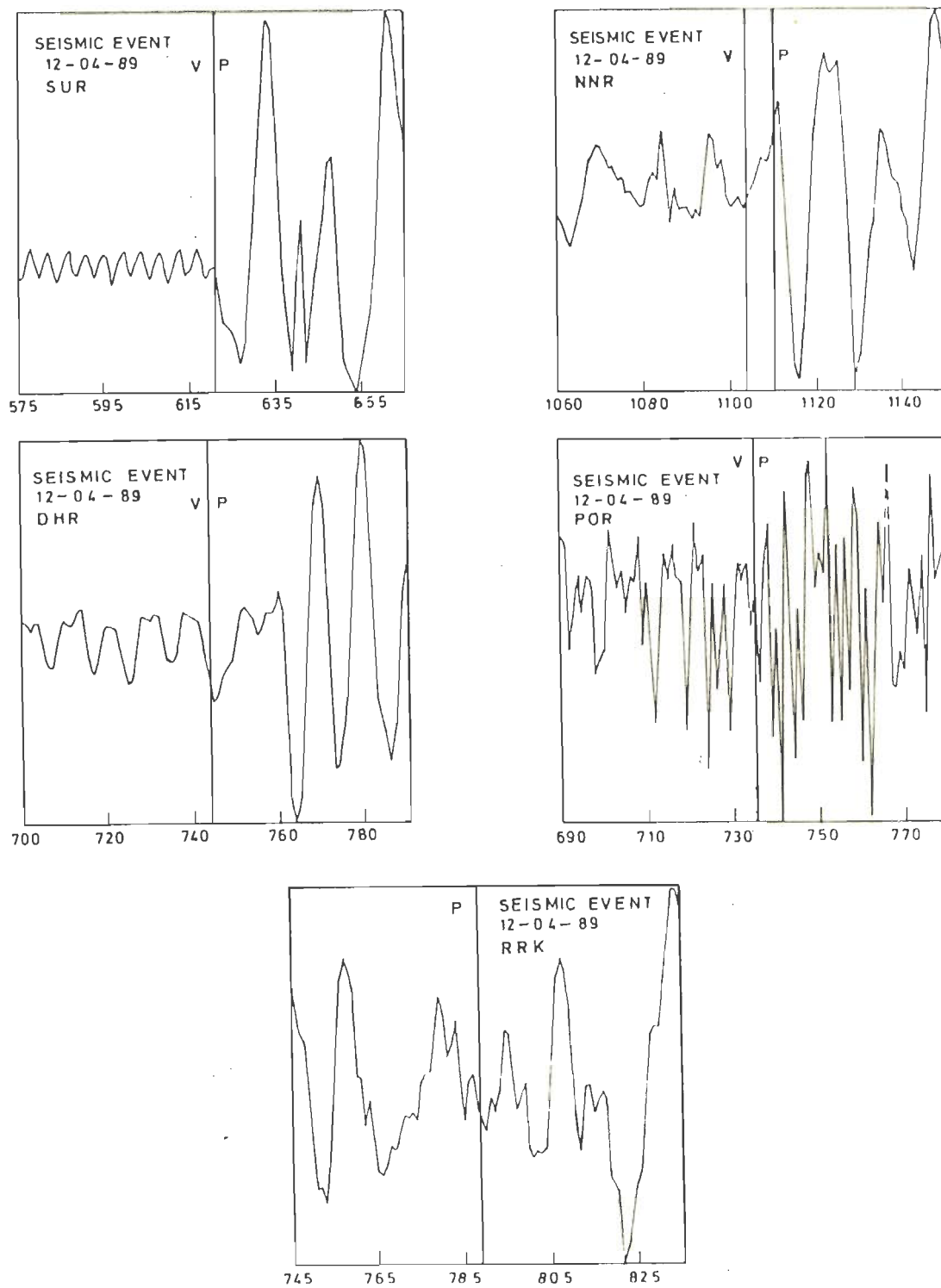


Fig. 6.5 - Example of P-phase picking by visual analysis (v) and APP (P) at five stations of seismic event dated 12-4-89. The blocks show display of 1 sec data containing the P-onset.

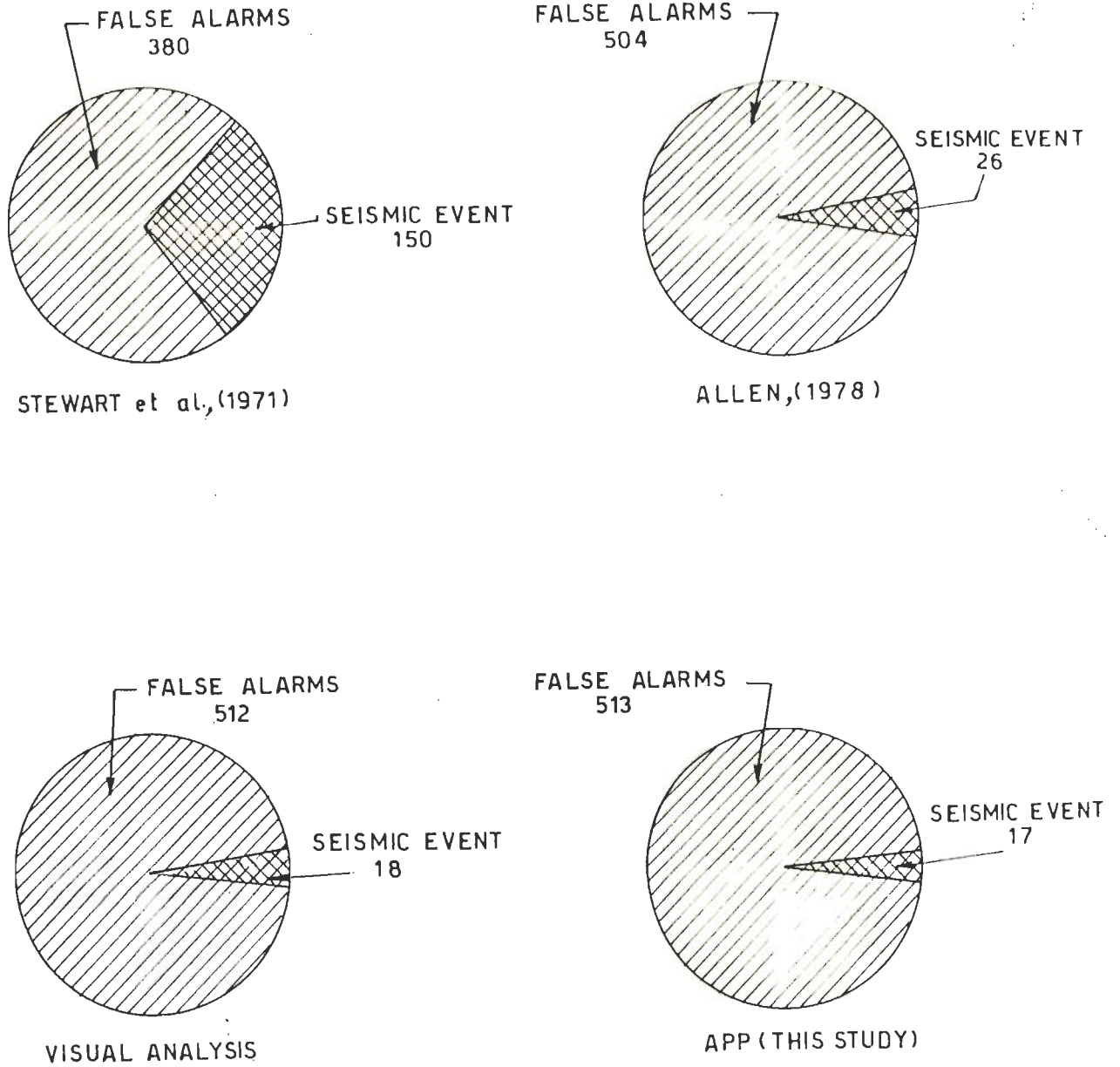


Fig. 6.6 - Comparison of the performance of different phase picker algorithms in confirming events at 3 or more stations as seismic events

TABLE 6.4 COMPARISON OF THE RESULTS OF APP WITH TWO OTHER ALGORITHMS AT VARIOUS STAGES TO CONFIRM THE TIME SERIES AS SEISMIC EVENT.

Test Criteria	Stewart, 1971		Allen, 1978		APP	
	P-Picks	EVENTS SE* / TE <sup>#</sup>	P-Picks	EVENTS SE / TE	P-Picks	EVENTS SE / TE
Tiggered for P-phase	638	218/530	439	188/530	403	178/530
Confirm by IInd trigger level	622	211/530	N.A.	N.A.	N.A.	N.A.
First Test (Frequency dispersion)	N.A.	N.A.	190	84/188	148	60/178
Second Test (Coda Shape)	N.A.	N.A.	152	58/84	85	31/60
Third Test (P-onset time)	N.A.	N.A.	N.A.	N.A.	68	17/31
P-phase pick at only one station	35	35/211	9	9/58	0	N.A.
P-phase pick at only two stations	52	26/211	46	23/58	0	N.A.
P-phase pick at more than two stations	353	150/211	97	26/58	68	17/17

\* - Seismic events selected by the algorithm

# - Total events on which the algorithm is applied

TABLE 6.5 HYPOCENTRAL PARAMETERS OF THE EVENTS AS COMPUTED FROM RESULTS OBTAINED BY VISUAL ANALYSIS (V) AND AUTOMATIC ANALYSIS (A).

SI No	Date	Origin Time			Epicentre		Focal depth (km)	No. of obs	RMS
		(H)	(M)	(S)	Lat [N <sup>o</sup> ]	Long [E <sup>o</sup> ]			
1	25 11 88V	05:36:56.50	31	58.02	78	53.88	15.41	5	0.19
		A 05:36:54.91	32	2.23	78	59.57	16.09	3	1.32
2	08 03 89V	11:36:39.70	30	26.18	78	23.93	6.22	4	0.27
		A 11:36:39.50	30	26.63	78	23.78	9.37	4	0.29
3	16 03 89V	22:06:35.07	30	28.06	78	23.83	10.15	4	0.01
		A 22:06:34.76	30	29.01	78	23.30	12.67	4	0.01
4	29 03 89V	10:59:15.15	30	25.00	78	35.96	10.00	4	0.60
		A 10:59:15.29	30	20.40	78	35.87	10.92	4	1.21
5	30 03 89V	03:04:44.77	30	25.00	78	23.78	2.94	4	0.05
		A 03:04:44.54	30	25.40	78	23.67	1.89	4	0.04
6	02 04 89V	10:38:57.97	30	16.64	79	14.36	10.00	3	0.82
		A 10:39:03.43	30	11.95	79	47.36	8.87	5	2.42
7	04 04 89V	01:12:40.85	30	16.17	78	35.34	24.09	4	0.06
		A 01:12:40.81	30	16.15	78	46.38	14.48	5	0.06
8	09 04 89V	08:03:41.35	30	24.00	79	01.52	20.00	3	0.01
		A 08:03:41.35	30	24.00	79	01.52	20.00	3	0.01

TABLE 6.5 CONTINUED

Sl No	Date	Origin Time (H) (M) (S)	Epicentre		Focal depth (km)	No. of obs	RMS	
			Lat [N <sup>o</sup> ]	Long [E <sup>o</sup> ]				
9.	11 04 89V	09:36:35.91	30	25.00 78	35.34	10.88	4	0.84
	A	09:36:35.84	30	27.26 78	35.27	10.65	5	1.04
10	11 04 89V	10:55:42.86	30	18.82 78	19.62	13.67	4	0.23
	A	10:55:42.86	30	18.82 78	19.62	13.67	4	0.23
11	12 04 89V	17:39:20.20	30	49.36 78	18.95	16.01	7	0.75
	A	17:39:24.59	30	25.00 78	38.89	15.27	5	1.98
12	16 04 89V	02:07:59.07	30	19.76 78	44.93	11.47	4	0.11
13	19 04 89V	04:38:54.37	30	06.75 79	05.18	4.19	4	0.22
	A	04:38:56.64	30	08.76 79	56.16	10.00	3	1.59
14	22 04 89V	21:40:37.42	31	05.29 78	04.63	16.13	4	0.50
	A	21:40:40.20	31	56.58 78	12.32	6.60	4	0.38
15	23 04 89V	11:42:32.59	30	33.97 78	25.84	14.91	4	0.02
	A	11:42:34.17	30	30.81 78	29.94	10.00	4	0.01
15	03 05 89V	11:26:52.89	30	21.88 79	44.60	10.00	3	0.00
	A	11:26:48.66	30	18.35 79	06.29	1.00	4	0.84
16	03 05 89V	21:15:23.81	30	20.68 78	49.65	10.00	4	0.00
	A	21:15:23.84	30	20.47 78	50.71	8.03	4	0.18
18	04 05 89V	01:33:27.84	30	36.40 78	18.00	1.00	3	1.50
	A	01:33:32.4	30	25.00 78	18.00	10.00	3	1.62



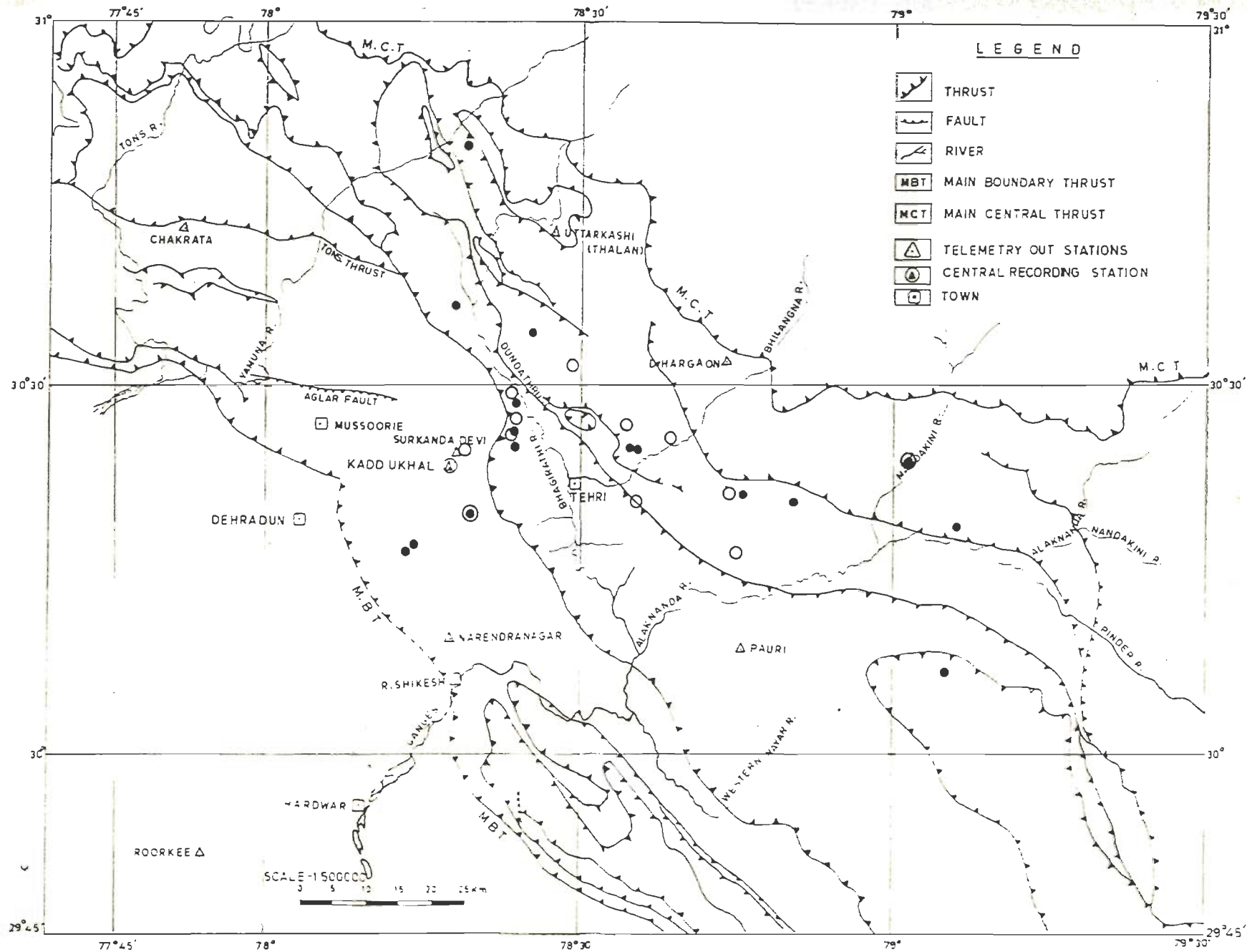


Fig. 6.7 - Hypocenter locations of seismic events using visual analysis (●) and APP (○)

hypocenters of the seismic events as located on the basis of visual analysis and the phase picker. There are a good number of hypocenters located near to the Dunda thrust. In this period no earthquake has been recorded close to MBT. As more constraints creep in while locating an event on the basis of arrival times, the accuracy of phase pickers should not be measured from the accuracy in locating the events. However, one can not rely on the residuals too heavily since they reflect the inadequacies of the velocity model and the computation power of the locating program more compared to the inaccuracies in the picks.

The determination of the size of the earthquake i.e., magnitude based on the amplitudes of ground motion is a complex procedure in case of a local array due to various reasons viz, resolution, dynamic range and standard response curves of the instruments, and the non-availability of attenuation laws for the region. Since the data recorded in digital form is used in the present study, most of these constraints are taken care of except the attenuation laws which are not known for this region. Richter, 1935 defined the local magnitude  $M_L$  of an earthquake observed at a station to be

$$M_L = \text{Log } A - \text{Log } A_0 (D) \quad (6.1)$$

where  $A$  is the maximum amplitude in microns recorded on the Wood Anderson seismograph with natural period of 0.8 sec, magnification as 2800 and critical damping of 0.8 for an earthquake at a

distance of  $D$  km and  $A_0(D)$  is the maximum amplitude at  $D$  km for a standard earthquake (79). To determine the magnitudes in Garhwal Himalaya region the amplitudes are modified for Wood Anderson seismograph and  $A_0(D)$  values are taken from the table given by Richter, 1957 as the attenuation laws for this region are not known (80). The local magnitude computed in the above manner are tabulated in Table 6.6 along with the source parameters.

### 6.7.2 Fault Plane Solutions

Composite fault plane solution have been obtained using the first P-motions of some of the seismic events at different stations. The seismic events located between latitude  $30^{\circ} 20'$  and  $30^{\circ} 30'$  and longitude  $78^{\circ} 25'$  and  $78^{\circ} 45'$  are considered to work out the composite fault plane solution. The first P-motions are plotted on the lower hemisphere at the source considering the azimuthal angle and the angle of emergence of the ray to a particular station from the source. The two planes are marked on the net as shown in Fig 6.8. One of the plane is NE dipping plane having strike  $N 52^{\circ} W - S 52^{\circ} E$  with dip  $50^{\circ}$  and the second plane is SE dipping plane having strike  $N 51^{\circ} E$  and  $S 51^{\circ} W$  with dip  $74^{\circ}$ . Keeping in mind the orientation of the existing tectonic environment as discussed in Section 3.2.4, the fault motion suggests reverse fault mechanism, which indicates that the recorded earthquakes are the result of the response of the upper crust in the ongoing under thrusting of the Indian plate due to continent-continent convergence (23,30,54).

○ DILATATION  
● COMPRESSION

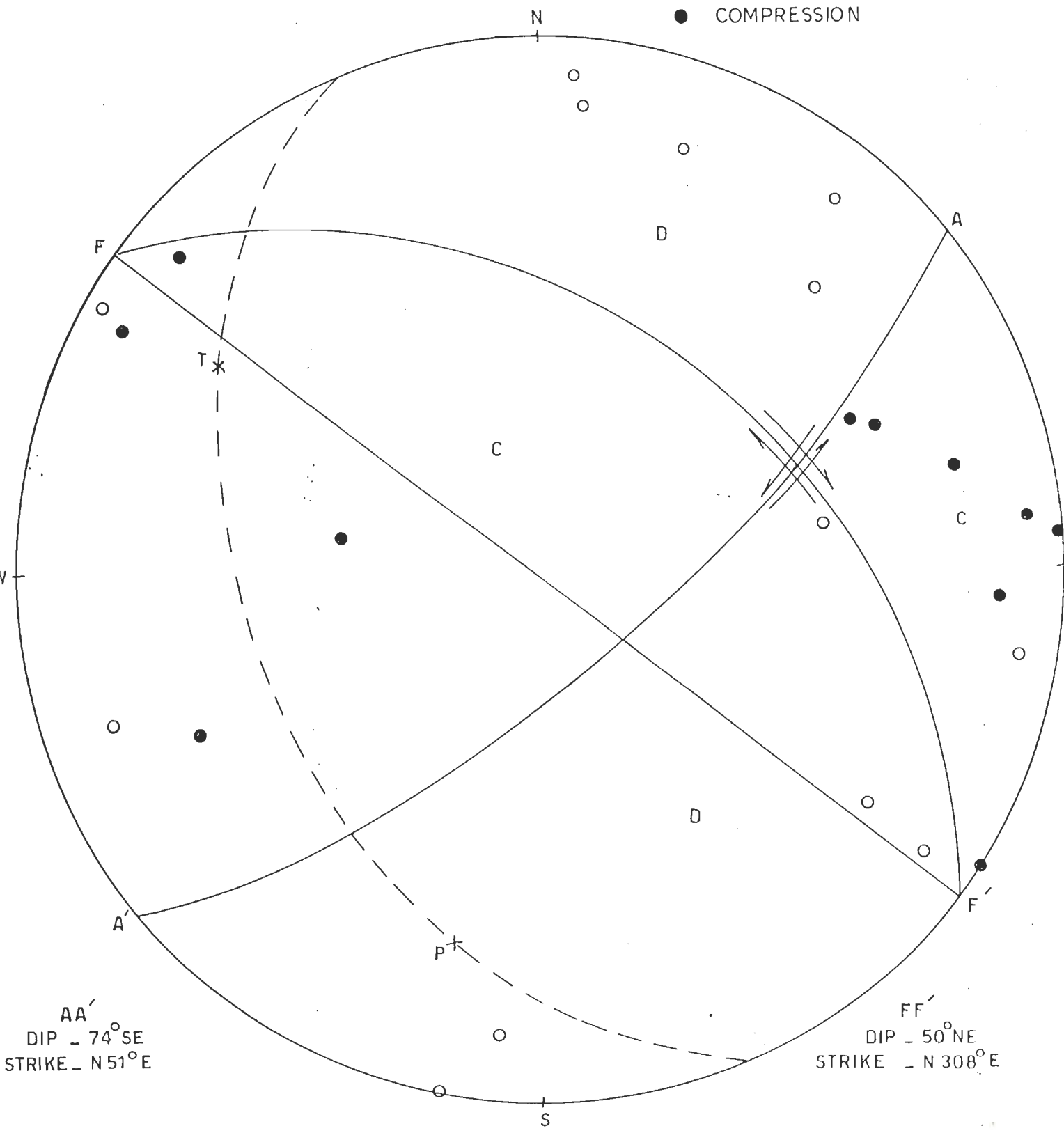


Fig. 6.8 - Composite fault plane solution of seismic events recorded by DAS

### 6.7.3 Source Parameters

The magnitude is widely used as the quantitative measure of the strength of an earthquake although its shortcomings are well known. It is also quite cumbersome to relate this parameter theoretically to other important source characteristics such as strain energy release, fault offset, stress drop, source dimension, seismic moment and radiated seismic energy. These source parameters are related to each other but their relationship to magnitude requires spectral description of the seismic source which in turn is obtained from complete temporal and spatial history of the faulting or stress release mechanism.

Brune, 1970 developed a powerful theory describing the nature of seismic spectrum radiated by the seismic source by considering the physical process of the energy release (20). In order to model the transverse elastodynamic radiations from an earthquake fault, Brune considered a sudden loss of traction over a circular dislocation surface of radius  $r$ . The fault is assumed to be opaque to shear waves during faulting so that energy from one side of the fault does not transmit to the other side. The sudden loss of traction radiates a shear wave in a direction normal to the fault. The near field and far field (including geometrical spreading and attenuation effects) phenomena are modelled and related to the corner frequency ( $f_0$ ) and low frequency asymptote ( $\Omega_0$ ).  $f_0$  and  $\Omega_0$  are, in turn, related to stress drop and the seismic moment of the source.

After the work of Brune in 1970, there has been a veritable explosion of papers on the seismic spectrum and its relation to source size, seismic moment, and stress drop. Observations of the spectra consistent with his theory have also been reported for microearthquakes with very low stress drops (29) and high stress drops (98) in addition to large earthquakes (44,105), thus covering a very wide range of computed values for parameters based on the theory.

Several observational studies from the early 1970s to the present time have used the corner frequency of the microearthquakes to determine their faulting dimensions and hence stress drops (11,31,98). These studies were largely motivated by the theoretical work of Brune, 1970 who developed a source model relating corner frequency to faulting dimension. A general result of these investigations is that the scaling behavior of small events ( $M < 3$ ) differs from that of larger events, implying a breakdown in the similarity of the rupture process of small earthquakes (33). Specifically, the corner frequencies of the small events are observed to increase very slowly or not at all with decreasing seismic moment. This is interpreted to signify that faulting dimensions of small events are relatively uniform as moment decreased below about  $10^{20}$  dynes cm so that stress drop decreased with decreasing moment (4,11,74). In contrast, studies of the spectra of larger events with  $M_L$  between 3.5 and 6 report constant stress drop with decreasing moment (96). In the present study site effects are not taken into account (13,69). The time window for 2.84 sec ( 256 samples @ 90 samples/sec) is applied

from the starting of the P-wave. This is being done to take only the samples containing the P-wave and no S-wave effect is present in the time series. The DC bias is removed by subtracting the mean of the samples from the time series. This window is cosine tapered with 10 per cent tapering at both the ends. The FFT algorithm by Cooley and Tuckey (27) has been used to compute Fourier spectra. The velocities are changed into displacement by applying the division by  $j\omega$  in Fourier domain. The spectra is then corrected for the attenuation characteristics of the region by taking an average value of the quality factor,  $Q$ , as 300 with a exponential decay. The value has been taken as an approximate as no specific work in this region has been carried out so far for the estimation of the  $Q$  value. The instrument correction is not required taking into account the frequency response of the system upto ADC (housed in modulator) which is flat from DC to 90 Hz, and the bit structure of the data word. The geometrical spreading correction is applied by multiplying the amplitudes by the epicentral distance of the station to the source. The Fourier spectra thus taken are shown in Fig 6.9 to Fig 6.26.

The frequency response of the Butterworth low pass filter is modified to include the effects of attenuation for estimating the spectral parameters i.e.,  $f_0$  and  $\Omega_0$  on an analytical model (48). This has the form

$$\Omega_0 [1 + (f/f_0)]^{-\gamma} \exp(-\pi f \tau) \quad (6.2)$$

where  $f$  is the frequency and  $\tau$  is the travel time divided by the quality factor  $Q$  and  $\gamma$  is the slope of the curve after  $f_0$ . In finding the corner frequency the effect of the  $Q$  is not taken into account while taking the Fourier transform, using this formulation. The above equation is used for making master curves for the spectral estimates. Fig 6.27 shows three cases of high frequency slope ( $\gamma$ ) for different values of  $\tau$ . These figures with the particular value of travel time of the P-wave are used as master curves to be overlain on the observed spectra and values of  $f_0$  and  $\Omega_0$  are read after a good matching is achieved. The method used here has the advantage of offering a uniform and systematic approach to the problem of estimating the spectral estimates. This method has the limitation that it can not be used obviously, to determine  $\tau$  and  $Q$  (48) in view of non-unique inverse solution. Hence  $\tau$  and  $Q$  must be either separately determined or assumed.

The physical parameters i.e., seismic moment, stress drop, source dimension, slip and energy are then computed from the spectral analysis of the recorded data based on Brune's model (1970). The corner frequency is the cut off frequency in the spectra after which the spectral amplitude decays at a much faster rate. The corner frequency method is being applied for computation of source parameters by several authors (29,47,50).

Explored by Keilis Borok, 1959 and then modeled by Brune, 1970 the formulations used in this study for the computation of source parameters are as follows :



DATE : 25 . 11 . 88

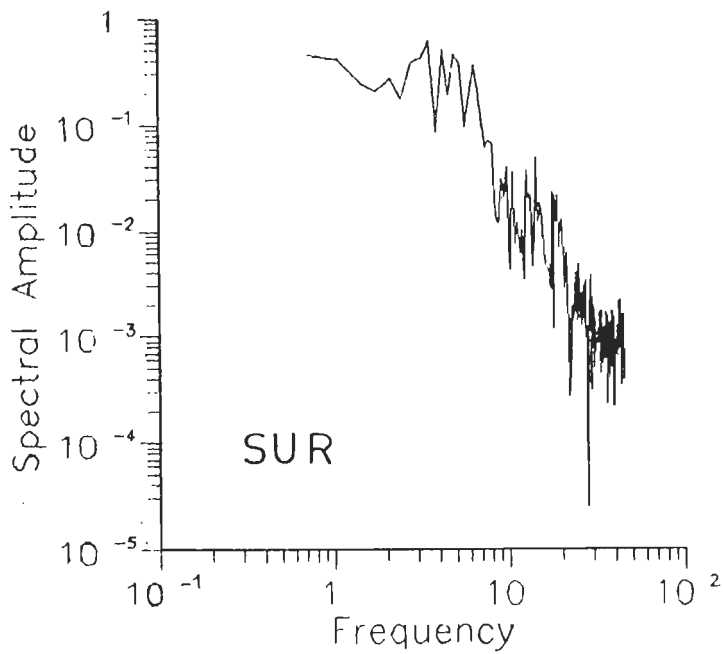
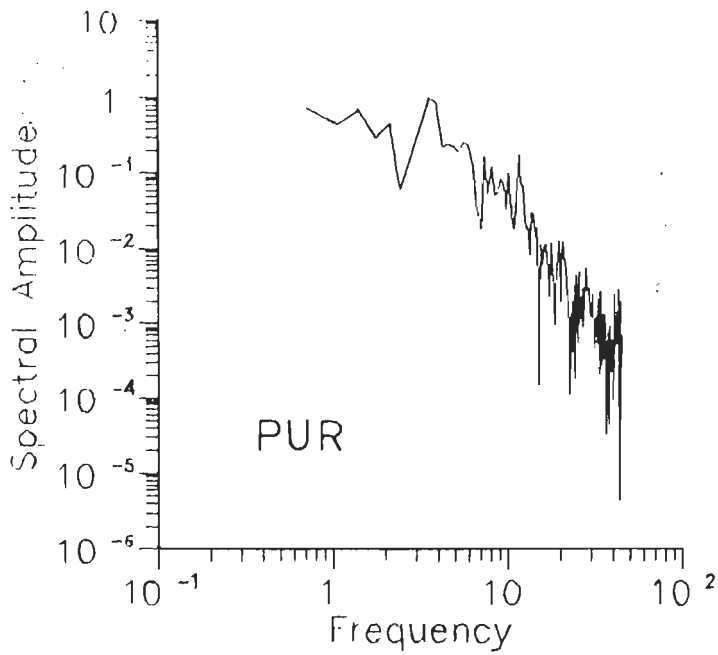


Fig. 6.9 - Displacement Spectra of P-wave for seismic event dated 25-11-88 used for computation of seismic source parameters

DATE: 8.3.89

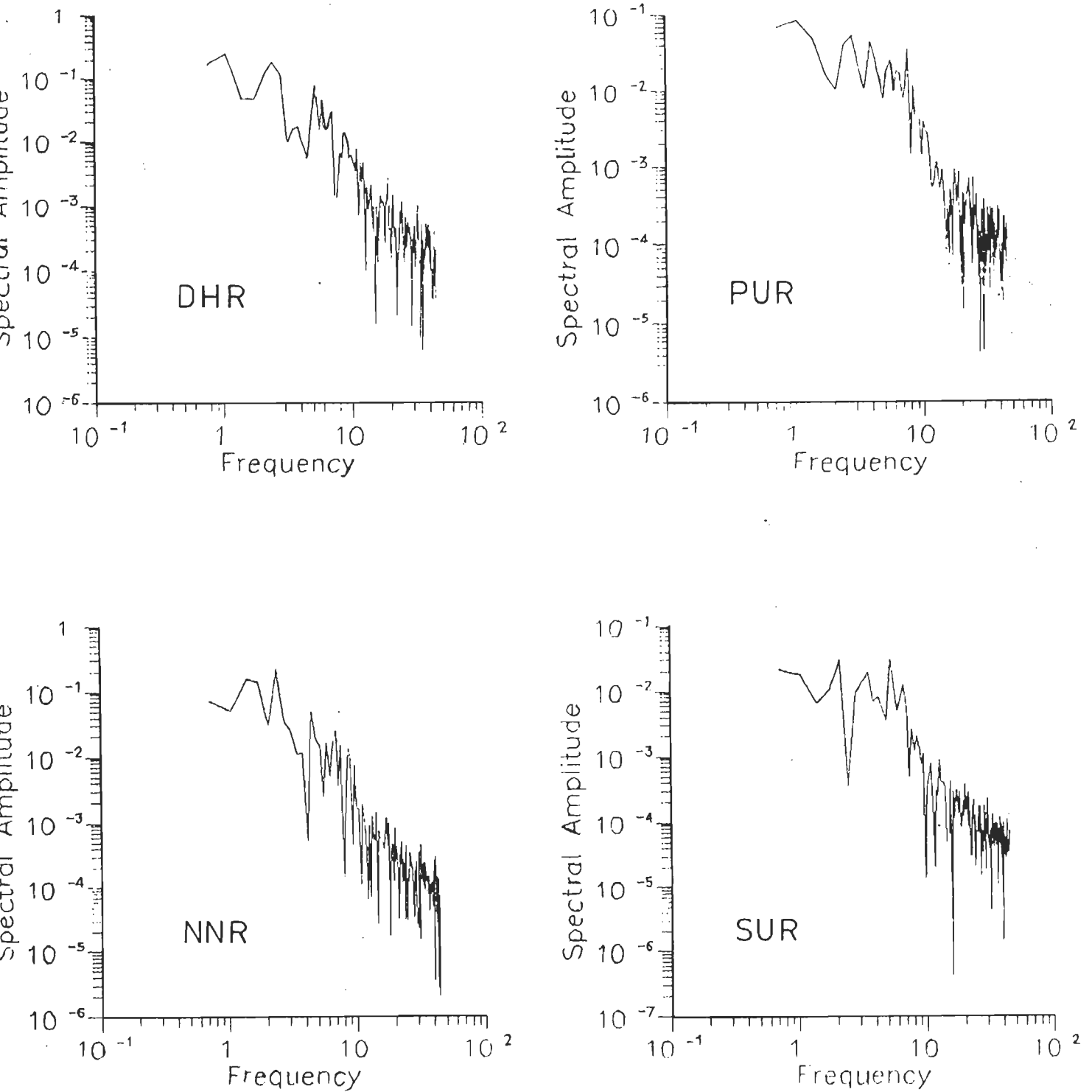


Fig.6.10\_Displacement Spectra of P-wave for seismic event dated 8-3-89 used for computation of seismic source parameters

DATE : 16.3.89

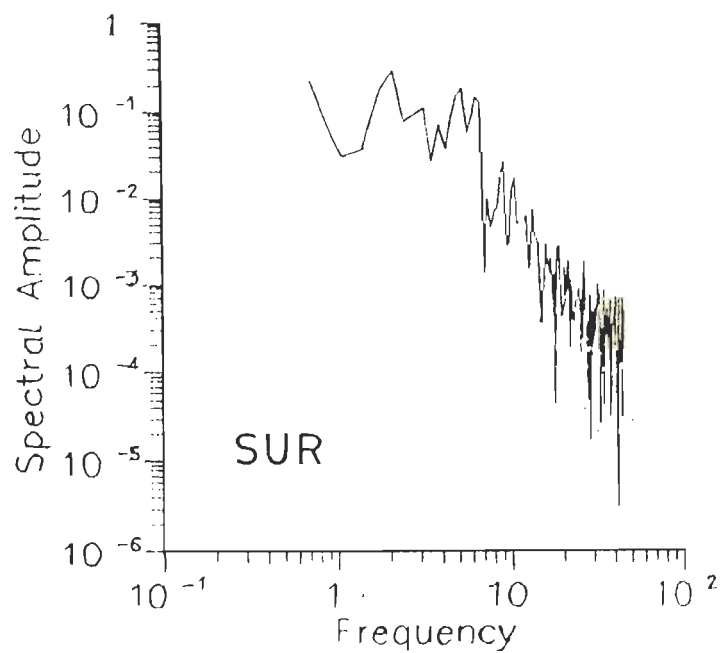
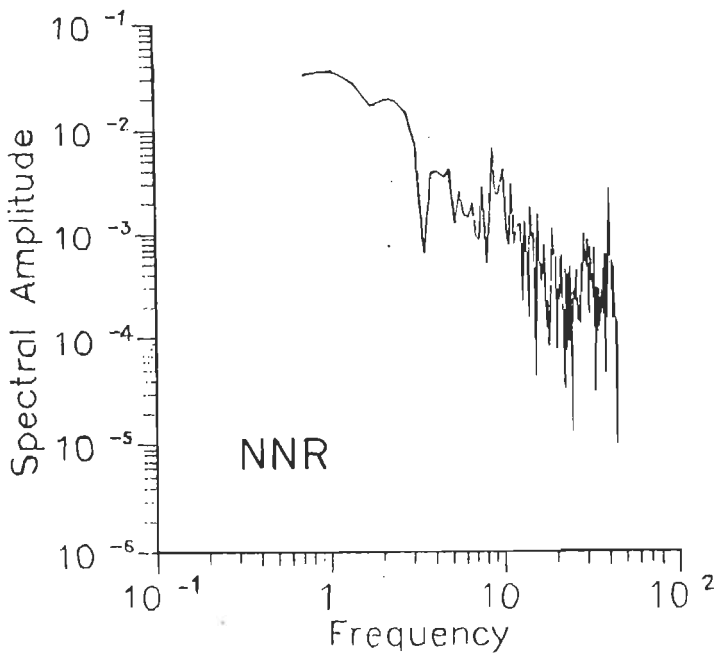
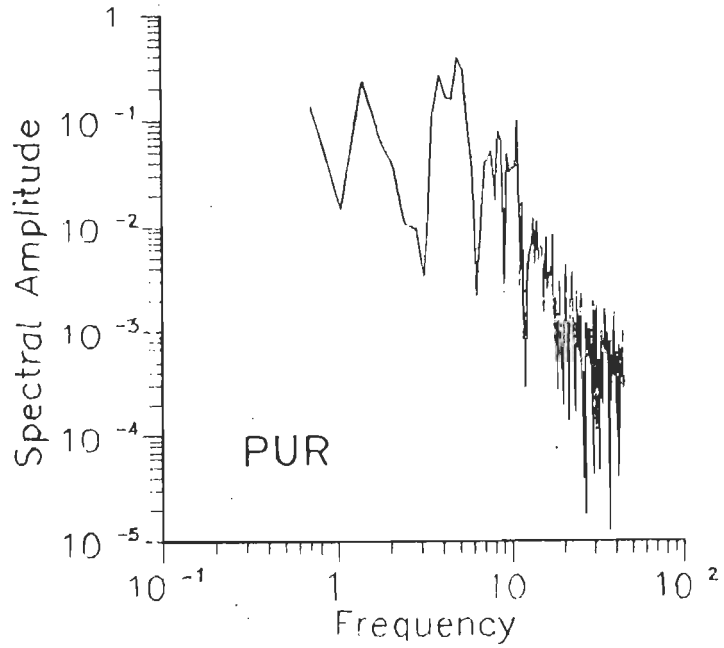
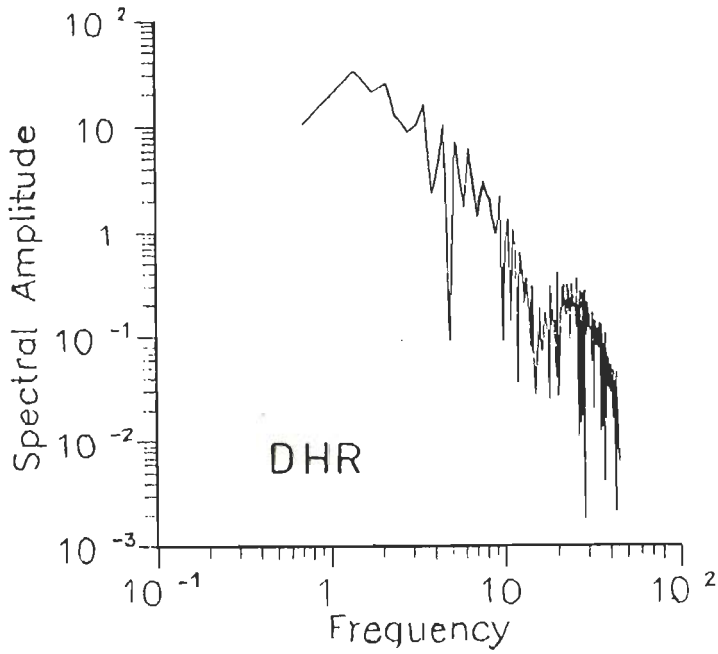


Fig.6.11 - Displacement Spectra of P-wave for seismic event dated 16-3-89 used for computation of seismic source parameters

DATE : 29.3.89

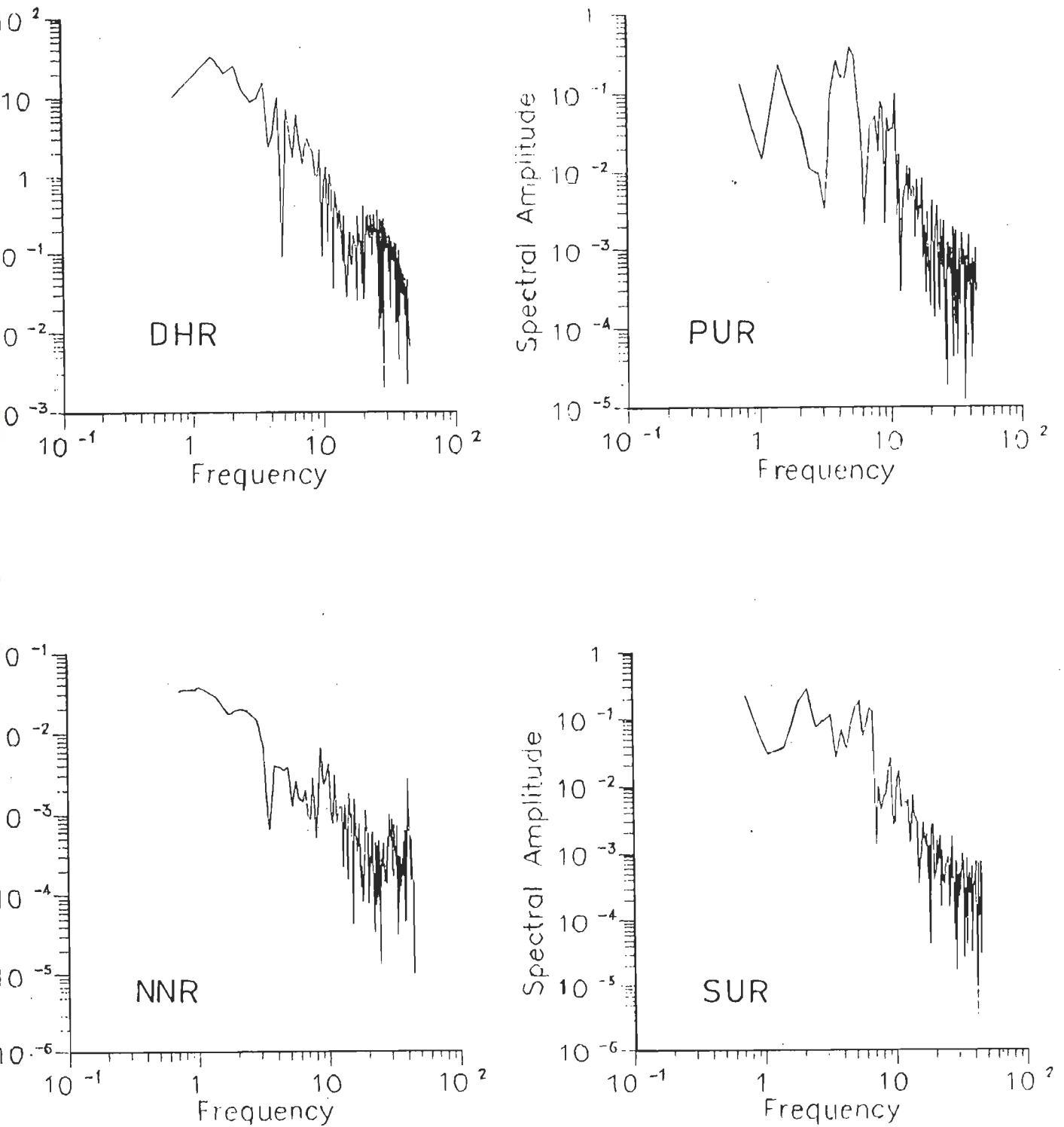


Fig.6.12 - Displacement Spectra of P-wave for seismic event dated 29-3-89 used for computation of seismic source parameters

DATE: 30. 3. 89

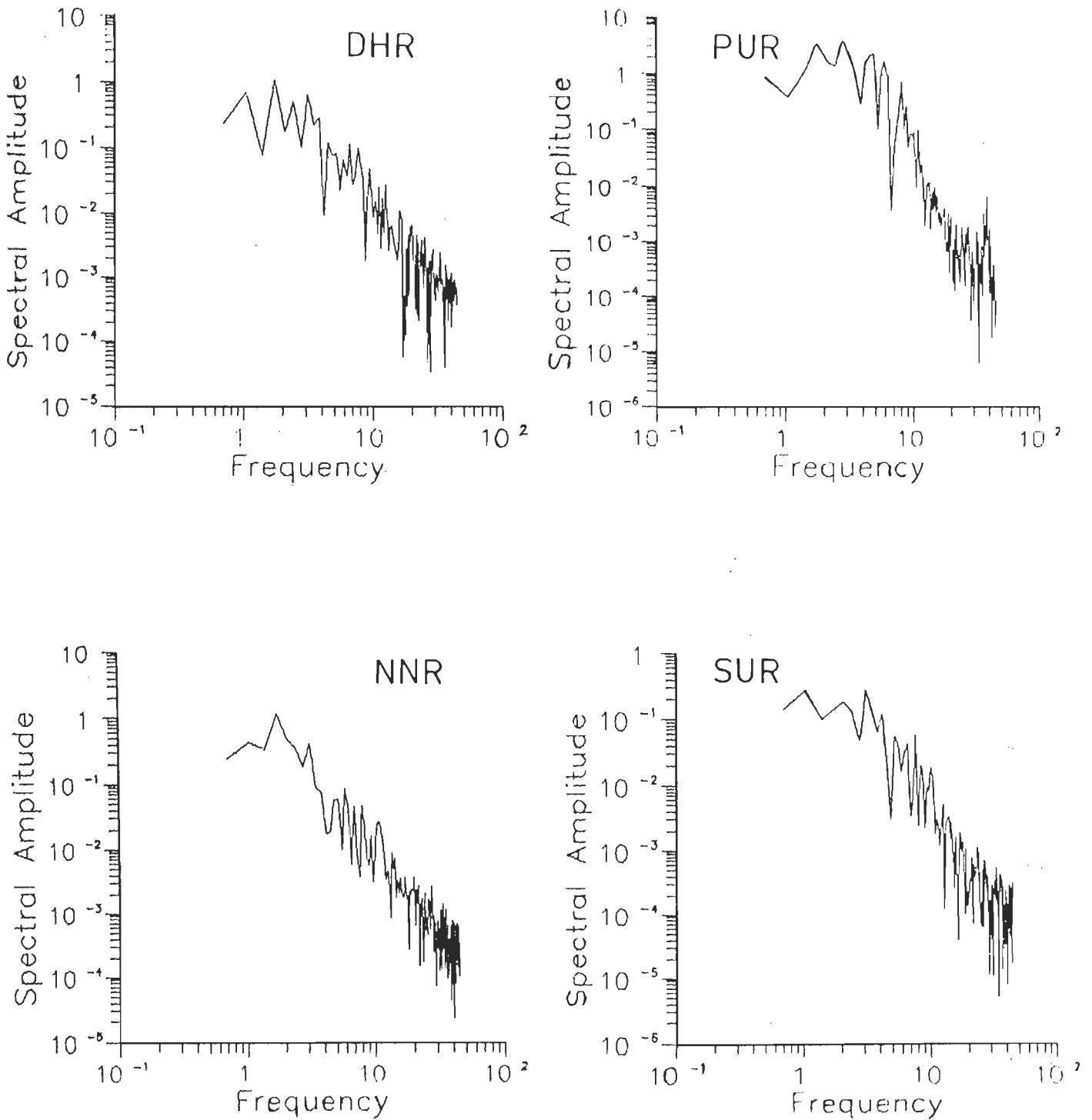


Fig.6.13 - Displacement Spectra of P-wave for seismic event dated 30-3-89 used for computation of seismic source parameters

DATE: 2.4.89

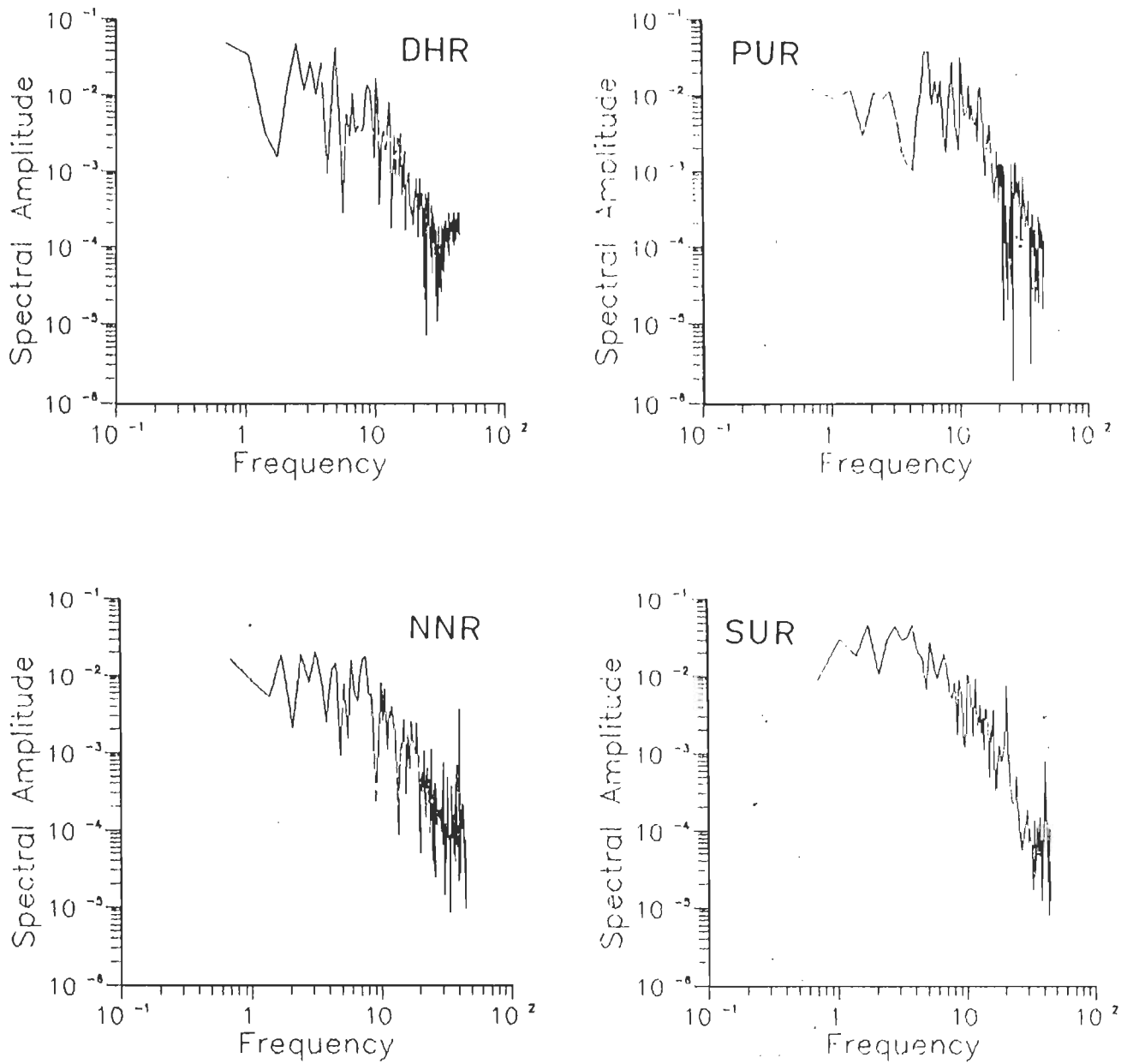


Fig.6.14 - Displacement Spectra of P-wave for seismic event dated 2-4-89 used for computation of seismic source parameters

DATE: 4.4.89

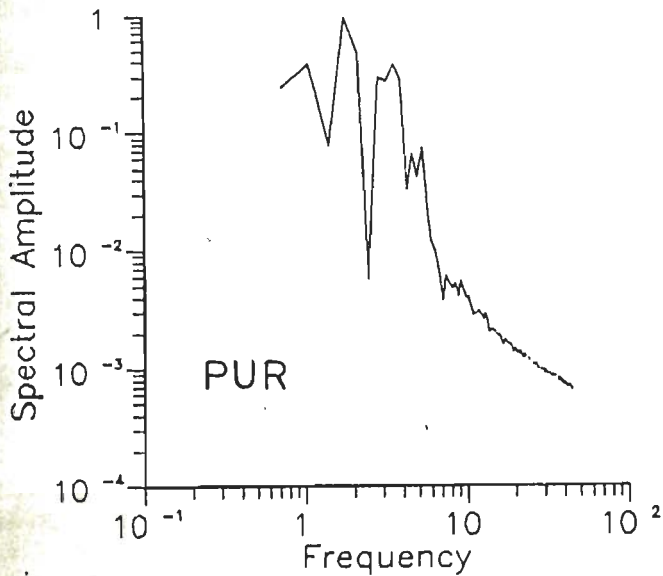
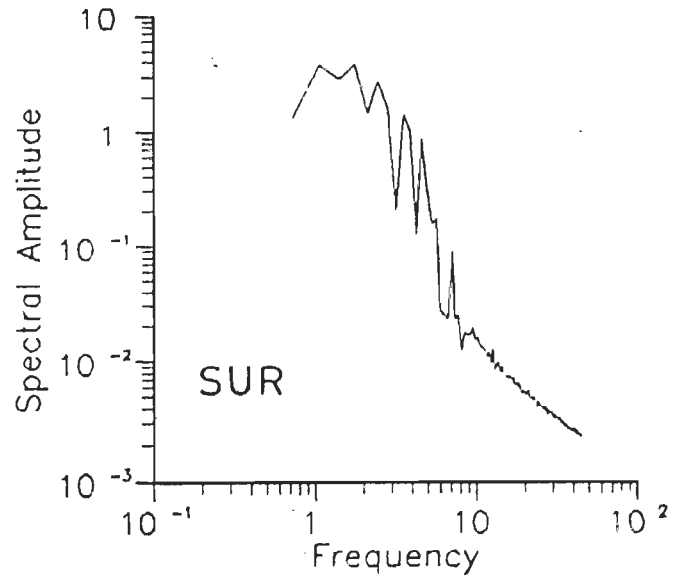
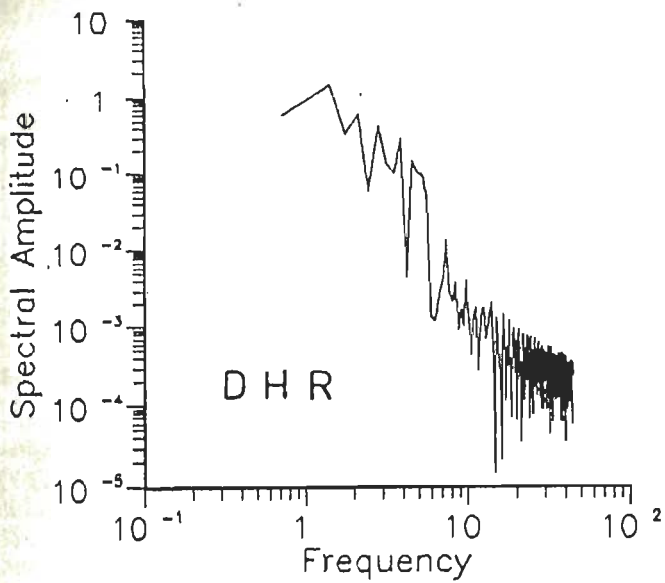


Fig.6.15 - Displacement Spectra of P-wave for seismic event dated 4-4-89 used for computation of seismic source parameters.

DATE: 9.4.89

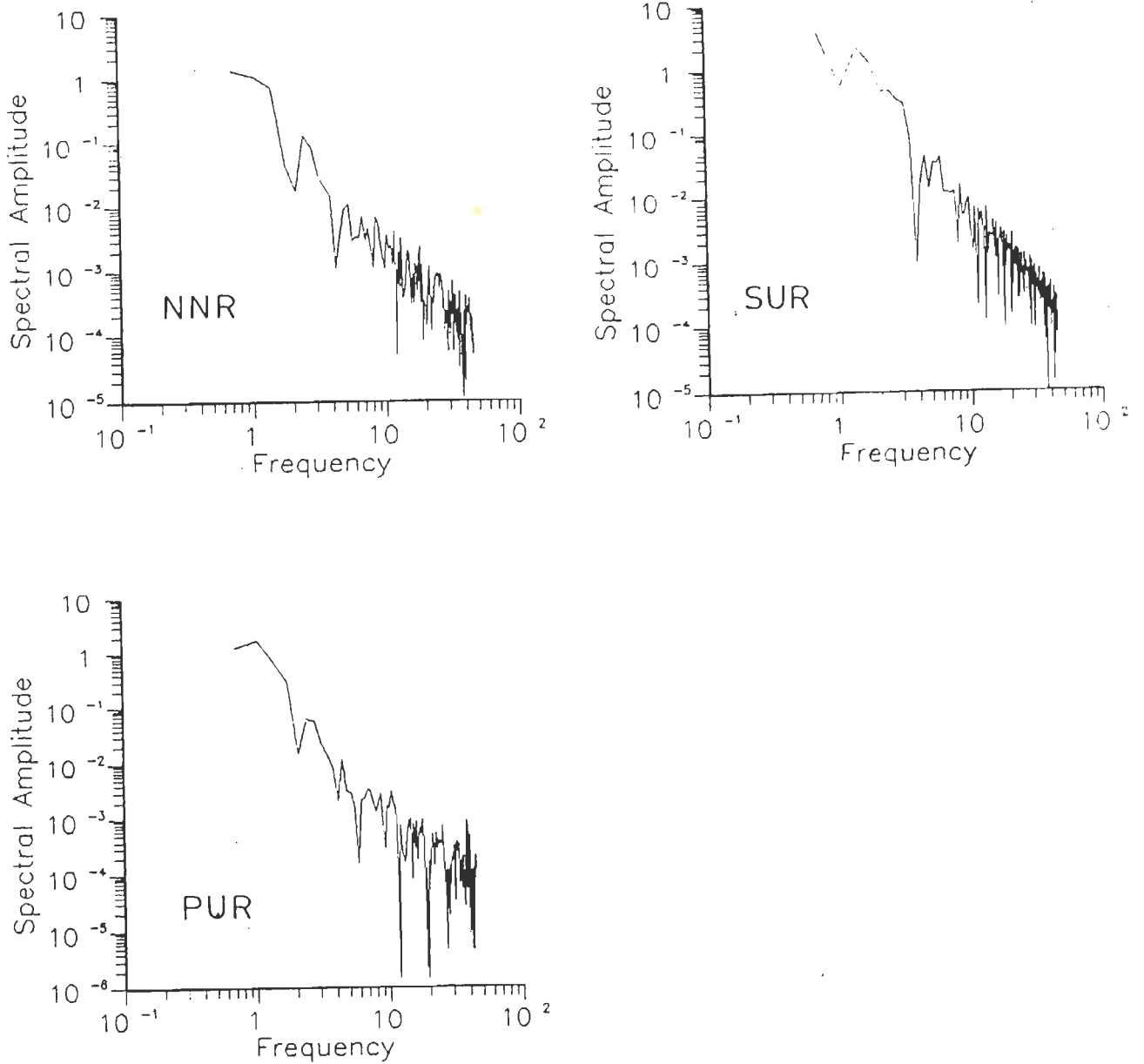


Fig.6.16 - Displacement Spectra of P-wave for seismic event dated 9-4-89 used for computation of seismic source parameters



DATE: 11.4.89 (I)

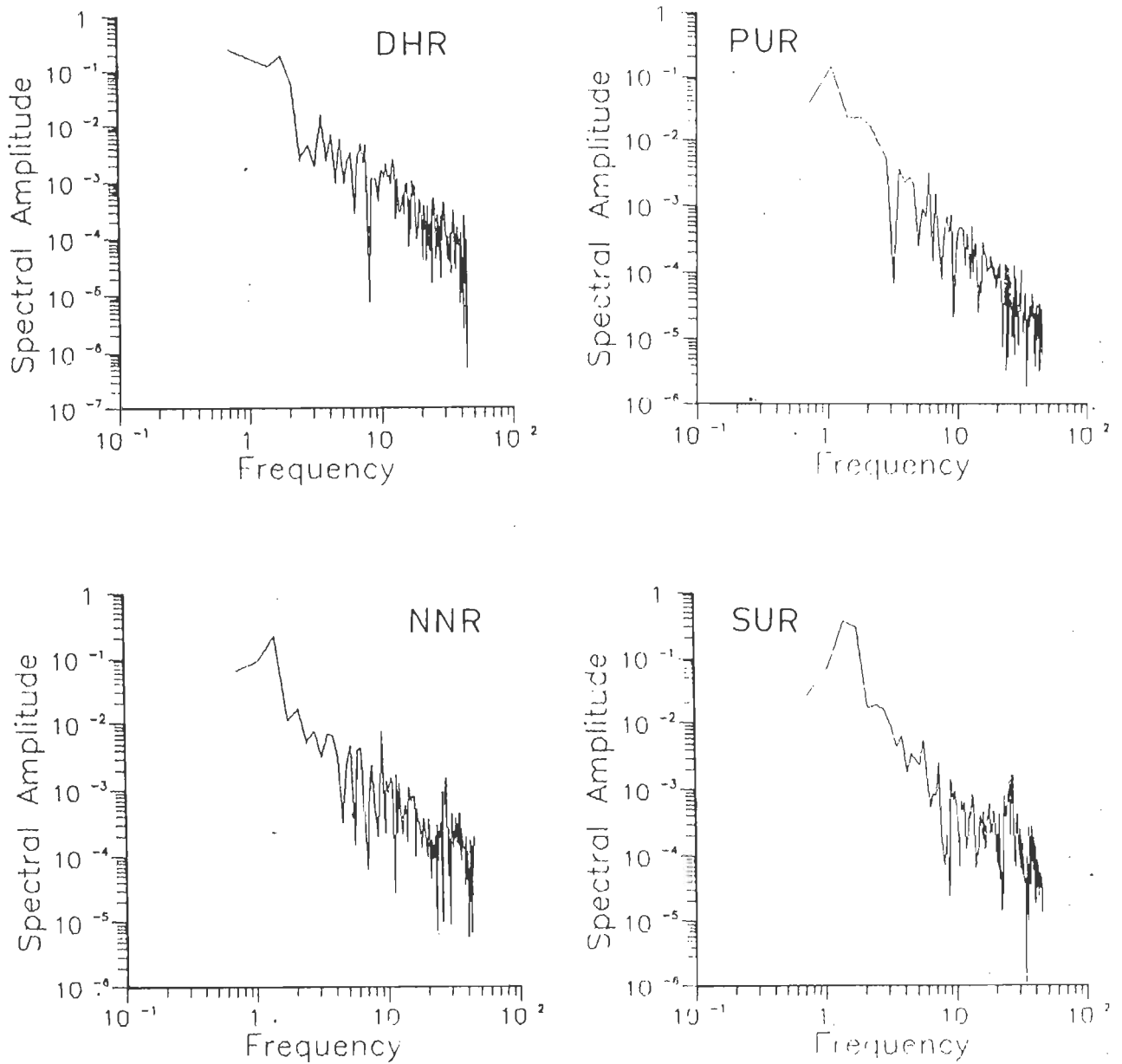


Fig. 6.17 Displacement Spectra of P-wave for seismic event dated 11-4-89 used for computation of seismic source parameters

DATE : 11.4.89 (II)

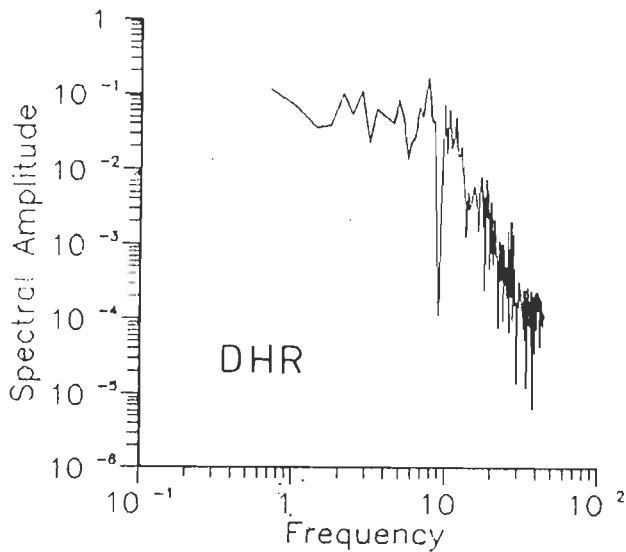
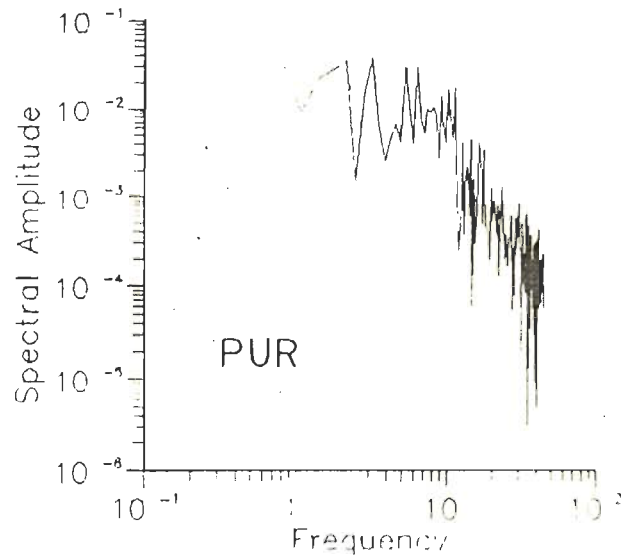
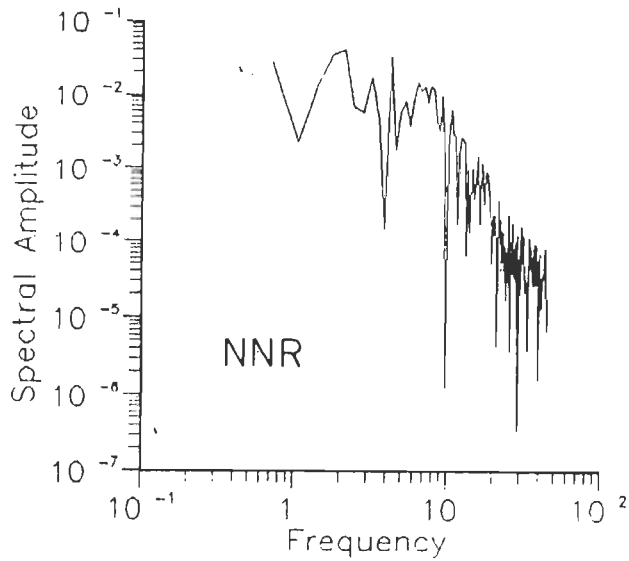


Fig. 6.18 - Displacement Spectra of P-wave for seismic event dated 11-4-89 used for computation of seismic source parameters

DATE: 12.4. 89

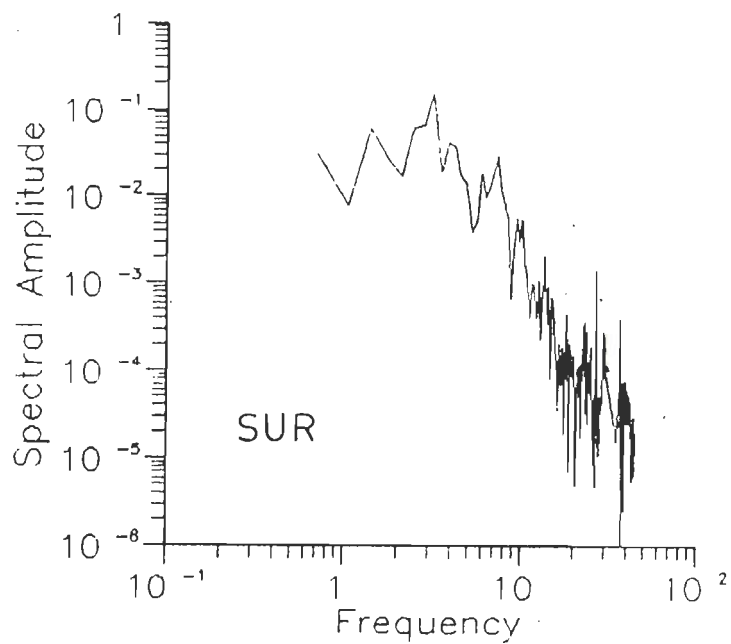
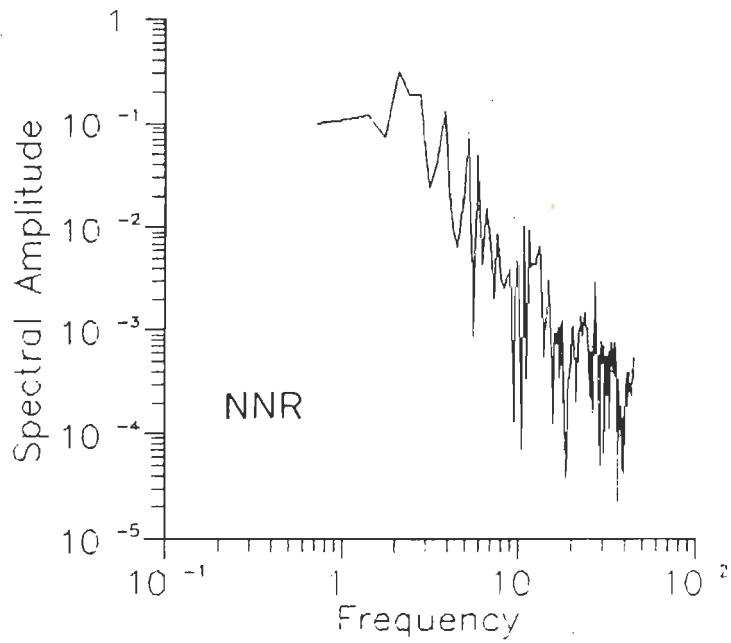


Fig.6.19 \_Displacement Spectra of P - wave for seismic event dated 12-4-89 used for computation of seismic source parameters

DATE : 16.4.89

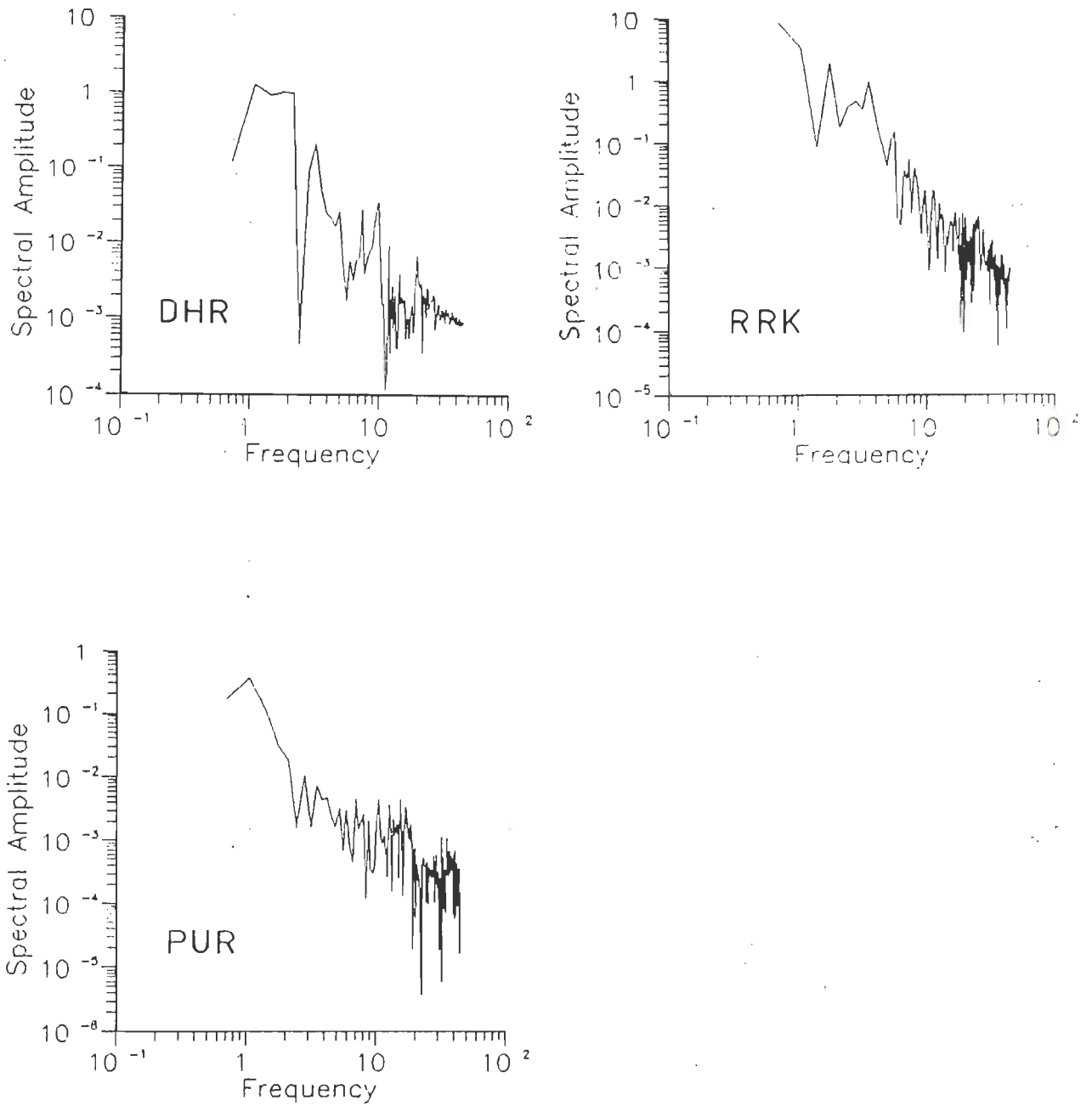


Fig.6.20 Displacement Spectra of P-wave for seismic event dated 16-4-89 used for computation of seismic source parameters

DATE : 19.4.89

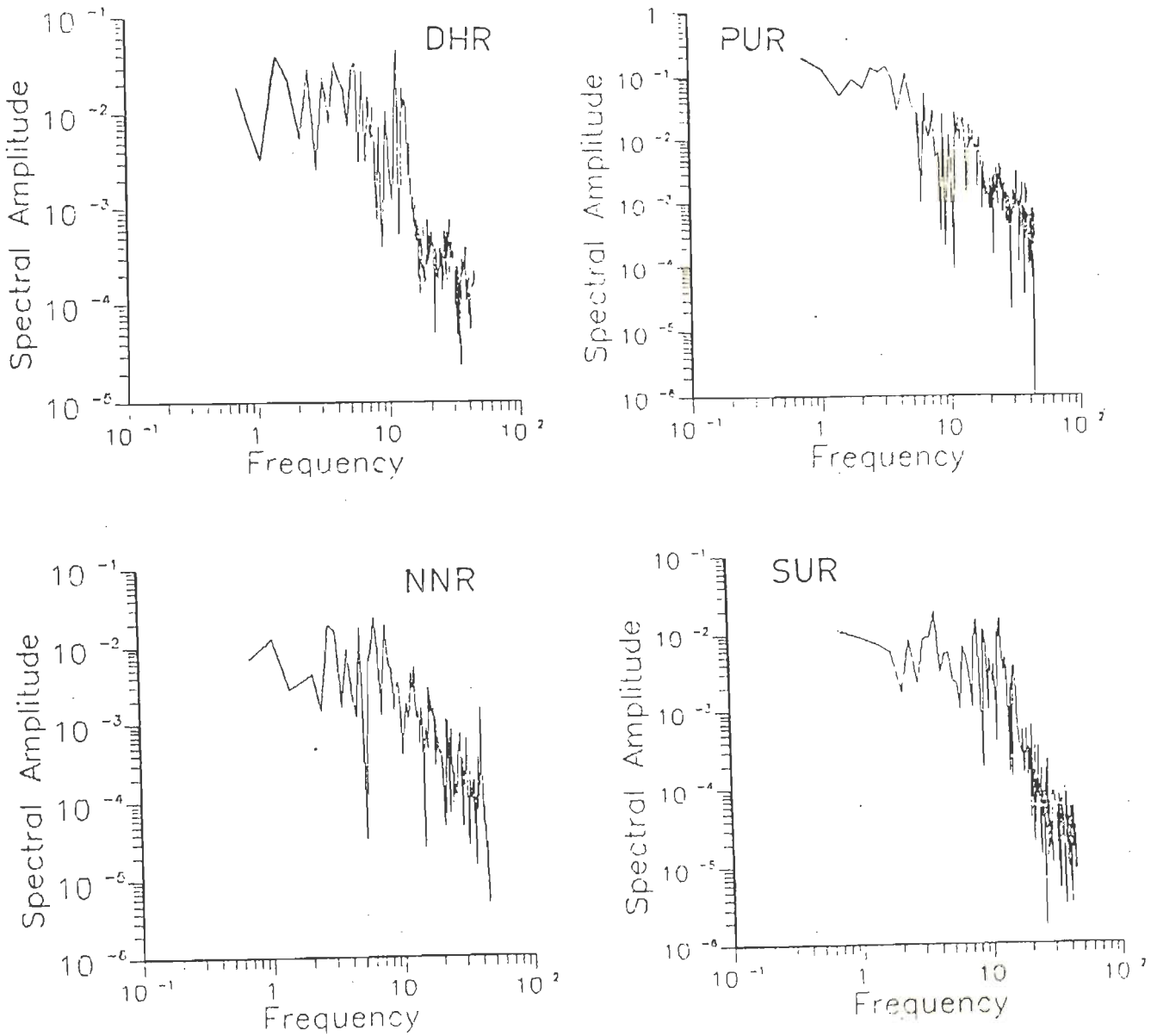


Fig. 6.21 - Displacement Spectra of P-wave for seismic event dated 19-4-89 used for computation of seismic source parameters

DATE: 22.4.89

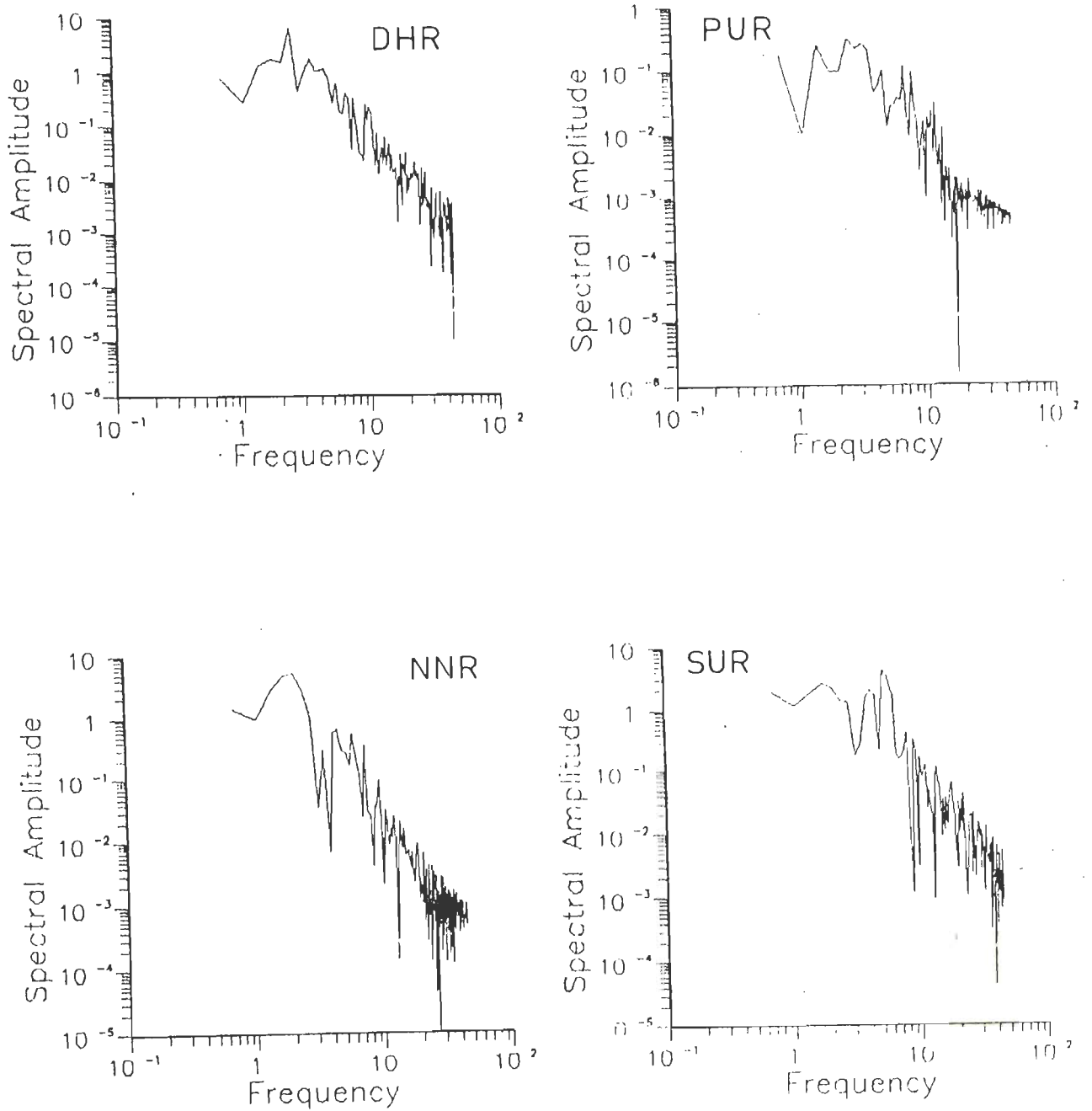


Fig.6.22 \_ Displacement Spectra of P - wave for seismic event dated 22-4-89 used for computation of seismic source parameters

DATE : 23 .4. 89

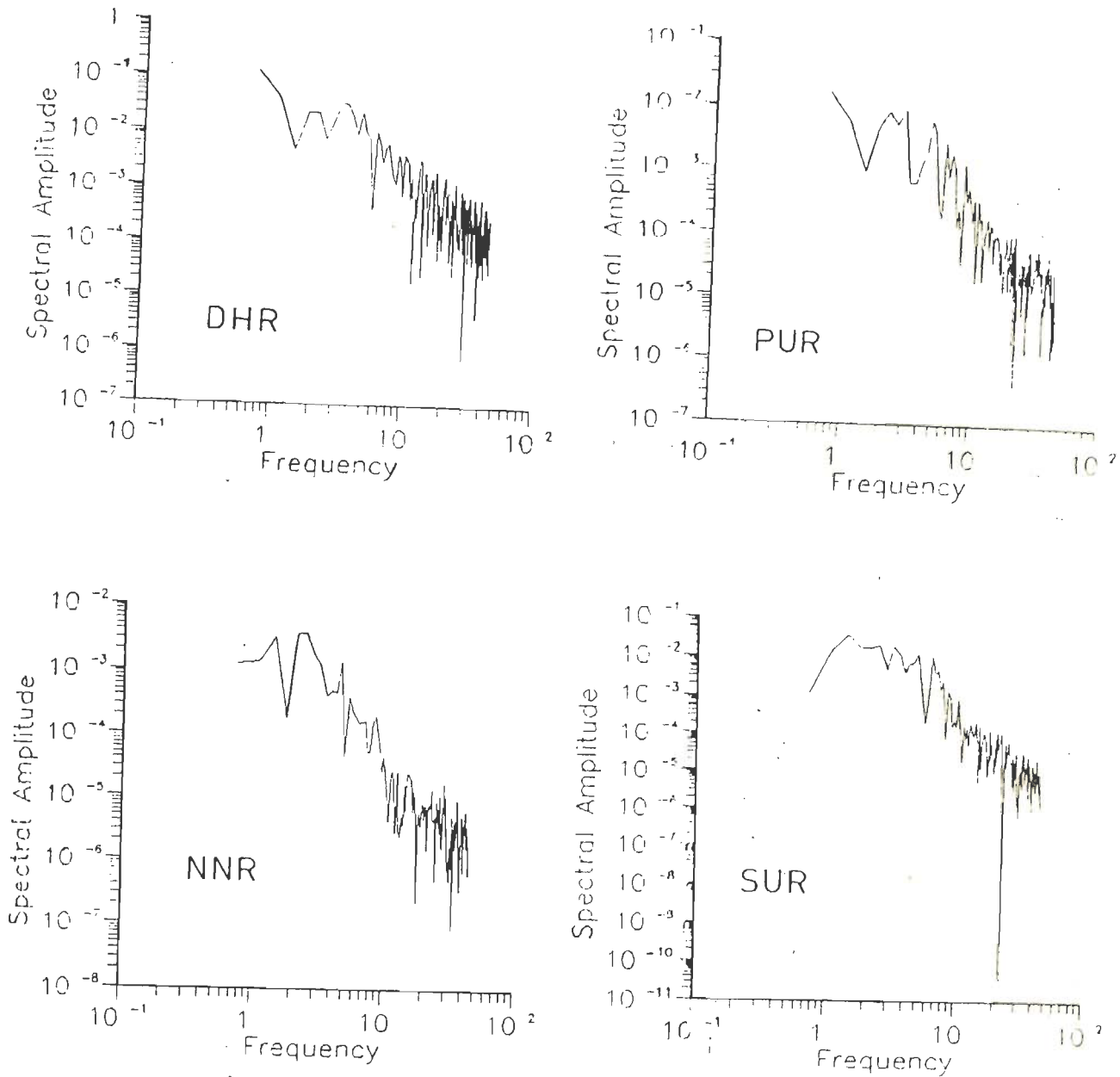


Fig.6.23 \_ Displacement Spectra of P-wave for seismic event dated 23-4-89 used for computation of seismic source parameters

DATE : 3.5.89 (I)

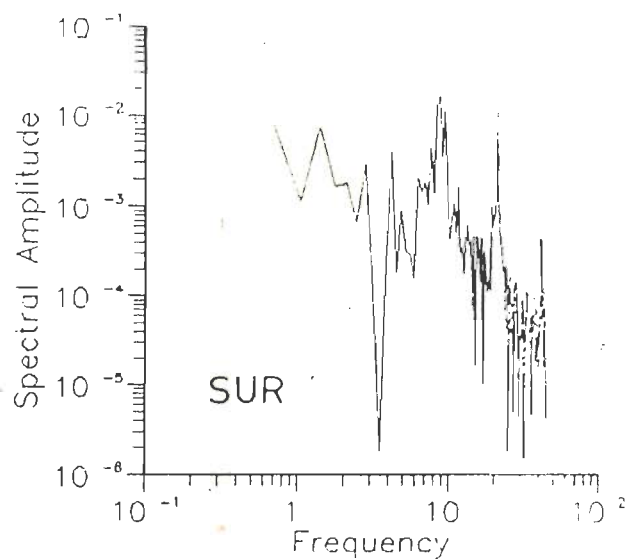
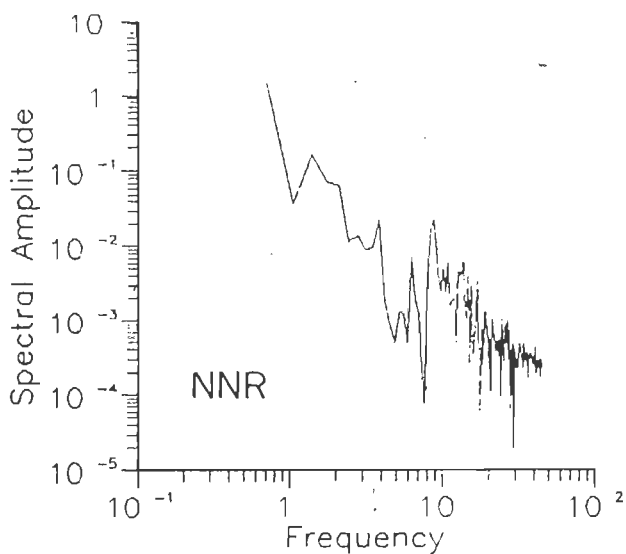
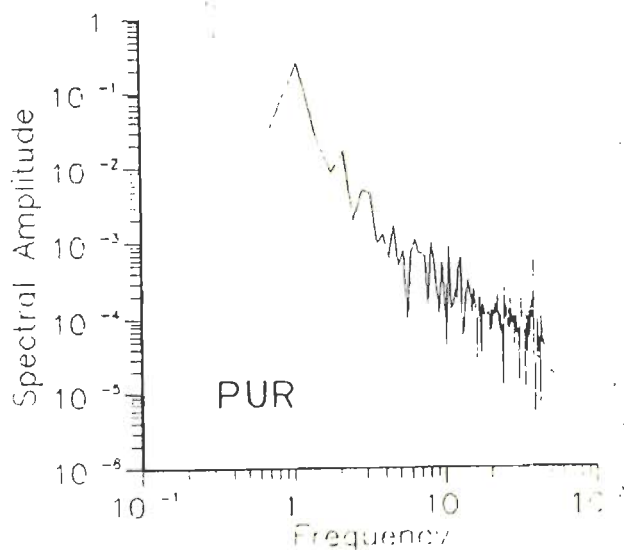
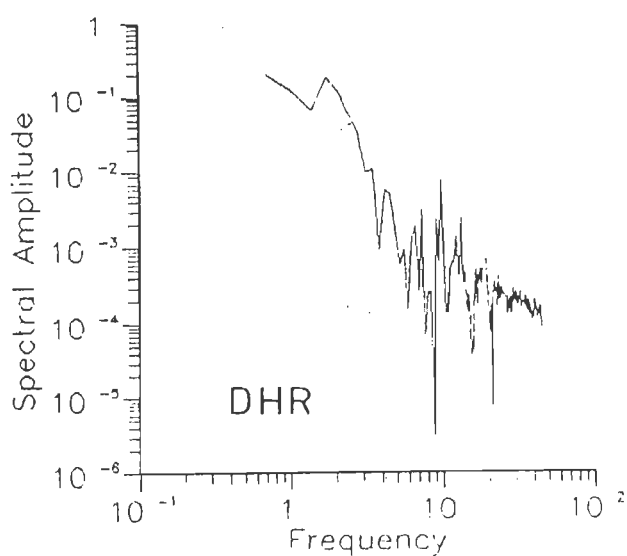


Fig. 6.24 \_ Displacement Spectra of P-wave for seismic event dated 3-5-89 used for computation of seismic source parameters



DATE : 3.5.89 (II)

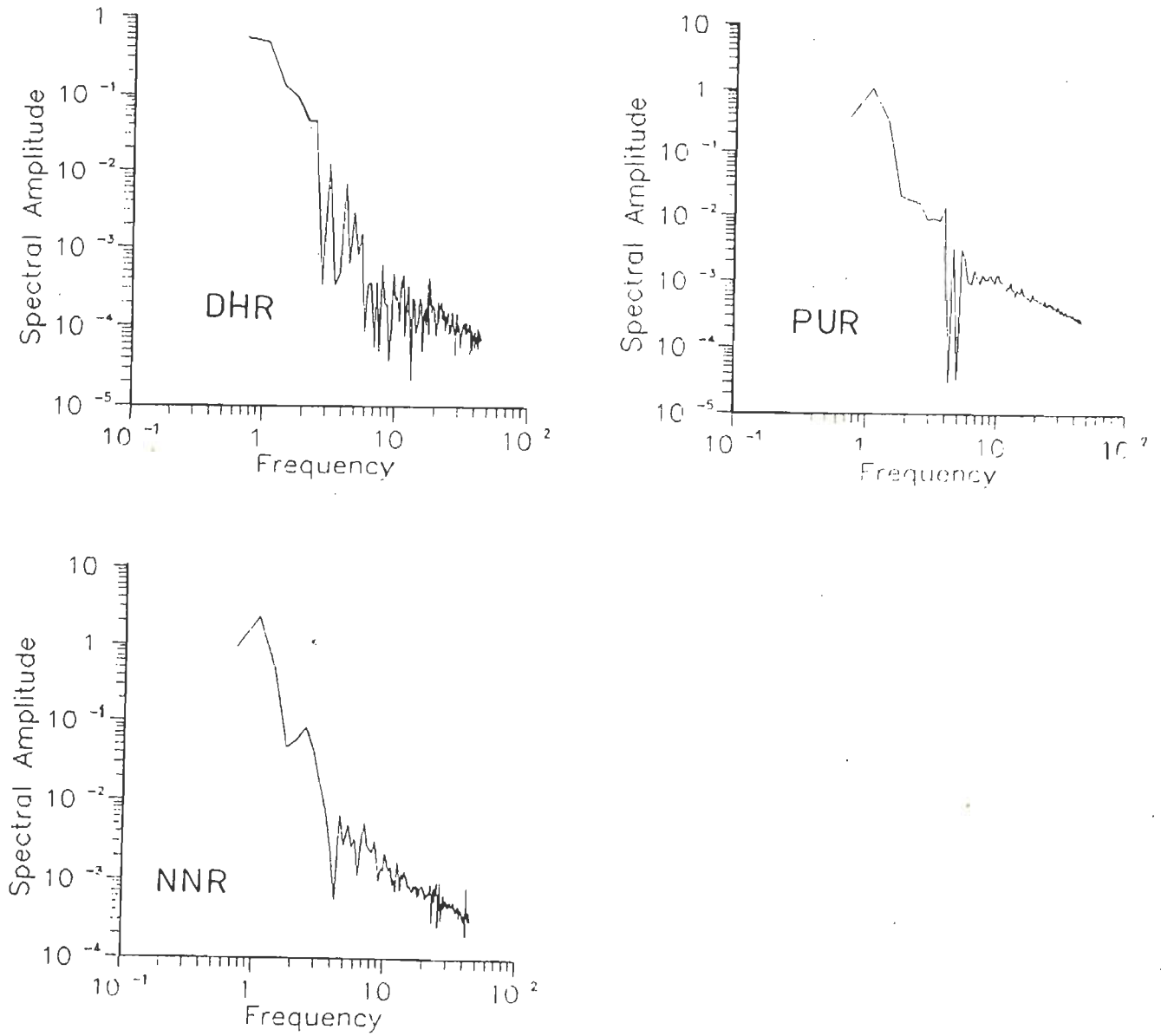


Fig.6.25 \_ Displacement Spectra of P-wave for seismic event dated 3-5-89 used for computation of seismic source parameters

DATE : 4. 5. 89

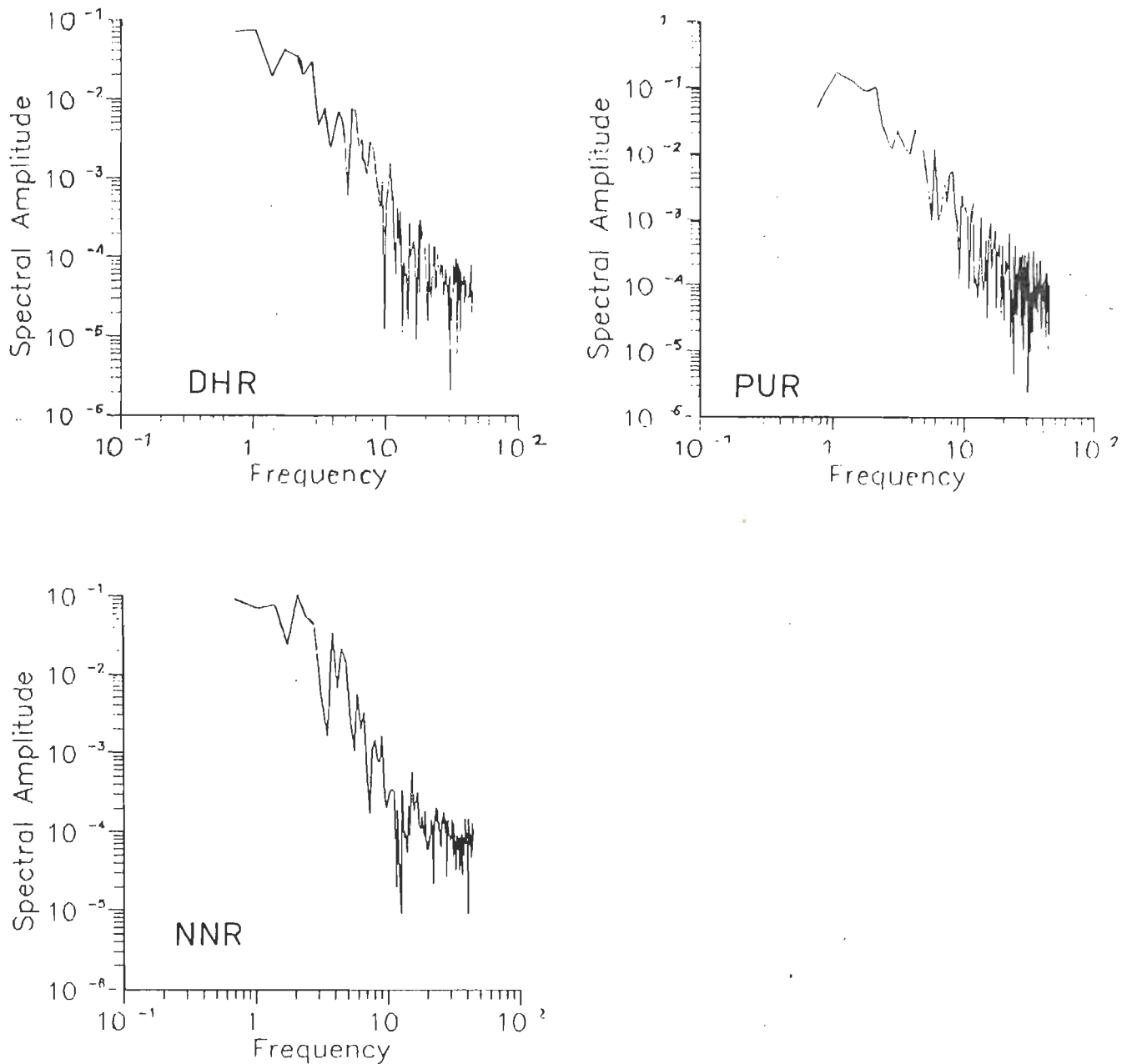


Fig. 6.26\_ Displacement Spectra of P-wave for seismic event dated 4-5-89 used for computation of seismic source parameters

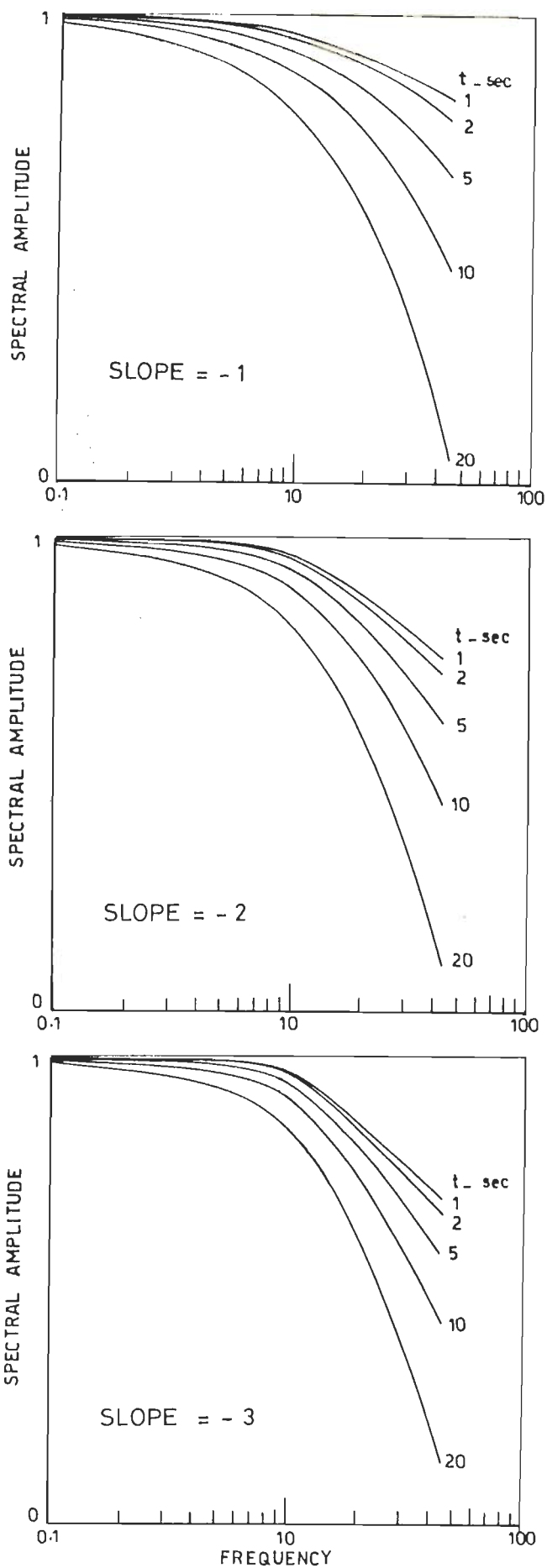


Fig. 6.27 - Master curves used to mark  $f_0$  and  $\Omega_0$ .

$$M_0 = 4 \pi \rho v^3 D \Omega_0 / R_{\theta\phi} \quad (6.3)$$

$$r = V_p / \pi f_0 \quad (6.4)$$

$$\Delta\sigma = 7 M_0 / (16 r^3) \quad (6.5)$$

$$u = M_0 / (4 \pi \mu r^2) \quad (6.6)$$

$$E = \Delta\sigma M_0 / 2\mu \quad (6.7)$$

where  $M_0$ ,  $r$ ,  $\Delta\sigma$ ,  $u$  and  $E$  are seismic moment, source radius, stress drop, slip and energy released respectively.  $\rho$  and  $\mu$  denote density and modulus of rigidity.  $D$  is the epicentral distance and  $R_{\theta\phi}$  is the radiation pattern. The above formulations have been widely used to compute the source parameters (21,32,43,45,48,51,53,76,77,78,96). For the computational purposes, the average velocity of P-wave is considered to be 6 km/sec and the average density of the material is taken as 2.77 gm/cm<sup>3</sup>. Since the fault plane solutions of the individual events could not be worked out due to less number of stations, the radiation pattern  $R_{\theta\phi}$  is approximately taken as 85 percent (76). The value of  $\mu$  computed from shear wave velocity by taking  $V_p/V_s$  equal to 1.71 is  $2.90 \times 10^{10}$  N/m<sup>2</sup> (54).  $M_0$  is taken as the average of seismic moments computed for different recording stations for an event. The source parameters computed viz, seismic moment, stress drop, source dimensions, slip and the energy released are listed in Table 6.6.

The individual values of  $M_0$ ,  $\Delta\sigma$ ,  $r$ ,  $u$  and  $E$  are plotted versus  $M_L$  on a semi-log scale as shown in Fig 6.28 to Fig 6.32. The straight line fit is obtained by least square fitting. This procedure is performed, firstly, to obtain useful empirical relationships between various parameters for Garhwal Himalaya region, and secondly, to see the confidence level of the estimation computed in the above manner. The relationships obtained with the slope and intercept of the straight line fit computed at 90% of confidence level using t-distribution (24) are as follows :

$$\log ( M_0 ) = (0.89 \pm 0.437) M_L + (18.18 \pm 0.21) \quad (6.8)$$

$$\log ( \Delta\sigma ) = (0.77 \pm 0.234) M_L - (1.78 \pm 0.468) \quad (6.9)$$

$$\log ( r ) = (0.69 \pm 0.016) M_L + (2.48 \pm 0.032) \quad (6.10)$$

$$\log ( u ) = (0.64 \pm 0.245) M_L - (3.11 \pm 0.490) \quad (6.11)$$

$$\log ( E ) = (1.67 \pm 0.449) M_L + (12.63 \pm 0.898) \quad (6.12)$$

Fig 6.28 to 6.32 show the graphical representation of the best fit lines and the observed data. Similar relationships for these parameters in relation to magnitude have been computed for other regions by different authors. Table 6.7 gives a list of the relationships obtained between magnitude and seismic moment

TABLE 6.6 SOURCE PARAMETERS OF THE SEISMIC EVENTS

Sl No	Date	Mag. $M_L$	$M_0$ (Dyn-cm) $\times 10^{20}$	$\Delta\sigma$ (Bars)	r (m)	u (cm)	E (Ergs)
1.	25 11 88	4.22	62.320	38.490	545	0.57	4.12E19
2.	08 03 89	2.05	0.816	0.62	363.7	0.016	8.70E15
3.	16 03 89	3.49	34.66	19.83	424.4	0.019	1.18E19
4.	29 03 89	2.41	22.84	19.25	373	0.44	7.56E18
5.	30 03 89	2.71	15.26	6.15	477	0.18	1.61E18
6.	02 04 89	3.16	2.55	0.92	493.5	0.028	4.03E16
7.	04 04 89	2.90	10.07	4.05	477	0.12	7.01E17
8.	09 04 89	2.56	7.29	2.57	498.6	0.08	3.22E17
9.	11 04 89	1.82	0.63	0.33	437	0.009	3.57E15
10	11 04 89	3.56	3.73	1.15	521	0.037	7.37E16
11	12 04 89	3.03	4.18	1.38	509.3	0.044	9.92E16
12	16 04 89	2.82	4.79	1.47	521.8	0.048	1.21E17
13	19 04 89	2.97	6.81	2.74	477	0.082	3.20E17
14	22.04.89	3.01	53.32	21.49	477	0.64	1.97E19
15	23 04 89	1.40	0.40	0.41	347.2	0.009	2.82E15
16	03 05 89	1.90	0.36	0.24	402.0	0.006	1.48E15
17	03 05 89	1.64	0.07	0.049	395.4	0.001	5.89E13
18	04 05 89	1.62	0.28	0.21	381.9	0.005	1.01E15

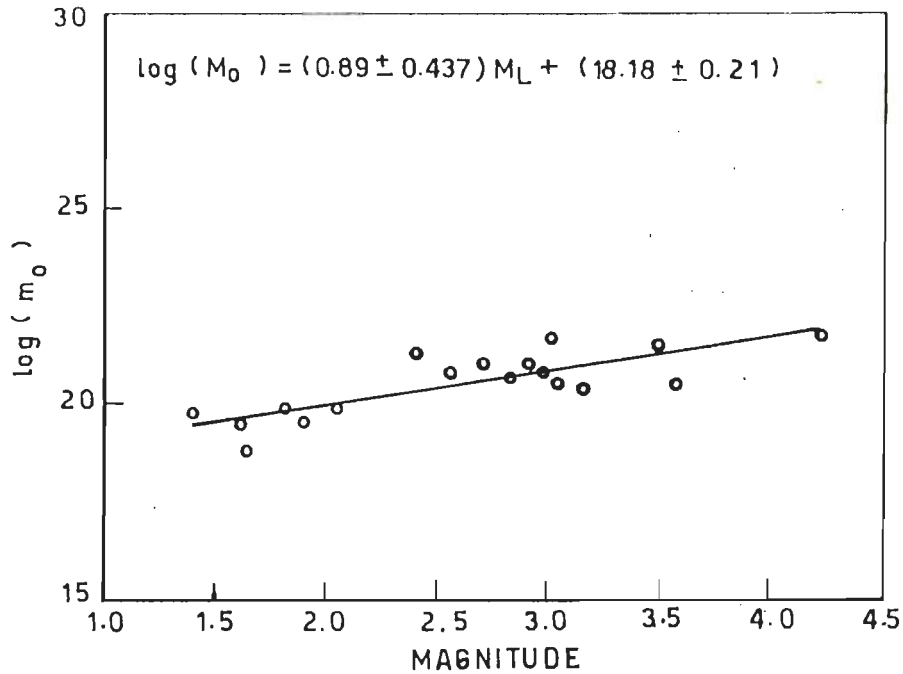


Fig. 6.28 - Linear regression curve of seismic moment ( $m_0$ ) with magnitude ( $M_L$ ) on semi-log scale

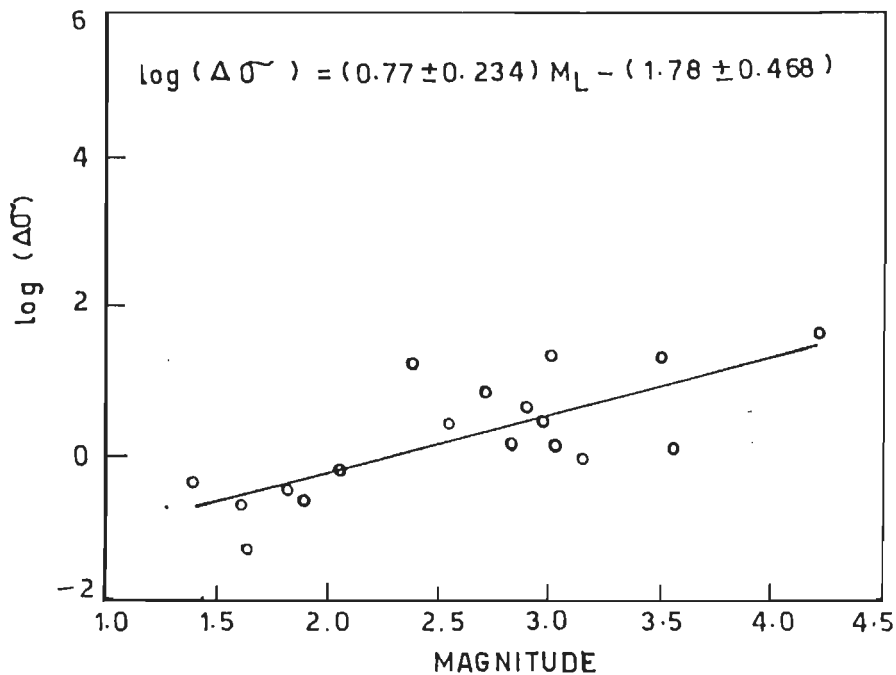


Fig. 6.29 - Linear regression curve of stress drop ( $\Delta\sigma$ ) with magnitude ( $M_L$ ) on semi-log scale

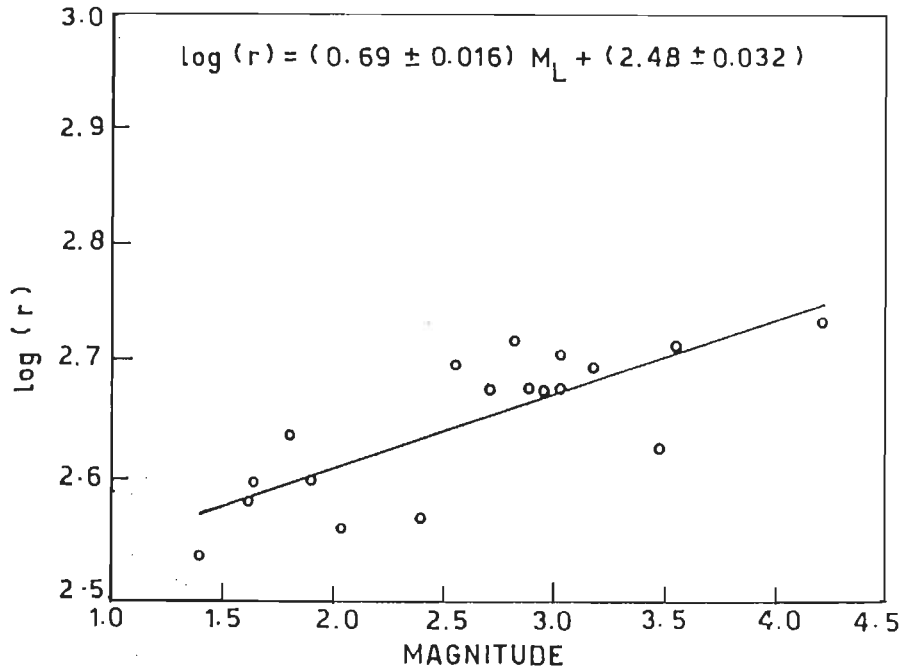


Fig. 6.30 - Linear regression curve of source dimension ( $r$ ) with magnitude ( $M_L$ ) on semi-log scale

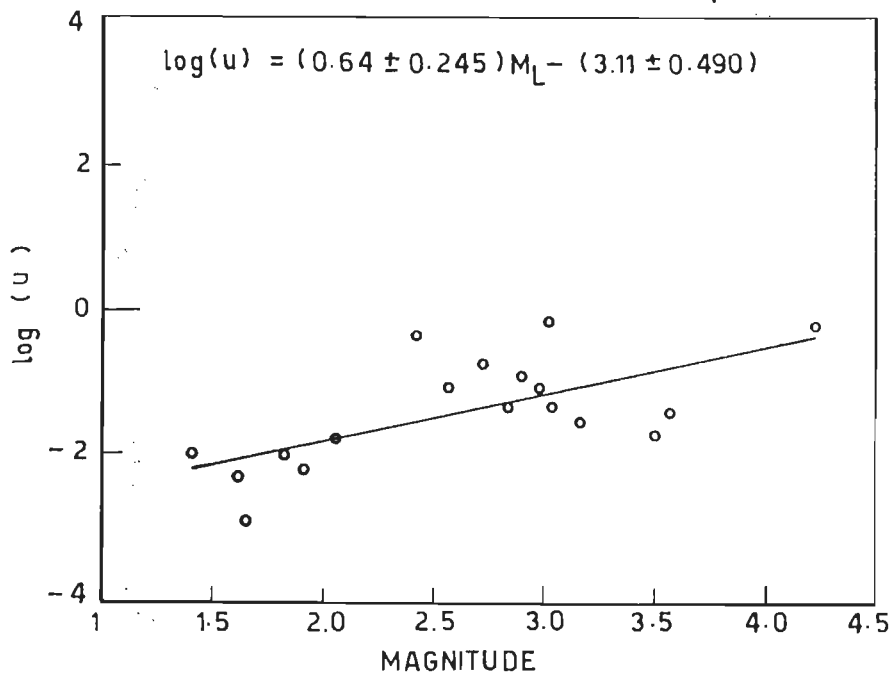


Fig. 6.31 - Linear regression curve of slip ( $u$ ) with magnitude ( $M_L$ ) on semi-log scale



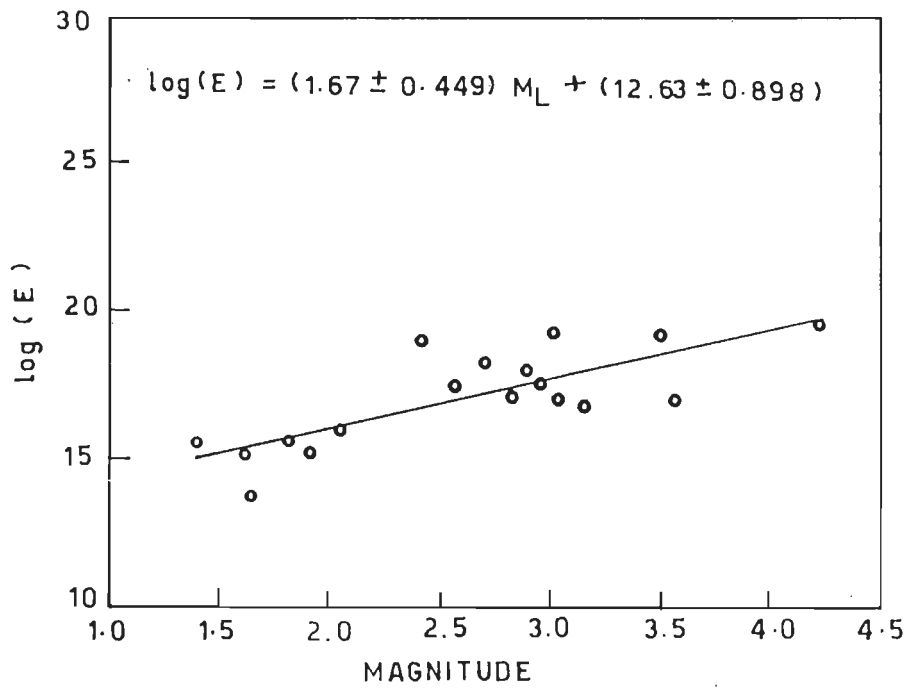


Fig. 6.32 - Linear regression curve of energy (E) with magnitude ( $M_L$ ) on semi-log scale

TABLE 6.7 'a' AND 'b' VALUES COMPUTED FOR SEISMIC MOMENT-MAGNITUDE RELATIONSHIP '(LOG  $M_o = a + b M_L$ ) FOR DIFFERENT AREAS BY VARIOUS AUTHORS.

Sl No.	Author	Region	a	b
1.	Present study	Garhwal Himalaya	18.18 $\pm$ 0.437	0.89 $\pm$ 0.21
2.	Wyss and Brune, 1968	San Andreas	17.0	1.4
3.	Thatcher and Hanks, 1973	Southern California	16.0	1.5
4.	Johnson and McEvelly, 1974	California	17.60 $\pm$ 0.28	1.16 $\pm$ 0.06
5.	Oncescu, 1983	Romania	18.0 $\pm$ 0.5	1.1 $\pm$ 0.1

for different area in comparison to Garhwal Himalaya region for which the relationships have been worked out in the present study.

#### 6.7.4 Interpretation of source parameters

The source parameters are computed for shallow earthquakes occurring in this part of the Himalaya. The linear regression curves show the trends of source parameters with respect to the local magnitude as given in equations (6.8) to (6.12). There are two basic types of explanations for low stress drop events - partial stress drop models (20) and low effective stress models (21). Partial stress drop events might occur when the fault locks (heals) itself soon after the rupture passes so that the average dynamic stress drops over the whole fault, or when the stress release is not uniform and coherent over the whole fault plane, but rather is more like a series of multiple events with parts of the fault remaining locked. In the low effective stress models the effective stress available for accelerating the fault is at all times low (not initially high, or high over parts of the fault as in partial stress drop models). These types of models have spectral shapes and far-field pulse shapes similar to that for large stress drop events and only the amplitudes are small (21).

In this part of Himalaya, the microearthquakes having shallow focal depths with low stress drops can be better understood with the partial stress drop model. These are the earthquakes with high frequency of occurrence arising due to

strain accumulation resulting from the adjustments going on in the region. The relative low stress drop at shallow depths shows that the rock mass constituting the upper crust in the region has little resilience for accumulation of strain and the rocks undergo brittle fractures and adjustments. The interpretation suggested above shall remain speculative until more data are obtained and possible sources of distortion and contamination of the spectra are better understood as the present spectra are not corrected for site response.

## CHAPTER # 7

### CONCLUSIONS AND SUGGESTIONS

---

CONCLUSIONS AND SUGGESTIONS FOR FURTHER WORK

---

7.1 CONCLUSIONS

The present study has attempted to formulate the methodology for processing of digital events data acquired by TDSA in the Garhwal Himalaya. The DAS records data on magnetic tapes using PDP 11/23 computer system in Industrial Compatible format. A software package TMD is developed under this study to transfer the recorded 16-bit data to 36-bit DEC 2050 computer system. This software also decodes the information and produces seismogram files for different stations recording an event with a common time and date file. Trigger parameters values suitable for this sample array were chosen and 530 events triggered at 3 or more stations were recorded during the period 13-2-89 to 7-5-89. The recorded data is processed to identify the seismic events and to determine their characteristic parameters. For the data processing two approaches are followed : (i) Visual analysis on the screen on PCs, and (ii) Automatic analysis using the phase pickers.

For the visual analysis of the recorded data on the PCs, the necessary methodology and procedures have been developed. The visual analysis of the recorded time series using these procedures identified 18 triggered events as seismic events and rest are rejected as false triggers. This shows that the trigger ratios for different stations are selected optimally ensuring that the low level seismic activity within the array, sensed by at least three stations is not missed.

The automatic mode of analysis is worked out by developing Automatic Phase Picker (APP) algorithm and its implementation in form of a computer program. The salient features of the phase picker (APP) include the use of a CF giving better S/N ratio compared to those used by others, STA/LTA computation combined with filters and confirmatory tests to check frequency dispersion (Test I) and shape of the coda (Test II). Test III checks the difference in the P-onset times marked at different stations after the time series have passed test I and II. APP has rejected 513 triggered events as false triggers and only 17 events are confirmed as seismic events, which is an excellent match with the visual analysis. The accuracy of APP in picking the P-onsets of seismic events is found as good as that of visual analysis on the PC's which in turn is more accurate than the conventional methods of measuring arrival times from analog records. For better accuracy, the station sites should have low background noise.

A comparison of the number of seismic events confirmed by other phase picker algorithms by Stewart, 1971 and Allen, 1978

using the same data set show that APP performs better and is more reliable.

The recording of higher number of false triggers shows that the event detector used by DAS at present is not sensitive to the shape (envelop) and frequency dispersion pattern of the time series to be recorded as seismic events. This drawback is taken care of by APP through its Test I and II. The event detection technique presently used in DAS should incorporate these features of the phase picker so as to decrease the number of false triggers recorded by the system.

The results of the visual analysis and APP are utilized to determine the hypocentral parameters and magnitude of the seismic events, and to work out their composite fault plane solution. Digital amplitude data has been utilized for the computation of the source parameters ; seismic moment, stress drop, source dimensions, slip and energy using Brune's model (1970). The estimated source parameters have the ranges : seismic moment -  $6.23 \times 10^{21}$  to  $7 \times 10^{18}$  dyne-cm, stress drop - 38.49 to 0.049 bars, source dimension - 545 to 347 m, slip - 0.57 to 0.001 cm and energy -  $4.1 \times 10^{19}$  to  $5.89 \times 10^{13}$  ergs. The shallow depth events with low stress drops imply the low resisting power of the upper crust to withhold the strain energy due to plate motions. This shows that the high magnitude earthquakes are more likely to occur below the upper crust in this interplate region.



As the data could only be acquired for intermittent periods, the small number of seismic events recorded by DAS and analysed in this study can be construed at best as a sample of seismicity of the region. There are a good number of hypocenters located near to the Dunda thrust. During this period no earthquake has been recorded close to MBT. The earthquakes recorded during this period are shallow focus earthquakes having focal depths less than 20 km except in one case where the focal depth is 24.09 km. Keeping in mind the orientation of existing fault planes, the composite fault plane solution suggests a reverse fault mechanism. This is in conformity with the data on past major earthquakes in the region which do not show surface breaks, as ruptures from such depths would not propagate to the ground surface in probable thrust/reverse fault mechanism.

Empirical relationships between the source parameters and the magnitudes of the seismic events for the region are obtained using linear regression analysis. The straight line fits with confidence level of 90 %, are as follows :

$$\begin{aligned} \log ( M_0 ) &= (0.89 \pm 0.437) M_L + ( 18.18 \pm 0.21) \\ \log ( \Delta\sigma ) &= (0.77 \pm 0.234) M_L - (1.78 \pm 0.468) \\ \log ( r ) &= (0.69 \pm 0.016) M_L + (2.48 \pm 0.032) \\ \log ( U ) &= (0.64 \pm 0.245) M_L - (3.11 \pm 0.490) \\ \log ( E ) &= (1.67 \pm 0.449) M_L + (12.63 \pm 0.898) \end{aligned}$$

These relationships may be used to estimate source parameters for any earthquake with magnitude  $M_L \leq 4$ .

The telemetered digital seismic arrays have advantages over conventional recordings in terms of higher dynamic range and resolution to record seismic activity of wider spread of magnitudes, common time base which yields more accurate hypocentral locations, facility for triggered event recording, real time processing of the data and minimal influence of spurious environmental disturbances

The optimal values of the trigger parameters depend on the characteristics of the region, aperture of the array, background noise levels at the outstations and the objectives of the data recording.

## 7.2 Suggestions for further work

To increase the reliability of the phase picking algorithms, the future algorithms should be developed taking into account the advantages of the Walsh transform. The algorithm should work in two distinct steps : (i) the detection of the seismic event should be done using the Walsh transform technique in the frequency domain and, (ii) the timing of the seismic arrivals should be worked out by the time domain algorithms. In this way, the algorithm will be using the superior detection technique of frequency domain and precise timing of the arrivals in the time domain.

The source parameters are computed without considering the effects of the sites on the seismograms. But a further re-examination of the source parameters is desirable to be made in light of the site responses at various stations. The hypocentral locations could be improved by experimenting different velocity models for the area. The attenuation characteristics should be worked out for the region for better estimates of different parameters.

The trigger parameters are selected for the sample array based on different characteristics of the region and the array. These parameters, particularly trigger ratios, should be worked out if the array geometry and/or the sites of the stations are altered. The DAS should have uninterrupted power and the lightning protectors of high quality at the outstations as well as at the CRS. In view of the high maintenance cost of the PDP 11/23 computer system, the PC based systems having the facility of post processing at CRS should be preferred.

## APPENDIX - I

```

      GO TO 10
C     START IT HERE
601   CONTINUE
      WRITE(25,*) ISSN
      DO 602 IU=1, ISSN
602   WRITE(25,*) KRSAMP(IU)
      CLOSE(UNIT=11)
      CLOSE(UNIT=12)
      CLOSE(UNIT=13)
      CLOSE(UNIT=14)
      CLOSE(UNIT=15)
      CLOSE(UNIT=16)
      CLOSE(UNIT=18)
      CLOSE(UNIT=25)
      STOP
      END
      SUBROUTINE SEREAL

```

```

*****
*     GIVES ACTUAL SAMPLE DATA WITH DATE & TIME     *
*     ARRANGES THE DATA SAMPLEWISE                 *
*****

```

```

      COMMON/A2/NINT(2048), N(3030), J, IJI, ISSN
      COMMON/A3/NST, LM(3030), M(3030)
      COMMON/A6/KRSAMP(10), NIN(4)
C     TAKE BITWISE
      I=1
      IF(IJI.EQ.1) GO TO 103
C     DATE AND TIME AS IT IS BCD
101   LA=MOD(NINT(I), 16)
      L1=NINT(I)/16
      LB=MOD(L1, 16)
      L2=L1/16
      LC=MOD(L2, 16)
      L3=L2/16
      LD=MOD(L3, 16)
      NINT(I)=LD*1000+LC*100+LB*10+LA
      I=I+1

```

```

      IF(I.LE.10) GO TO 101
      DO 1211 IO=6,9
1211  NIN(IO)=NINT(IO)
      WRITE(25,*) (NIN(IIO),IIO=6,9)
      IJI=1
C     STORE IT NINT---M( )
103   I1=1
104   M11=128+NST+(I1-1)*ISSNN
      M(I1)=NINT(M11)
      I1=I1+1
      I11=1920/ISSNN
      IF(I1.LE.I11) GO TO 104
C     NEXT BLOCK
      RETURN
      END
      SUBROUTINE SAMPLE
*****
*     COMPUTE DATA IN INTEGER FORM     *
*****
      COMMON/A2/NINT(2048),N(3030),J,IJI,ISSNN
      COMMON/A3/NST,LM(3030),M(3030)
      COMMON/A6/KRSAMP(10),NIN(4)
C     VARIABLES-----
C           NS--SIGN BIT
C           N2,N4--REST
C           NR--RANGE
C           ND--DATA NOT VALID
C           NE--PARITY IF PRESENT
C           ND+NE--COLLAP
      MK=1
102   N(MK)=MOD(M(MK),512)
      N1=M(MK)/512
      NS=MOD(N1,2)
C     COMPLEMENT FOR NEGATIVE DATA
      IF(NS.EQ.1) N(MK)=512-N(MK)
      N2=N1/2
      NR=MOD(N2,4)

```

```
N4=N2/16
ND=MOD(N4,2)
NE=N4/2
IF(NE.EQ.1) GO TO 603
IF(ND.EQ.0) GO TO 604
603 IF(MK.GT.1) GO TO 105
C   GIVE 0000 TO COLLAP
    LM(MK)=0
    GO TO 104
105 LM(MK)=LM(MK-1)
    GO TO 104
C   RANGE IT 00,04,16,64
604 IF(NR.EQ.3) GO TO 201
    IF(1-NR) 202,203,204
202 NI=16
    GO TO 205
203 NI=4
    GO TO 205
204 NI=1
    GO TO 205
201 NI=64
205 N(MK)=NI*N(MK)
    IF(NS.EQ.0) GO TO 301
    LM(MK)=-N(MK)
    GO TO 104
301 LM(MK)=N(MK)
C   REALIZE IT
104 MK=MK+1
    I11=1920/ISSNN
    KRSAMP(NST)=KRSAMP(NST)+1
    IF(MK.LT.I11) GO TO 102
    MS=NST+10
    WRITE(MS,*) (LM(I),I=1,MK)
C   NEXT BLOCK PLEASE
    RETURN
END
```

## 1.2 Computer Program APP

{ THE PROGRAM APP - AUTOMATIC PHASE PICKER' TEST A TIME SERIES FOR SEISMIC EVENT. THE PROGRAM MODIFIES THE TIME SERIES TO CHARACTERISTIC FUNCTION AND THEN RUN STA-LTA ALGORITHM (INCLUDING FILTERING PROCEDURES) TO MARK THE P-PHASE AND THEN CHECK THE TIME SERIES FOR SEISMIC EVENT USING CONFIRMATORY TESTS. (Developed in TURBO PASCAL VER. 5.0)

AUTHOR    ::     M. L. SHARMA  
 DATE      ::     OCT 1989

```

}
{*****}
program seismic(input,output);
  uses dos,crt,turbo3,graph3,graph;
  const
    a1=1;
    c1=0.995;{high pass filter time constant}
    k1=30;k2=150;{event conts}
{*****}
type
  aqq=array[1..3000] of real;
  bqq=array[1..3000] of integer;
  {
    sqq=array[1..3000] of real;}
  var
    zx: integer;
    c5: real;{CONSTANT FOR THRESHOLD}
    wxy: char;
att,f1,f2,f3,f4,xx,f11: text;
bool,bb1: boolean;
name:string;
    r1,sta1,lta1,r,cf,lta,sta,ref,sr,ta,delta,l,qw,s: real;
mean,samprate,slope,std,a5,a6: real;
    zerocounter,m,i,j,k5,s11,abstime: integer;
    qee,wee,p11,j11,i11,r11,m1,l11: integer;
    {M is peak index number}
    zerocrosstime: bqq;

```



```

    am: aqq;
{
    ed: sqq;
}
{THESE ARRAYS STORE THE ZEROCROSSTIMES AND PEAKS
OF THE CODA(EVENT)}
    b3, b4, b5, b8, b2: boolean;
{LOOP VARIABLES}
    c3, c4, sum1, sum2: real;
    currentamp, currentderi, noislevel: real;
{THESE ARE THE IMPORTANT PARAMETERS OF THE EVENT AT ONSET}
    provispeak: real;
{THIS IS THE CURRENT PEAK VALUE}

{
    P R O C E D U R E S
}
procedure setvideo(attribute: integer);
    var
        blinking, bold: integer;
    begin
        blinking:=(attribute and 4)*4;
        if(attribute and 1)=1 then
            begin
                bold:=(attribute and 2)*4;
                textcolor(blinking+bold);
                textbackground(3);
            end
        else
            begin
                bold:=(attribute and 2)*5 div 2;
                textcolor(7+blinking +bold);
                textbackground(1)
            end
        end;
procedure putstring(outstring: string;
    line, col, attrib: integer);
    begin
        setvideo(attrib);
        gotoxy(col, line);
        write(outstring);

```

```

        setvideo(0)
        end;
procedure putprompt(outstring:string;
    line,col:integer);
    begin
        gotoxy(col,line);
        clreol;
        putstring(outstring,line,col,3)
    end;
procedure getstring(var instring:string;
    line,col,attrib:integer;strlength:integer);
    const
        bell=#7;
        backspace=#8;
        carriagereturn=#13;
        special=#0;
        rightarrow=#77;
        leftarrow=#75;
        downarrow=#80;
        uparrow=#72;
    var
        oldstr:string;
        inchar:char;
        ii:integer;
    begin
        oldstr:=instring;
        putstring(instring,line,col,attrib);
        for ii:=length(instring) to strlength-1 do
            putstring(' ',line,col+ii,attrib);
        gotoxy(col,line);
        inchar:=readkey;
        if inchar<>carriagereturn then
            instring:='';
        while inchar<>carriagereturn do
            begin
                if inchar = backspace then
                    begin

```

```

if length(instring) >0 then
    begin
        instring[0]:=chr(length(instring)-1);
        write(backspace);
        write(' ');
        write(backspace)
    end
end
else
if inchar=special then
    begin
        inchar:=readkey;
        if inchar=rightarrow then
            begin
                if length(oldstr)>length(instring)
then
                    begin
                        instring[0]:=chr(length(instring)-1);
                        inchar:=oldstr[ord(instring[0])];
                        instring[ord(instring[0])]:=inchar;
                        write(inchar)
                    end
                end
            end
        else
            write(bell)
        end
    end
else
        if length(instring)<strlength then
            begin
                instring[0]:=chr(length(instring)+1);
                instring[ord(instring[0])]:=inchar;
                write(inchar)
            end
        end
else
write(bell) ;
inchar:=readkey
end;

```

```

    putstring(instring, line, col, attrib);
    for ii:=length(instring) to strlength -1 do
    putstring(' ', line, col + ii, 0);
    end;
procedure getpromptedstring(var instring:string;
    inattr, strlength: integer; strdesc:string; descline,
    descacol: integer; prompt:string; prline, prcol: integer);
    begin
    putstring(strdesc, descline, descacol, 2);
    putprompt(prompt, prline, prcol);
    getstring(instring, descline, descacol + length(strdesc) ,
    inattr, strlength);
    putstring(strdesc, descline, descacol, 0)
    end;
procedure getreal(var number:real; line,
    col, attrib, numlength, numdec: integer);
    const bell=#7;
    var
    valcode: integer;
    originalstr, tempstr: string;
    tempreal: real;
    begin
    str(number: numlength: numdec, originalstr);
    repeat
    tempstr:=originalstr;
    getstring(tempstr, line, col, attrib, numlength);
    while tempstr[1]=' ' do
    tempstr:=copy(tempstr, 2, length(tempstr));
    val(tempstr, tempreal, valcode);
    if valcode<>0 then
    write(bell);
    until valcode =0;
    number:=tempreal;
    str(number: numlength: numdec, tempstr);
    putstring(tempstr, line, col, attrib)
    end;

```

{THIS PROCEDURE DOES:

- 1) READS DATA FROM FILE SEQUENTIALLY
- 2) PRE-FILTERS THE DATA
- 3) GENERATES CHARACTERISTIC-FUNCTION (TIME SERIES)
- 4) GENERATES SHORT & LONG TIME AVERAGES}

```

procedure p4(var xyz:text; var bb:boolean; r1,sta1,lta1:
real; var d, r2,cf2,lta2,sta2,ref2: real; var a3,a4:real
; var i:integer; c5:real);
    const
        c1=0.995;
    var
        deltar:real;
x1:real;
j7:integer;
    begin{1}
        bb:=true;
    if(i=1) then
    begin
        read(xyz, j7, x1);
        a3:=x1
    end
    else
        read(xyz, j7, x1);
        if eof(xyz) then bb:=false;
        a4:=x1;
    if(i=1)
    then
        r2:=a3
    else
    begin{2}
        r2:=r1*c1+(a3-a4);{high pass filter to remove d.c}
        d:=r2-r1;
        deltar:=a3-a4
    end;{2}
    { sum1[1]:=0;
    sum2[1]:=0; }
    {sum1[i]:=sum1[i-1]+(r2*r2);

```

```

        sum1[i]:=sum1[i-1]+(deltar*deltar);}
    if(i=1) then
    begin{3}
    cf2:=2*sqr(r2)
    end {3}
    else
    {$r-}
        cf2:=sqr(r2)+sqr(deltar);
if (i=1)then
begin{4}
                                sta2:=0.67*cf2;
                                lta2:=0.008*cf2
end{4}
    else
    begin{5}
                                lta2:=(1-0.008)*lta1+(0.008*cf2);
                                sta2:=(1-0.67)*sta1+(0.67*cf2)
    end; {5}
                                ref2:=c5*lta2;
i:=i+1;
a3:=a4 ;
    end;
procedure getpromptedreal(var innumber:real;inattr,
numlength,inumdec:integer; strdesc:string;descline,
descacol:integer; prompt:string;prline,prcol:integer);
begin
    putstring(strdesc,descline,descacol,2);
    putprompt(prompt,prline,prcol);
    getreal(innumber,descline,descacol+length(strdesc),
inattr,numlength,inumdec);
    putstring(strdesc,descline,descacol,0);
end;
{THIS PROCEDURE VERIFIES THE PRESENCE OF ZERO CROSSINGS}
    procedure p3(a1,a2:real;var b8:boolean);
    begin
        if((a1>0.0)and(a2>0.0)) then b8:=false else
        if((a1<0.0)and(a2<0.0)) then b8:=false else

```

```

        b8:=true
    end;
{THIS PROCEDURE ANALYSE THE FREQUENCY DISPERSION}
    procedure frequency(var peakindex:bqq;var mean,
        std,samprate:real;eventstart,eventend:integer);
    type
        a1=array [1..1550] of integer;
    var
        freq:a1;
        b6:boolean;
        n,i1,j1,k1:integer;
    m,s:real;
    begin
        n:=trunc((eventend-eventstart)/(samprate*0.5));
{   writeln('n:',n);}
        j1:=1;
            for i1:=1 to n do
                begin
                    b6:=true;
                    k1:=0;
{   writeln('k1:',k1); }
                    while(b6) do
                        begin
                            if(peakindex[j1]>trunc(i1*0.5*samprate))
                                then b6:=false
                                else
                                    begin
                                        k1:=k1+1 ;
                                        j1:=j1+1
                                        end
                                    end;
                                {$r-}
                                freq[i1]:=k1;
{   writeln(freq[i1],' i1:',i1);}
                                end;
                                m:=0;
                                for i1:=1 to n do

```

```

        m:=m+freq[i1];
{ writeln('m:',m); }
        mean:=(m/n);
{ writeln('mean:',mean);}
        s:=0;
        for i1:=1 to n do
            s:=s+(freq[i1]-mean)*(freq[i1]-mean);
{ writeln('s:',s);}
        std:=sqrt(s/n);
{ writeln('std:',std)}
        end;
        {THIS PROCEDURE RESETS THE PEAK INDEX}
        procedure p0(var g:integer);
        begin
            g:=1;
        end;
procedure codaslope(var pm:aq;pi:bqq;var slope,samprate:
real;eventstart,eventend:real);
    var
        up,down:real;
n,i1,j1,k1:integer;
        b7:boolean;
        temp1,temp2:real;
    begin
        up:=0.0;
        down:=0.0;
        n:=trunc((eventend-eventstart)/(samprate*0.5));
        temp1:=0.0;
j1:=2;
        for i1:=1 to n do
            begin
                b7:=true;
                while(b7) do
                    begin
                        if (pi[j1]>trunc(i1*samprate*0.5)) then
                            b7:=false
                        else

```



```
begin
```

```
  if (pm[j1]>pm[j1-1])then
```

```
    temp2:=pm[j1]
```

```
  else
```

```
    temp2:=pm[j1-1];
```

```
  j1:=j1+1
```

```
end
```

```
  end;
```

```
  if (temp2>temp1)then
```

```
    up:=up+sqr(temp2-temp1)
```

```
  else
```

```
    down:=down+sqr(temp1-temp2);
```

```
  temp1:=temp2
```

```
  end;
```

```
  slope:=sqr(up/down)
```

```
  end;
```

```
procedure convert(var file2:text);
```

```
var
```

```
  file1:text;
```

```
  i:integer;
```

```
  x:char;
```

```
  www:string;
```

```
begin
```

```
getpromptedstring(www,1,30,' FILE NAME  :',10,2,
```

```
'TYPE INPUT FILE NAME AND PRESS ENTER',24,2);
```

```
clrscr;
```

```
gotoxy(19,10);
```

```
writeln('PLEASE WAIT ! ');
```

```
gotoxy(12,12);
```

```
writeln('THE FORMAT IS BEING CONVERTED FROM FREE
```

```
TO APPROPRIATE FORMAT');
```

```
  assign(file1,www);
```

```
  reset(file1);
```

```
  assign(file2,'cs10.dat');
```

```
  rewrite(file2);
```

```
  i:=1;
```

```
  write(file2,i:6,' ');
```

```

while not eof(file1) do
begin
    read(file1,x);
    if(ord(x)<>44)then
    begin
        if((ord(x)<>32)and(ord(x)>31))then
        if not(x='@') then
        write(file2,x)
        end
    else
    begin
        i:=i+1;
        writeln(file2);
        write(file2,i:6,'      ')
        end
    end;
    close(file2)
end;

```

```

{*****}

```

```

{MAIN PROGRAM}

```

```

    begin;
    clrscr;
    assign(att,'ar.dat');
    rewrite(att);
assign(f2,'q.dat');
    rewrite(f2);
    assign(f3,'s.dat');
    rewrite(f3);
    assign(f4,'s1.dat');
    rewrite(f4);
    assign(xx,'result');
    rewrite(xx);
        assign(f11,'filtered.dat');
        rewrite(f11);
gotoxy(10,3);

```

```

writeln('-----')
-----');
gotoxy(10,24);
writeln('-----')
-----');
for i:=4 to 23 do
begin
  gotoxy(10,i);
  write('I
                                I')

end;
gotoxy(12,5);
writeln(' APP - AUTOMATIC PHASE ');
gotoxy(12,6);
writeln(' -----');
gotoxy(12,10);
writeln(' PICKER & ANALYSER');
gotoxy(12,11);
writeln(' -----');
gotoxy(11,18);
writeln(' M L SHARMA ');
  gotoxy(22,25);
  write('PRESS ANY KEY TO CONTINUE:');
  gotoxy(49,25);

repeat
until keypressed;
clrscr;
  bool:=false;
  gotoxy(9,3);
writeln('-----')
-----');
gotoxy(9,20);
writeln('-----')
-----');
for i:=4 to 19 do
begin
  gotoxy(9,i);

```

```

write('I
                                     I')

end;
gotoxy(11,5);
writeln('THIS SOFTWARE IS DEVELOPED TO PICK THE P-PHASE
ARRIVAL OF SEISMIC EVENTS');
gotoxy(11,7);
    writeln('THIS PROGRAM REJECTS TRANSIENT NOISE BURSTS
AND SELECT SEISMIC EVENTS. ');
gotoxy(11,9);
    writeln('THE DATA IS PASSED THROUGH D.C OFFSET REMOVERS,
PRE-FILTERS, ');
gotoxy(11,11);
writeln('TO REMOVE NOISE-PEAKS. ') ;
gotoxy(11,15);
    writeln('THE TIME SERIES IS MODIFIED TO CHARACTERISTIC
FUNCTION ');
gotoxy(11,17);
    writeln('AND STA LTA ALGORITHM MARK P PHASE. ');
    gotoxy(72,21);
    delay(10);
    clrscr;
gotoxy(9,3);
writeln('-----
-----');
gotoxy(9,20);
writeln('-----
-----');
for i:=4 to 19 do
begin
    gotoxy(9,i);
    write('I
                                     I')

end;
gotoxy(11,5);
    writeln('TO UNDERSTAND THE LOGIC OF DETECTION, PLEASE
RUN "VIEWER.COM"');

```

```

gotoxy(11,7);
    writeln('THIS SOFTWARE SIMULATES AN ON-LINE PROCESS
    BY TREATING');
gotoxy(11,8);
writeln('          -----');
gotoxy(11,9);
writeln('DATA SEQUENTIALLY. ');
gotoxy(11,11);
    writeln('THIS SOFTWARE PRESERVES MEMORY SINCE ONLY
    THE EVENT IS') ;
gotoxy(11,12);
writeln('          -----');
gotoxy(11,13);
writeln('IS STORED AND THE NOISE IS REJECTED.THE
ANALYSES IS ');
gotoxy(11,15);
    writeln('STORED IN AN OUTPUT FILE CALLED "RESULT" ');
    gotoxy(72,20);
    delay(50);
    clrscr;
    writeln('CHOOSE FORMAT : (1) FOR FREE FORMAT ,ANY OTHER
    DIGIT TO CONTINUE');
    read(zx);
    clrscr;
    if (zx<>1) then
    begin
        gotoxy(9,3);
writeln('-----
-----');
gotoxy(9,20);
writeln('-----
-----');
for i:=4 to 19 do
begin
    gotoxy(9,i);
    write('1
1')

```

```

end;
gotoxy(11,5);
writeln('PLEASE NOTE');
gotoxy(11,8);
writeln('-----');
gotoxy(11,7);
    writeln('THE INPUT DATA FILE SHOULD HAVE FORMAT AS:');
gotoxy(11,8);
    writeln('      S.No          DATA          ');
gotoxy(11,9);
    writeln('      1              XX ');
gotoxy(11,11);
    writeln('      2              XX ');
gotoxy(11,12);
gotoxy(11,13);
writeln(' ');
gotoxy(11,15);
    writeln(' ');
    gotoxy(72,20);
    delay(3000);
    clrscr;
    getpromptedstring(name,1,30,' FILE NAME  :',10,2,'TYPE
INPUT FILE NAME AND PRESS ENTER',24,2);
    assign(f1,name)
    end
    else
        convert(f1);
    reset(f1);
    clrscr;
    getpromptedreal(samprate,1,30,1,'SAMPLING RATE
: ',10,2,'ENTER SAMPLING RATE',24,2);
    clrscr;
    getpromptedreal(c5,1,30,1,'TRIGGER RATIO  :',10,2,
'ENTER TRIGGER RATIO',24,2);
    clrscr;
        gotoxy(9,3);

```

```

writeln('*****
*****');
gotoxy(9,20);
writeln('*****
*****');
for i:=4 to 19 do
begin
  gotoxy(9,i);
  write(' *
                                     *')

end;
gotoxy(11,10);
writeln('          THE SEISMIC DATA IS BEING MONITORED');
  gotoxy(72,20);
k5:=1;
j:=1;
  s:=0;
r:=0.0;
sr:=0.0;
cf:=0.0;
sta:=0.0;
lta:=0.0;
ref:=0;
r1:=0.0;
sta1:=0.0;
lta1:=0.0;

  i:=1;
  bb1:=true;
  b2:=true;
      while (b2=true) do
        begin {*}
          p0(j);
          b3:=true;
          while(b3=true) do
            begin {&}
              p4(f1,bb1,r1,sta1,lta1,sr,r,cf,lta,sta,ref,a5,a6,i,c5);
              r1:=r;

```

```

noiselevel:=lta1;
sta1:=sta;
lta1:=lta;
        if ((sta>ref)and (i>350))
then
begin
    b3:=false;
    qw:=ref
end
        else
            b3:=true ;
                if(bb1=false) then
                    begin{@@}
                        b3:=false
                    end{@@}
end;{&}
    p11:=0;
    j11:=1;
{ declare event and store onset value }
    abstime:=i-1;
    currentamp:=r;
    currentderi:=sr;
    noiselevel:=noiselevel+10.0;
    { ed[j11]:=r; }
    p11:=p11+1;
    j11:=j11+1;
    if (bb1=false)then
        begin
            b4:=false ;
            b5:=false
        end
    else
        begin
            b5:=true;
            b4:=true
        end;
    while(b4=true) do

```



```

begin{1}
provispeak:=abs(r);
b5:=true;
while(b5=true) do
begin {2}
ta:=r;
p4(f1,bb1,r1,sta1,lta1,sr,r,cf,lta,sta,ref,a5,a6,i,c5);
r1:=r;
sta1:=sta;
lta1:=lta;
{ed[j11]:=r;}
p11:=p11+1;
j11:=j11+1;
{ writeln(att,i:6,'      ',sta);}
delta:=qw+(k5-1);
k5:=k5+1;
p3(r,ta,b8);
if (b8=false)
then
begin {3}
if (abs(r)< provispeak)
then
begin {4}
b5:=true ;
b4:=false;
if(bb1=false) then
begin
b4:=false;
b5:=false
end
end {4}
else
begin {5}
b5:=false;
b4:=true;
if(bb1=false) then
begin

```

```

b4:=false;
b5:=false
end

                                end{5}
                                end{3}
                                else
                                    begin{6}
                                        zerocrosstime[j]:=i-abstime;
                                        am[j]:=provispeak;
                                        j:=j+1;
                                        {determine the end of event}
                                        if(lta>noiselevel)
                                            then
                                                begin{9}
                                                    b5:=false;
                                                    b4:=true;
if(bb1=false) then
    begin
        b4:=false;
        b5:=false
    end
                                end{9}
                                else
                                    begin{10}
                                        b4:=false;
                                        b5:=false
                                    end{10}
                                end{6}
                                end{2}
                                end;{1}
                                    m1:=i- abstime;
                                    if (j>k2)
                                        then
                                            begin
{INITIALISING THE PARAMETERS}
        mean:=0.0;
        std:=0.0;

```

```

slope = 0.0;
wee = abstime;
qee = 1;
frequency(zerocrosstime, mean, std, samprate, wee, qee);
if(std>0.9) then
begin
  clrscr;
  writeln('FREQUENCY DISPERSION PASSED');
  delay(1000);
  codaslope(am, zerocrosstime, slope, samprate, wee, qee);
  if (slope>0.9) then
  begin
    writeln('CODA SLOPE PASSED');
    delay(1000);
    s11:=p11;
    r11:=abstime;
    gotoxy(12,12);
    writeln('RESULT AND ANALYSIS:');
    gotoxy(12,13);
    writeln('-----');
    gotoxy(12,14);
    writeln('THE EVENT STARTS AT SAMPLE NO : ',abstime);
    gotoxy(12,16);
    writeln('THE EVENT ENDS AT : ',i);
    gotoxy(12,18);
    writeln('NUMBER OF PEAKS IN THE EVENT:',j);
    gotoxy(12,20);
    writeln('THE FREQUENCY DISPERSION OF THE EVENT:',
    std);
    gotoxy(12,22);
    writeln('THE AVERAGE NUMBER OF PEAKS/0.5sec : ',mean);
    gotoxy(12,24);
    writeln('THE SLOPE OF THE EVENT(CODA SHAPE): ',slope);
    writeln(xx, 'RESULT AND ANALYSIS:');
    writeln(xx, '-----');
    writeln(xx, 'THE EVENT STARTS AT SAMPLE NO : ',abstime);
    writeln(xx);
  end
end

```

```

writeln('THE MONITORING OF THE EVENT IS OVER!');
gotoxy(22, 12);
writeln('THE ANALYSIS IS STORED IN FILE-"RESULT"');
    gotoxy(72, 24);
    delay(3000);
        clrscr;
    end.
{ procedure convert();
  var
    file1, file2: text;
    i: integer;
    x: char;
  begin
    getpromptedstringname();
    assign(file1, www);
    reset(file1);
    assign(file2, 'cs10.dat');
    rewrite(file2);
    i:=1;
    write(file2, i:6, ' ');
    while not eof(file1) do
      begin
        read(file1, x);
        if(ord(x)<>44)then
          begin
            if((ord(x)<>32)and(ord(x)>31))then
              write(file2, x)
            end
          else
            begin
              i:=i+1;
              writeln(file2);
              write(file2, i:6, ' ')
            end
          end
        end;
      }
  { END OF THE PROGRAM}

```

## APPENDIX - II

## APPENDIX - II

### DETAILS OF THE MAGNETIC TAPE FORMAT USED IN PDP 11/23 SYSTEM

#### 2.1 The configuration block

This is the first block on the magnetic tape. This block contains information about how the system was configured when the magnetic tape was written. This block has the following format :

WORD	CONTENT
0000	Reserved
0001	Reserved
0002	Reserved
0003	Reserved
0004	STA interval in 1/10ths of a second.
0005	LTA interval in 1/10ths of a second.
0006	Trigger window interval in 1/10ths of a second.
0007	The pre-event recording period in 1/10ths of a second.
0008	The post-event recording period in 1/10ths of a second.
0009	The maximum recording period in seconds.
0010	The number of stations involved in the trigger.
0011-0015	Reserved
0016	One word containing the identification/type and trigger ratio for the first station to be recorded.

- The high byte contains the trigger ratio required to contribute to an event.
- 0017-0079 Station order list. One word for each of the other stations being recorded.
- 0080-0111 A list of 32 entries containing the identification of a station to be output to the chart recorder DAC outputs.
- 0112 A value in seconds which when non zero will be taken as the period of data to be sent to the chart recorder as pre-event data.
- 0113 A value in seconds which when non zero will be taken as the period of data to be sent to the chart recorder as post-event data.
- 0114-0127 Reserved
- 0128-0158 Up to 32 ascii bytes containing the identification of the site and issue data of the software.
- 0159-0225 Reserved
- 0256-0287 32 words allocated to each active station containing the following information.
- 0256 One word identical to word 0016 with the exception that 0rrrrrrr indicates the station is not to be recorded 1rrrrrrr indicates the station is to be recorded.
- 0257 Station latitude in degrees held as a 16 bit binary integer 0-259.
- 0258 Station latitude in 1/100ths of a minute held as a 16 bit binary integer 0-999.

0259	Station longitude in degrees.
0260	Station longitude in 1/100ths of a minute.
0261	Station calibration volts/metre/sec.
0262	Spare.
0264	Spare.
0266-0287	Reserved.
0288-2047	32 words for the next station.

## 2.2 Event data block format

Event data is recorded onto the magnetic tape in 4096 byte blocks. An event is recorded as a number of these blocks terminated with an End Of File mark (EOF). Each block has a 128 word/256 byte preamble which contains time information for that particular block. The time code is inserted as the block is started so the first data sample will correspond to the time encoded in the data block header. After this header one word is stored for each station in turn up to the end of the block continuing onto the next block in sequence.

WORD	CONTENT
0000	An incrementing block serial number.
0001	A sixteen bit unsigned integer containing an Internal Record Sequence Number (IRSN). This word is used for internal diagnostic reference only.
0002	A sixteen bit unsigned integer containing an Internal Sequence Address word (IRSA). This word is used for internal diagnostic reference only.



0003	Reserved	
0004	Reserved	
	Hi-byte	Lo-byte
0005	Seconds	1/100 seconds count
0006	Hour	Minute
0007	Month	Day
0008	Spare	Year
0009	Reserved	
0010	ID of the last station written to the last block.	
00011-0014	Reserved.	
0015	One word either zero or containing a BCD code of seconds and 1/100 second time. This represents the time that the system has detected a trigger.	
0016-0047	One word for each of the stations currently being recorded. These words will either be zero or contain a BCD code of seconds and 1/100 second time. This represents the time that a particular station has exceeded its trigger time.	
0048-0079	A copy of the station order list as defined for word 16 onwards in the configuration block.	
0080	The short term averaging time of the system contained as a 16 bit integer whose value is the STA interval in 1/10ths of a second.	
0081	The long term averaging time of the system contained as a 16 bit integer whose value is the LTA interval in 1/10ths of a second.	

- 0082        The trigger window time interval of the system contained as a 16 bit Integer whose value is the window interval in 1/10ths of a second.
- 0083        The pre-event record time contained as a 16 bit integer whose value is the period in 1/10ths of a second.
- 0084        The post-event record time contained as a 16 bit integer whose value is the period in 1/10ths of a second.
- 0085        The maximum recording period of an event contained as a 16 bit integer whose value is this period in seconds.
- 0086        The number of stations involved in the trigger which when triggered will cause an event to be recorded onto magnetic tape. This is represented as 16 bit binary integer.
- 0087        Reserved
- 0088-0089    Two words as four ascii bytes containing the site identification as displayed in the banner on the console VDU.
- 0090-0127    Reserved
- 00128-2047   One word data sample for every station that is included in the record. The station order of these samples are as listed in words 16 to 79 in the configuration block. This list also determines the format of the data.

## REFERENCES

## REFERENCES

1. Acharya, H. R., L. M. Tyrala, J. M. Ganzales and J. A. Hileman (1989) Microearthquake monitoring of the Texas Panhandle, Bull. Seis. Soc. Am., 79, 1645-1650.
2. Agrawal, P. N. and A. Kumar (1982) Microearthquake recording for engineering applications, Engineering geosciences (ed) B. B. S. Singhal, Meerut : Sarita Prakashen, 181-186.
3. Agrawal, R. C., B. Kumar and S. K. Jain (1988) Contemporary seismicity of a portion of MCT in Tehri Garhwal region, Proc. ECE/UN seminar on prediction of earthquakes, Nov. 14-18, 897-907.
4. Aki, K. (1984) Asperities, barriers, characteristic earthquakes and strong motion prediction, J. Geophys. Res., 89, 5867-5872.
5. Allen, R.V. (1978) Automatic earthquake recognition and timing from single traces, Bull. Seis. Soc. Am., 68, 1521-1532.
6. Allen, R.V. (1982) Automatic phase pickers : their present use and future prospects, Bull. Seis. Soc. Am., 72, S225-S242.

7. Allen, R.V. and J.O. Ellis (1980) An automatic on-line monitor for microearthquake networks, Trans. Am. Geophys. Union, 61, S-41.
8. Ambuter, B.P. and S.C. Solomon (1974) An event recording system for monitoring small earthquakes, Bull. Seis. Soc. Am., 64, 1181-1188.
9. Anderson, K.R. (1978) Automatic analysis of microearthquake network data, Geoexploration, 16, 159-175.
10. Andrew J. M., P.G. Stephen and J. L. Pulli, (1982) A real time digital seismic event detection and recording system for network applications, Bull. Seis. Soc. Am., 72, 2339-2348.
11. Archuleta, R.J., E. Cranswick, C. Mueller and P. Spudich (1982) Source parameters of the 1980 Mammoth Lakes, California, earthquake sequence, J. Geophys. Res., 87, 4595-4607.
12. Baer, M., and U. Kradolfar (1987) An Automatic phase picker for local and teleseismic events, Bull. Seis. Soc. Am., 77, 1437-1445.

13. Bakun, W. and C.G. Bufe (1975) Shear wave attenuation along the San Andreas fault zone in central California, Bull. Seis. Soc. Am., 65, 439-459.
14. Baranowski, J., J. Armbruster, L. Seeber and P. Molnar (1984) Focal depths and fault plane solutions of earthquakes and active tectonics of the Himalaya, J. Geophys. Res., 89, 6918-6928.
15. Barazangi, M. and J. Ni (1982) Velocities and propagation characteristics of  $P_n$  and  $S_n$  beneath the Himalayan arc and the Tibetan plateau, possible evidence of underthrusting of Indian continental lithosphere beneath Tibet, Geology, 10, 179-185.
16. Bibbo, J., D. Etter and D. Breding (1991) A software package for processing of seismic data, Computers and Geosciences, 17, 301-305.
17. Bird, P. (1978) Initiation of intracontinental subduction in the Himalaya, J. Geophys. Res., 83, 4975-4987.
18. Bolt B. A., J. E. Friday and R. A. Uhrhammer (1988) A PC - based broad band digital seismograph network, Geophys. J., 93, 565-573.

19. Borchardt, R. D., J. B. Fletcher, E. G. Jenson, G. L. Maxwell, J. R. Vanshaack, R. E. Warrick, E. Cranswick and M. J. S. Johnson (1985) A general earthquake observation system (GEOS), Bull. Seis. Soc. Am., 75, 1783-1825.
20. Brune, J.N. (1970) Tectonic stress and the spectra of seismic shear waves from earthquakes, J. Geophys. Res., 75, 4997-5009.
21. Brune, J.N., J. Fletcher, F. Vernon, L. Haar, T. Hanks, and J. Berger (1986) Low stress-drop earthquakes in light of new data from the ANZA, California telemetered digital array, in Earthquake Source Mechanics, Geophys monograph 37, Maurice Ewing 6, S. Das, J. Boatwright, and C.H. Scholz, Editors, Am. Geophys. Union, Washington D.C.
22. Chander, R., I. Sarkar, K.N. Khattri and V.K. Gaur (1986) Upper crustal compressional wave velocity in the Garhwal Himalaya, Technophysics, 124, 133-140.
23. Chandra, U. (1978) Seismicity, earthquake mechanisms and tectonics along the Himalayan mountain range and vicinity, Phys. Earth Planet. Int., 16, 109-131.
24. Chatfield, C. (1989) Statistics for technology - A course in applied statistics, Third edition (revised), Chapman and Hall, London.

25. Chen, W.P. and P. Molnar (1981) Constraints on the seismic wave velocity structure beneath the Tibetan plateau and their tectonic implications, *J. Geophys. Res.*, 86, 5937-5962.
26. Chin, J. M., G. Steiner, R. Smalley, Jr. and A. C. Johnston (1991) PANDA : A simple, portable seismic array for local to regional scale experiments, *Bull. Seis. Soc. Am.*, 81, 1000-1014.
27. Claerbout, J.F. (1985) *Fundamentals of Geophysical data processing with application to Petroleum prospecting*, Blackwell Scientific Publications, California.
28. Crampin, S. and C.J. Fyfe (1974) Automatic analysis of tape recordings from seismic networks, *Geophys. J. Roy. Astron. Soc.*, 39, 155-168.
29. Douglas, B. M. and A. Ryall (1972) Spectral characteristics and stress drop for microearthquakes near *Palmer Peak, Nevada*, *J. Geophys. Res.*, 77, 351-359.
30. Fitch, T.J. (1970) Earthquake mechanisms in the Himalaya, Burmese and Andman regions and continental tectonics in central Asia, *J. Geophys. Res.*, 75, 2699-2709.



31. Fletcher, J.B. (1980) Spectra from high-dynamic range digital recordings of Oroville, California aftershocks and their parameters, *Bull. Seis. Soc. Am.*, 70, 735-755.
32. Fletcher, J., L. Haar, T. Hanks, L. Baker, F. Vernon, J. Berger and J. Brune (1987) The Digital Array at ANZA, California, Processing and initial interpretation of source parameters, *J. Geophys. Res.* 92, 369-382.
33. Frankel, A. and L. Wennerberg (1989) Microearthquake spectra from the ANZA, California, seismic network: Site response and source scaling, *Bull. Seis. Soc. Am.*, 79, 581-609.
34. Fuchs, G. (1975) Contribution to the geology of north western Himalayas, *Abh. Geol.*, B-A, 32, Wein, 1-59.
35. Fuchs, G. and A. K. Sinha (1978) The tectonics of the Garhwal-Kumaon Lesser Himalaya, *Sonderchuck aus dem Jahrb. Geol. B. - A.*, Bd. 121 Heft 2, Wein 1978, S 219-241.
36. Gane P. G., H. G. Logie and J. H. Stephen (1949) Triggered telerecording seismic experiment, *Bull. Seis. Soc. Am.*, 39, 117-143.
37. Gansser, A. (1964) *Geology of the Himalayas*, Inter Science Publisher, New York, 298pp.

38. Gaur, V.K., R. Chander, I. Sarkar, K.N. Khattri and H. Sinvhal (1985) Seismicity and state of stress from investigations of local earthquakes in kumaon Himalaya, Tectonophysics, 118, 243-251.
39. Gledhill, K. R. and M. J. Randall (1986) SNARE : an earthquake detection and recording system for small seismograph networks, Bull. Seis. Soc. Am., 76, 1485-1489.
40. Goforth, T. and E. Herrin (1981) An automatic seismic signal detection algorithm based on the Walsh transform, Bull. Seis. Soc. Am., 71, 1351-1360.
41. Grant, F.S. and G.S. West (1965) Interpretation theory in applied Geophysics, McGraw Hill, New York.
42. Gutenberg, B. and C. F. Richter (1941) Seismicity of the Earth, Geol. Soc. Am., Spec Pap., 34,1-33.
43. Hanks, T.C. and H. Kanamori (1979) A moment magnitude scale, J. Geophys. Res., 84, 2348-2350.
44. Hanks T.C. and M. Wyss (1972) The use of body wave spectra in the determination of seismic source parameters, Bull. Seis. Soc. Am., 62, 561-589.

45. Helmlberger, D.V. and L.R. Johnson (1977) Source parameters of moderate size earthquakes and importance of receiver crustal structure in interpreting observations of local earthquakes, Bull. Seis. soc. am., 67, 301-313.
46. IS : 1893- 1962, Recommendations for earthquake resistant design of structures, Indian Standard Institutions, New Delhi.
47. Ishida, M. (1964) Determination of fault parameters of small earthquakes in the Kii peninsula, J. Phys. Earth, 22, 177-212.
48. Johnson, L.R. and T.V. McEvelly (1974) Near field observations and source parameters of Central California earthquakes, Bull. Seis. Soc. Am., 64, 1855-1886.
49. Kaila, K.L., P.R. Reddy and H. Narain (1968) Crustal structure in the Himalaya foot hills of north India from P-wave data of shallow earthquakes, Bull. Seis. Soc. Am., 58, 597-612.
50. Kasahara, K. (1981) Earthquake mechanics, Cambridge University Press, London, pp-248.
51. Keilis-Borok, V. I. (1959) An estimation of the displacement in earthquake source and of source dimensions, Ann. Geofis., 12, 205-214.

52. Khattri, K.N. (1987) Great earthquakes, seismicity gaps and potential for earthquake disaster along the Himalaya plate boundary, *Tectonophysics*, 138, 79-92.
53. Khattri, K.N., A.K. Saxena and H. Sinval (1977) Determination of seismic source parameters for the 1967 earthquake in Koyna Dam Region, India, using body wave spectra, *Proc. 6th World Conference on Earthquake Engineering*, New Delhi, India, 2-308-2-316.
54. Khattri, K. N., R. Chander, V. K. Gaur, I. Sarkar and S. Kumar (1989) New seismological results on the tectonics of the Garhwal Himalaya, *Proc. Ind. Acad. Sci. (Earth Planet. Sci.)*, 98-1, 91-109.
55. Kolvanker, V. G., V. N. Nadre and C. Shiv Kumar (1987) A rock burst data acquisition system at Kolar gold fields, Report no 1393, B.A.R.C., Bombay.
56. Kolvanker, V.G., V.N. Nadre and D.S. Rao (1989) Instrumentation for wireless telemetered seismic network at Bhatsanagar, Fifteen annual convention of AEG, Madras.
57. Kumar, S., R. Chander and K.N. Khattri (1987) Compressional wave speed in the second crustal layer in Garhwal Himalaya, *J. Ass. Expl. Geophys.*, VIII, 219-225.

58. Le Fort, P. (1975) Himalaya - the collided range, present knowledge of the continental arc, *Am. J. Sci.*, 275 A, 1-44.
59. Lee, W.H.K. and J.C. Lahr (1975), Hypo71 (revised) : A computer program for determining hypocenter, magnitude and first motion pattern of local earthquakes. U.S.G.S. Open-File Rept. 75-311, 1-116.
60. Lee, W. H. K. and S. W. Stewart (1981) Principles and applications of microearthquake networks, *Advances in Geophysics*, Academic Press Inc. London.
61. Massinon, B. and J. L. Plantet (1976) A large aperture seismic network in France : description and some results concerning epicenter location and upper mantle anomalies, *Phy. Earth. Planet. Inter.*, 12, 118-127.
62. Matsumura, S. and K. Hamada (1976) Determination of P-wave onset times by a digital computer, *XISIN* 229 383-394 (in Japanese)
63. McEvelly, T.V. and E.L. Major (1982) An automated seismic processor for microearthquake network, *Bull. Seis. Soc. Am.*, 72, 303-375.

64. Michael, A. J., S. P. Gildea and J. J. Pulli (1982) A real time digital seismic event detection and recording system for network applications, Bull. Seis. Soc. Am., 72, 2339-2348.
65. Miyamura, S., M. Hori and H. Matumoto (1966) Local earthquake observation network in Kii peninsula, central Japan. Part 5. Development of microearthquake observation network in Kii peninsula during 1957-1962 and observed seismicity, Bull. Earthquake Res. Inst. Univ. Tokyo, 44, 709-729.
66. Molnar, P. (1984) Structure and tectonics of the Himalaya: Constraints and implications of geophysical data, Ann. Rev. Earth Pla. Sci., 12, 489-518.
67. Molnar, P., W.P. Chen, T.J. Fitch, P. Tapponier, W.E.K. Warsi and F. T. Wu (1977) Structure and tectonics of the Himalaya, a brief summery of the relevant geophysical observations, editions de C.N.R.S., 268, 269-294.
68. Molnar, P and W.P. Chen (1983) Focal depths and fault plane solutions of earthquakes under the Tibetan Plateau, J. Geophys. Res., 88, 1180-1196.

69. Mueller, C. S. and E. Cranswick (1985) Source parameters from locally recorded aftershocks of the 9 Jan. 1982, Miramichi, New Brunswick, earthquake, Bull. Seis. Soc. Am., 75, 337-360.
70. Ni, J. and M. Barazangi (1984) Seismotectonics of the Himalayan collision zone. Geometry of the underthrusting Indian plate beneath the Himalaya, J. Geophys. Res., 89, 1147-1163.
71. Oncescu, M. C. (1983) Automatic source parameter determination of local events, Proc. Symp of Digital data acquisition and processing , G. D. R., Reinhansburg ed Ch. Teusper, 114-123
72. Ottnes, R. K. and L. Enochson (1978) Applied time series analysis Vol 1, Basic techniques, John Wiley and sons, New York.
73. Pandey, I. G. (1991) Himalayan tectonogenesis vis-a-vis metamorphic episodes, First Professor Jhingran Memorial lecture, Department of Geology, University of Delhi, 23rd Dec.
74. Papageorgiou, A.S. and K. Aki (1983) A specific barrier model for the quantitative description of inhomogeneous faulting and prediction of strong ground motion, Bull. Seis. Soc. Am., 73, 693-722.

75. Peterson, J., H. M. Butler, L. G. Holcomb and L. R. Hutt (1976) Seismic research observatory, Bull. Seis. Soc. Am., 66, 2049-2068.
76. Prochazkova, D. (1980) Determination of source parameters, Proc. of the 17th Assembly of the ESC Budapest, 217-221.
77. Randall, M.J. (1973) The spectral theory of seismic sources, Bull. Seis. Soc. Am., 63, 1133-1144.
78. Rautian, T.G., V.I. Khaltium, V.G. Martynov and P. Molnar (1978) Preliminary analysis of the spectral content of P and S waves from local earthquakes in the Garm, Tadzhikistan, region, Bull. Seis. Soc. Am., 68, 949-971.
79. Richter, C.F. (1935) An instrumental earthquake magnitude scale, Bull. Seis. Soc. Am., 25, 1-32.
80. Richter, C.F. (1958) Elementary Seismology, W.H. Freeman and Co., San Francisco, 768 pp.
81. Sarkar, I. (1983) On seismological investigations of the Kumaon Himalaya using local earthquake data, Ph.D. Thesis, University of Roorkee, India.



82. Searle, M.P., B.F. Windley, M.P. Coward, D.J.W. Cooper, A.J. Rex, D. Rex., Li Tingdong, Xiao Xuchang, M.Q. Jan, V. C. Thakur and S. Kumar (1987) The closing of Tethys and the tectonics of the Himalaya, Geol. Soc. Am. Bull., 98, 678-701.
83. Seeber, L. and J.G. Armbruster (1981) Great detachment earthquakes along the Himalayan arc and long term forecasting in earthquake prediction, An International Review, Maurice Ewing Series 4, Am. Geophys. Union, 259-277.
84. Seeber, L., J.G. Armbruster and R.C. Quittmeyer (1981) Seismicity and continental subduction the Himalayan arc in Zagros, Hindukush, Himalaya, Geodynamic evolution, Geodyn, Ser. Vol. 3, ed. H.K. Gupta and F.M. Dalany, A.G.U, Washington, D.C., 215-242.
85. Sharma, M. L. (1990) Data management and software for short aperture digital telemetered array in Ganga Yamuna Valley, Earthquake Engineering report EQ 90-3, Earthquake Engineering Department, University of Roorkee, India.
86. Sharma, M. L. (1991) Sample telemetered digital seismic array in Garhwal Himalaya - Software and data management, Journal of Geological society of India (under publication).

87. Sharma, M. L., S. C. Gupta and H. R. Wason (1990) An automatic phase picker for earthquakes, Proc. International conf. on Automatic Robotics and computer vision, Singapore, 247-250
88. Sharma, M. L. and H. R. Wason (1989) Data acquisition aspects of digital telemetered microearthquake networks, presented in silver jubilee symp. of ISET, Roorkee, Feb 25-26.
89. Sharma, M. L., H. R. Wason and L. S. Srivastava (1987) Telemetered digital seismic event recording system, Proc. Vith Indian Geological Congress, Roorkee, Feb 21-24, 127-130.
90. Singh, S. R., K. K. Subbaramu, R. N. Bhartur, S. S. H. Sharma, M. K. Bhat and T. R. Ramanunny (1969) Technical aspects of Gouribidanour seismic array, Proc. Symp. Use of Gouribidanour data for seismological research, Gouribidanour, July 4-5.
91. Srivastava, H.N. (1992) Seismic instrumentation in India, Current Science, special issue - seismology in India, an overview, 62, NOS 1 and 2, 199-212.
92. Stebbings, J. (1982) The assessment of a site for VHF, Radio Communications, 1050-1053.

93. Stevenson, P.R. (1976) Microearthquakes at Flathead Lake, Montana: A study using automatic earthquake processing, Bull. Seis. Soc. Am., 66, 61-80.
94. Stewart, S.W. (1977) Real time detection and location of local seismic events in central California, Bull. Seis. Soc. Am., 67, 433-452.
95. Stewart S. W., W. H. K. Lee and J. P. Eaton (1971) Location and real time detection of microearthquakes along the San Andreas fault system in central California, Bull. R. Soc. N. Z., 9, 205-209.
96. Thatcher, W. and T.C. Hanks (1973) Source parameters of southern California earthquakes, J. Geophys. Res., 78, 8547-8576.
97. Tondon, A.N. and R.K. Dube (1973) A study of the crustal structure beneath the Himalaya from body waves, Pure and Applied Geophys., VIII, 2207-2216.
98. Tucker, B. E. and J. N. Brune (1977) Source mechanism and  $m_b - M_s$  analysis of aftershocks of the San Fernando earthquake, Geophys. J., 49, 371-426.
99. Valdiya, K.S. (1981) Tectonics of the central sector of Himalaya, in Zagros, Hindukush, Himalaya, Geodynamic Evolution, Geody. Ser., Vol III ed. H.K. Gupta and F.M., Dalany, A.G.U. Washington D.C., 81-110.

100. Verma, G.S. (1974) Structure of foot hills of the Himalayas, Pure and Applied Geophys., VII2, 18-26.
101. Wadia, D.N. (1953) Geology of India, Macmillan and Co., London, 531 pp.
102. Wason, H. R., M. L. Sharma, Kirat Pal and L. S. Srivastava (1986) Digital telemetered array in Ganga Yamuna Valley, Proc. 8th symp. of earthquake engineering, Dec 29-31, 91-99
103. Windley, B.F. (1983) Metamorphism and tectonics of the Himalaya, J. Geol. Soc. Lon., 140, 849-865.
104. Wyss, M. and J.N. Brune (1968) Seismic moment, stress, and source dimensions for earthquakes in the California-Nevada region, J. Geophys. Res., 73, 4681-4694.
105. Wyss, M. and T.C. Hanks (1972) The source parameters of the San Fernando earthquake inferred from teleseismic body waves, Bull. Seis. Soc. Am., 62, 591-602.